

# Characterization of Natural Polymers for Cosmetic Applications

by

**Carlo B. Botha**

*Dissertation presented in partial fulfilment of requirements*

*for the degree of*

***Master of Science (Polymer Science)***

*at the*

Pectora cuberant cultus recti

***University of Stellenbosch***

Supervisor: Prof H. Pasch

December 2015

Co-supervisor: Dr H. Pfukwa

## **Declaration**

By submitting this thesis electronically, I declare that the entirety of the work contained therein is my own, original work, that I am the authorship owner thereof (unless to the extent explicitly otherwise stated) and that I have not previously in its entirety or in part submitted it for obtaining any qualification.

Date: .....

Carlo Bennet Botha  
Stellenbosch University

## Abstract

The characterization of the molar mass and the chemical composition distributions of hyaluronic acid (HA), a linear polysaccharide, is an important task for developing structure-property correlations and for the advancement of various industrial applications. Some of the current techniques to obtain these distributions exhibit problems related to the poor sample solubility of virgin and modified HA since chemical composition and molecular size separations are typically conducted in solution. Therefore, there is a need for characterization techniques enabling the analysis of virgin and modified hyaluronic acid that are accurate, robust and reproducible.

In the first part of this work solubility studies were performed on unmodified HA as well as HA modified with acrylic moieties. The aim of this work was to obtain suitable solvent systems for both species that can be used for size and chemical composition analysis. The solubility tests provided useful insight into solvents applicable for the chromatographic fractionation of the HA samples. The results gave a guideline for which solvent system is the most suitable for dissolving all the HA's, irrespective of their degree of modification (degree of substitution, DS). For a first overview, the HA's were analysed by bulk methods such as proton nuclear magnetic resonance ( $^1\text{H-NMR}$ ) and Fourier transform infrared (FT-IR) spectroscopy. From the bulk analyses, the average degrees of substitution of the HA's were quantitatively determined by  $^1\text{H-NMR}$  spectroscopy. FT-IR spectroscopy was shown to provide fast and reliable information on DS of chromatographic fractions and is, therefore, complementary to  $^1\text{H-NMR}$ .

In the present work, different analytical approaches have been developed for the chemical composition and molar mass characterization of HA and its derivatives. The combination of size exclusion chromatography (SEC) and multi-angle laser light scattering (MALLS) detection provided accurate molar mass distributions. The chemical composition separation was conducted by gradient high performance liquid chromatography (HPLC). In further investigations, these fractionation techniques were hyphenated with an information-rich detector such as FT-IR to obtain information on the degree of acrylate substitution of HA as a function of either molar mass or chemical composition.

The results of this research showed that carefully conducted solubility tests are an important prerequisite for developing accurate and robust fractionation techniques. For very polar

polymers such as HA and its derivatives, solvent systems must be found that suppress aggregate formation and enable the macromolecules to adopt random coil conformations. To our knowledge, the first gradient HPLC separation of HA bearing acrylate functionalities was successfully achieved in this work. The hyphenation of gradient HPLC with FT-IR provided insight into the separation mechanism and the functional group distribution of these polymers.

## Opsomming

Die karakter analise van die verspreidings funksies, wat die beskrywing van grootte, en chemiese verwante parameters, van hialuroniese suur (HA) 'n lineêre polisakaried insluit, in oplossing beklemtoon die noodsaaklikheid ten opsigte van struktuur-eienskap verhoudings, vir die vooruitgang van spesifieke industriële toepassings. Sommige van die huidige tegnieke wat bogenoemde verspreidings aanbetref het veelvuldige probleme geassosieer daarmee in terme van swak monster ontbinding van beide ongemodifiseerde en gemodifiseerde HA, sienende dat chemiese komposisie en grootte skeidings tipies in oplossing plaasvind. Daarom is karakter analitiese tegnieke wat die analise van gemodifiseerde en ongemodifiseerde HA moontlik maak, van kardinale belang om informasie te verkry, wat dus ook akkuraat, duursaam en herproduseerbaar is.

In die eerste gedeelte van die werk was oplosbaarheids studies uitgevoer met betrekking tot ongemodifiseerde HA asook gemodifiseerde HA gefunksioneer met akriel groepe. Die doel van die werk was om 'n geskikte oplossings sisteem te vind vir beide spesies wat dus ook gebruik kon word vir grootte en chemiese komposisie ontleding. Die in diepte ondersoek van die oplosbaarheid van HA het insiggewende informasie gebied vir oplosmiddels wat van toepassing is met betrekking tot die chromatografiese fraksionering van die HA monsters. Die resultate het 'n duidelike indikasie aangedui met betrekking tot watter oplosmiddel sisteem die mees gepaste sou wees vir die HA's ten spyte van die graad van substitusie (DS). Vir 'n eerste oorsig was die HA's dus ook ge-analiseer deur middel van grootmaat opsporing metodes soos: proton kern magnetiese resonansie ( $^1\text{H-KMR}$ ), en Fourier transform infra-rooi (FT-IR) spektroskopie. Van die grootmaat analise was die gemiddelde graad van substitusie van die HA's kwantitatief bepaal deur  $^1\text{H-KMR}$  spektroskopie. FT-IR spektroskopie het getoon om voorsiening te maak vir vinnige en betroubare inligting ten opsigte van die DS van chromatografiese fraksies en is dus aanvullend ten opsigte van  $^1\text{H-KMR}$  spektroskopie.

In die huidige werk was verskeie analitiese benaderings ook ontwikkel vir die chemiese komposisie en molêre massa karakterisering van HA en sy afleibares. Die gekombineerde gebruik van grootte uitsluiting chromatografie (SEC) met 'n multi hoek laser lig verstrooiing (MALLS) detektor het akkurate molêre massa verspreidings voorsien. Die chemiese komposisie skeiding was uitgevoer deur middel van gradiënt hoë veringting vloeistof chromatografie (HPLC). In verdere ondersoeke was die fraksionerings tegnieke ook

gekoppel met 'n informasie-reike detektor soos FT-IR met die doel om informasie te verkry ten opsigte van die graad van akriel substitusie van HA as 'n funksie van óf molêre massa óf chemiese komposisie.

Die resultate van die navorsing het getoon dat noukerig uitgevoerde oplosbaarheids studies 'n belangrike voorvereiste is vir die ontwikkeling van akkurate en duursame fraksionerings tegnieke. In die geval van hoogs polêre polimere soos HA en sy afleibares moet oplosmiddels gevind word wat die vorming van konglomerasie onderdruk en die makromolekule in staat stel om lukrake spoel konformasies aan te neem. Tot ons kennis is die eerste gradiënt hoë verrigting vloeistof chromatografie (HPLC) skeidings van die HA's gemodifiëer met akrilaat funksionele groepe suksesvol bereik in die navorsings werk. Die koppeling van gradiënt hoë verrigting vloeistof chromatografie met Fourier transform infra-rooi spektroskopie het insig verskaf op die skeidings meganisme en die graad van funksionele groep verspreiding van die polimere.

## Acknowledgements

I want to start off by firstly thanking God Almighty for all my abilities and His guidance throughout the research endeavour.

My utmost gratitude goes to my supervisor and co-supervisor, **Prof Harald Pasch** and **Dr Helen Pfukwa**, for their input, support and encouragement throughout the course of my study. I would also like to thank Prof Pasch and L'Oréal (Paris, France) for their financial support regarding the study.

My most sincere appreciation goes out to my family and my girlfriend Ashley Carine de Lange for all their support through difficult times.

Finally my sincere thanks go to the following people:

**Ms Chantelle Human**, **Ms Nedine van Deventer** and **Mr Piere Siebert** for their friendship and support throughout the study, especially during difficult times.

**Dr Jaco Brand** and **Mrs Elsa Malherbe** for all the solution NMR analyses.

**Dr Maggie Brand** and **Mr Guillaume Greyling** for their help and advice with AF<sup>4</sup> and ThFFF analysis.

**Mr Anthony Ndiripo** for his help and guidance with the LC-Transform and data processing of FT-IR analysis.

**Dr Nadine Makan** for all her help regarding instrumentation, with reference to the hardware of instruments.

All members and staff of the Department of Chemistry and Polymer Science; **Mrs Erinda Cooper**, **Mrs Aneli Fourie**, **Mr Deon Koen**, **Mr Jim Motshweni** and **Mr Calvin Maart**.

All members of Prof Pasch's group, past and present; **Trevor**, **Douglas**, **Kerissa**, **Mohau**, **Paul**, **Ashwell**, **Lebogang**, **Khumo**, **Pritish**, **Lucky**, **Zanelle** and **Timo**.

**Dr Céline Farcet** from L'Oréal for the opportunity to work on an interesting and very challenging project.

# Table of Contents

<b>Declaration</b> .....	<b>ii</b>
<b>Abstract</b> .....	<b>iii</b>
<b>Opsomming</b> .....	<b>v</b>
<b>Acknowledgements</b> .....	<b>viii</b>
<b>Table of Contents</b> .....	<b>viii</b>
<b>List of Figures</b> .....	<b>x</b>
<b>List of Tables</b> .....	<b>xiviv</b>
<b>List of Abbreviations</b> .....	<b>xv</b>
<b>List of Symbols</b> .....	<b>xvii</b>
<b>Chapter 1</b> .....	<b>1</b>
Introduction and Objectives .....	1
1.1 Introduction .....	1
1.2 Objectives .....	2
1.3 Layout of Thesis .....	3
<b>References</b> .....	<b>5</b>
<b>Chapter 2</b> .....	<b>6</b>
Historical and Theoretical Perspectives .....	6
2.1 Polysaccharides .....	6
2.1.1 Hyaluronic Acid: Structure and Properties .....	6
2.1.2 Hyaluronic Acid Derivatization .....	8
2.1.3 Hyaluronic Acid Derivative Characterization .....	12
2.2 High Performance Liquid Chromatography (HPLC) .....	14
2.2.1 Size Exclusion Chromatography (SEC) .....	17
2.2.2 Liquid Adsorption Chromatography (LAC) .....	19
2.2.3 Liquid Chromatography at Critical Conditions (LC-CC) .....	20
2.2.4 Gradient LAC .....	22
2.2.5 Detectors .....	22
2.3 Hyphenated Liquid Chromatography Techniques: Coupling with Chemically Selective or Molar Mass sensitive Detectors .....	25
2.3.1 Liquid Chromatography–Infrared Spectroscopy (LC-IR) .....	25
2.3.2 Size Exclusion Chromatography–Multi-Angle Laser Light Scattering (SEC- MALLS) .....	26
<b>References</b> .....	<b>30</b>
<b>Chapter 3</b> .....	<b>34</b>
Solubility Studies and Spectroscopic Analysis .....	34
3.1 Solubility Studies of Hyaluronic Acid with respect to DS .....	34



3.1.1	Introduction.....	34
3.1.2	Experimental Procedure.....	35
3.1.3	Results and Discussion .....	36
3.2	Spectroscopic Analysis of HA Polysaccharides .....	43
3.2.1	Introduction.....	43
3.2.2	Experimental .....	43
3.2.3	Results and Discussion .....	44
3.3	Conclusions.....	51
<b>References .....</b>		<b>52</b>
<b>Chapter 4 .....</b>		<b>53</b>
Development of a SEC Method for Modified and Unmodified HA.....		53
4.1	Introduction.....	53
4.2	Experimental .....	53
4.3	Results and Discussion .....	57
4.3.1	Molar Mass Determination of HA's .....	57
4.3.2	SEC Method Development for HA's in DMSO-Water.....	60
4.3.3	SEC Coupled to LC Transform with FTIR .....	71
4.4	Conclusion.....	72
<b>References .....</b>		<b>73</b>
<b>Chapter 5 .....</b>		<b>75</b>
LAC Method Development for the HA's.....		75
5.1	Introduction.....	75
5.2	Experimental .....	76
5.3	Results and Discussion .....	77
5.3.1	Separation of the HA's According to DS.....	77
5.3.2	Sample Stability Studies.....	88
5.3.3	Gradient LAC Coupled to LC Transform with FTIR .....	89
5.3.4	Preliminary C8 Column Results .....	92
5.4	Conclusion.....	94
<b>References .....</b>		<b>95</b>
<b>Chapter 6 .....</b>		<b>96</b>
Summary, Conclusions and Future Work.....		96
6.1	Summary .....	96
6.2	Conclusions.....	96
6.3	Recommendations for Future Work.....	98
<b>Appendix A.....</b>		<b>99</b>
<b>Appendix B.....</b>		<b>104</b>
<b>Appendix C.....</b>		<b>105</b>

## List of Figures

<b>Figure 2.1:</b>	Schematic illustration of the repeat unit in hyaluronic acid (HA).....	7
<b>Figure 2.2:</b>	Schematic illustration of the hydrogen bonds of HA in water.....	8
<b>Figure 2.3:</b>	Illustration of the (A) sixteen different substitution patterns of HA and (B) chemical heterogeneity among polymer chains (1 <sup>st</sup> order) and along the polymer chain (2 <sup>nd</sup> order).....	11
<b>Figure 2.4:</b>	Schematic illustration of the chromatographic behaviour of elution volume dependence on the molar mass in SEC, LC-CC, LAC and gradient LAC mode.....	17
<b>Figure 2.5:</b>	Schematic illustration of an ELSD (modified from reference 94).....	24
<b>Figure 2.6:</b>	Schematic illustration of an LC-Transform coupling.....	26
<b>Figure 2.7:</b>	A simplified schematic illustration of a MALLS detector.....	29
<b>Figure 3.1:</b>	Hyaluronic acid before and after modification (DS = 2).....	37
<b>Figure 3.2:</b>	Sample recoveries after filtration in the presence of the following solvent systems; (A) DMSO:H <sub>2</sub> O (20:80); (B) DMSO:H <sub>2</sub> O (60:40); (C) ACN:H <sub>2</sub> O (20:80) and (D) ACN:H <sub>2</sub> O (50:50).....	40
<b>Figure 3.3:</b>	Sample recoveries after filtration in the presence of DMSO:H <sub>2</sub> O (60:40) + 0.1M ammonium acetate.....	40
<b>Figure 3.4:</b>	Sample recoveries after filtration using a 0.1M NaCl + NaN <sub>3</sub> solution solvent system.....	41
<b>Figure 3.5:</b>	Schematic illustration of the maximum DS of each HA repeat unit.....	44
<b>Figure 3.6:</b>	<sup>1</sup> H-NMR spectrum of sample HAM 04 (DS = 2.6) in D <sub>2</sub> O.....	45
<b>Figure 3.7:</b>	Stacked IR spectra of unmodified and modified (HAM 09, DS = 2.5) HA samples.....	47
<b>Figure 3.8:</b>	Overlaid FTIR spectra of the modified HA samples (DS range of 0.4–3.4). The inset represents an expansion of the frequency range 600–1800 cm <sup>-1</sup> .....	48
<b>Figure 3.9:</b>	The interrelationship of specific FT-IR signal area ratios (C=O ester and C–O skeleton) with that of the DS values obtained by <sup>1</sup> H-NMR spectroscopy of the modified HA samples.....	50
<b>Figure 4.1:</b>	“Staircase” intervals obtained at different sample concentrations, sample HAM 04 (DS = 2.6) is used as illustration, in the presence of DMSO:H <sub>2</sub> O/LiBr at 40 °C.....	56

- Figure 4.2:** Linear fit ASTRA 6.0 software performs after the different concentrations have been defined to produce the  $dn/dc$  value. HAM 04 (DS = 2.6) is used as illustration, in the presence of DMSO:H<sub>2</sub>O/LiBr at 40 °C.....56
- Figure 4.3:** SEC-RI traces of the HA samples dissolved in 0.1 M NaCl eluent; injection volume: 100 µL (conc. = 1.5 mg/mL); Eluent: 0.1 M NaCl water solution with 300 mg/L NaN<sub>3</sub>; column: PSS-Suprema set at 40 °C; RI temperature: 40 °C; Flow rate: 1.0 mL/min; Detectors: RI; Samples: (A) HA03 (unsubstituted), (B) HAM01 (DS = 3.1), (C) HAM03 (DS = 2.9) and (D) HAM 06 (DS = 0.8). The dotted line at a  $V_e = 37.5$  mL is representative of the exclusion limit of the column set.....58
- Figure 4.4:** RI- (solid red line) and corresponding LS-traces (blue star-lines) of the HA samples dissolved in DMSO:H<sub>2</sub>O; injection volume: 100 µL (conc. = 1.5 mg/mL); Eluent: DMSO:H<sub>2</sub>O (60:40)(v/v%); column: PSS-GRAM set at 40 °C; RI temperature: 40 °C; Flow rate: 0.30 mL/min; Detectors: MALLS and RI; Samples: (A) HA1 (unsubstituted), (B) HAM09 (DS = 2.5) and (C) HAM10 (DS = 1.5).....61
- Figure 4.5:** RI traces of sample HAM 10 (DS = 1.5) in DMSO:H<sub>2</sub>O (60:40) at (A) 30 °C, (B) 40 °C, (C) 50 °C and (D) 55 °C. Experimental conditions were the same as in **Figure 4.4**.....62
- Figure 4.6:** Overlays of the RI- and LS-traces (A) HA 02 (unsubstituted) and (B) HAM 11 (DS = 1.6) in DMSO:H<sub>2</sub>O/LiBr; Injection volume: 100 µL (conc. = 1.5 mg/mL); Sample solvent and eluent: DMSO: H<sub>2</sub>O (60:40, v/v%) + 50 mmol/L LiBr; Column: PSS-GRAM 1000 Å (300 mm x 80 mm I.D., 10 µm) at 40 °C; RI temperature, 40 °C; Flow rate: 0.350 mL/min; Detectors: MALLS and RI.....64
- Figure 4.7:** Overlays of the RI- and LS-traces (inset) for (A) HA1 (unsubstituted); (B) HAM07 (DS = 0.4); (C) HAM09 (DS = 2.5) and (D) HAM10 (DS = 1.5) at variable LiBr salt concentrations in the presence of DMSO:H<sub>2</sub>O/LiBr; Injection volume: 100 µL (conc. = 1.5 mg/mL); Sample solvent and eluent: DMSO: H<sub>2</sub>O + X mmol/L LiBr (X = 50 (black), 100 (red) and 200 (blue)); Column: PSS-GRAM 1000 Å (300 mm x 80 mm I.D., 10 µm) at 40 °C; RI temperature, 40 °C; Flow rate: 0.350 mL/min; Detectors: MALLS and RI.....66
- Figure 4.8:**  $dn/dc$  values obtained in DMSO:H<sub>2</sub>O (60:40)/ 0.05M LiBr at 40 °C as a function of DS.....68
- Figure 4.9:** Overlaid RI traces at variable concentrations for samples (A) HA1 (unmodified) and (B) HAM10 (DS = 1.5) in the presence of DMSO:H<sub>2</sub>O/LiBr; Injection volume: 100 µL; Sample solvent and eluent: DMSO: H<sub>2</sub>O + 50 mmol/L LiBr; Column: PSS-GRAM 1000 Å (300 mm x 80 mm I.D., 10 µm) at 40 °C; RI temperature, 40 °C; Flow rate: 0.350 mL/min; Detector: RI.....69
- Figure 4.10:** Sample deposition on Germanium disc after SEC. 5 min. after removal from the LC-Transform instrument, the presence of moisture is apparent due to the presence of the LiBr salt.....72
- Figure 5.1:** Chromatograms of HA's having different DS values; Sample solvent: DMSO:H<sub>2</sub>O (60:40) (v/v%); Injection volume: 30 µL (conc. = 0.5 mg/mL); Gradient profile: linear gradient from 100% ACN to 100% H<sub>2</sub>O. (A) sample HA1 (un-substituted), (B) sample HAM 01 (DS = 3.1), (C) sample HAM 06

- (DS = 0.8), (D) HAM 09 (DS = 2.5) and (E) sample HAM 10 (DS = 1.5).....80
- Figure 5.2:** Illustration of the reproducibility of overlaid chromatograms of two HA samples varying in DS value; Sample solvent: DMSO:H<sub>2</sub>O (60:40) (v/v%); Injection volume: 30 μL (conc. = 0.5 mg/mL); Gradient profile: linear gradient from 100% ACN to 100% H<sub>2</sub>O. (A) Sample HAM 10 (DS = 1.5), (B) sample HAM 01 (DS = 3.1).....81
- Figure 5.3:** Influence of variable injected volumes of sample HAM 09 (DS = 2.5) on the CN column; Sample solvent: DMSO:H<sub>2</sub>O (60:40)(v/v%); Gradient profile: linear gradient from 100% ACN to 100% water in 30 min. The dashed line is a representative of the mobile phase composition at the detector.....83
- Figure 5.4:** Illustration of variable injected concentrations on the retention behaviour of sample HAM 10 (DS = 1.5) on the CN column; Sample solvent: DMSO:H<sub>2</sub>O (60:40)(v/v%); Injection volume: 20 μL; Gradient profile: linear gradient from 100% ACN to 100% water in 35 min. The dashed line is a representative of the mobile phase composition at the detector.....84
- Figure 5.5:** Illustration of the chromatographic retention as a function of the DS for all the HA samples (DS range of 0.4–3.1).....86
- Figure 5.6:** Overlaid chromatograms of HA samples representing the biggest part of the DS range. Experimental conditions are the same as in **Figure 5.1**.....87
- Figure 5.7:** Illustration of samples (A) HA 1 (unmodified) and (B) HAM 01 (DS = 3.1) before and after exposure to light. Same experimental conditions as used in **Figure 5.4**.....88
- Figure 5.8:** (A) Linked FT-IR spectra and (B) selected chemigram of the gradient LAC-FTIR analysis of sample HAM 09 (DS = 2.5). Stationary phase: CN column; Sample solvent: DMSO:H<sub>2</sub>O (60:40)(v/v%); Sample concentration: 1 mg/mL; Injection volume: 100 μL; Gradient profile: linear gradient from 100% ACN to 100% water in 35 min. Additional experimental conditions as explained in section 5.2.....89
- Figure 5.9:** The area corresponding to the specific regions incorporated for the DS determination as a function of elution volume by gradient LAC-FTIR. Refer to **Figure 5.8** for experimental conditions.....90
- Figure 5.10:** The absorbance and wavenumbers as a function of time determined by gradient LAC-FTIR. Refer to **Figure 5.8** for experimental conditions.....91
- Figure 5.11:** Chromatograms of HA's with different DS values separated on a C8 column; Sample solvent: DMSO:H<sub>2</sub>O (60:40) (v/v%); Injection volume: 20 μL (conc. = 0.5 mg/mL); Gradient profile: linear gradient from 100% H<sub>2</sub>O to 100% ACN. (A) sample HAM 03 (DS =2.9), (B) sample HAM 04 (DS = 2.6), (C) sample HAM 06 (DS = 0.8), (D) HAM 09 (DS = 2.5), (E) sample HAM 10 (DS = 1.5) and image F an overlay of samples A–E.....93
- Figure C.1:** Influence of mobile phase composition on the ELSD response; No column; flow rate: 0.50 mL/min.; Temperature 30 °C; Injected volume 30 μL; sample codes: (1) HA 1 (unmodified), (2) HAM 01 (DS = 3.1), (3) HAM 02 (DS = 3.4),

---

(4) HAM 03 (DS = 2.9), (5) HAM 04 (DS = 2.6), (6) HAM 05 (DS = 2.2), (7) HAM 06 (DS = 0.8), (8) HAM 07 (DS = 0.4), (9) HAM 08 (DS = 2.6), (10) HAM 09 (DS = 2.5), (11) HAM 10 (DS = 1.5), (12) HAM 11 (DS = 1.6). Eluent profile: 3 min isocratic run with the desired solvent or solvent mixture; Detector: ELSD (Nebulization temp. = 100 °C, evaporation temp. = 100 °C and gas flow = 3.0 bar).....	105
---------------------------------------------------------------------------------------------------------------------------------------------------------------------------------------------------------------------------------------------------------------------------------------------------------------------------------------------------------------------------------------------------------	-----

## List of Tables

<b>Table 2.1:</b>	Categorization of LC detectors with regard to their applicability.....	23
<b>Table 3.1:</b>	Description of different solvent systems tested on the HA's.....	37
<b>Table 3.2:</b>	Description of most effective solvent systems.....	38
<b>Table 3.3:</b>	Sample information as obtained from L'Oréal.....	39
<b>Table 3.4:</b>	Recoveries after filtration using DMSO:H <sub>2</sub> O/NaCl as solvent.....	42
<b>Table 3.5:</b>	Summary of the DS for the modified polysaccharides as obtained from <sup>1</sup> H-NMR spectroscopy.....	46
<b>Table 3.6:</b>	FT-IR spectral assignments for the modified HA's.....	49
<b>Table 4.1:</b>	Average molar masses and molar mass dispersities as determined by SEC with the HA's dissolved in 0.1M NaCl water solution and 300 mg/L NaN <sub>3</sub> on a PSS Suprema column set using a pullulan calibration.....	59
<b>Table 4.2:</b>	Description of the molar mass data obtained for samples HA01–HAM11.....	70
<b>Table 5.1:</b>	Description of the optimized linear gradient profile.....	77
<b>Table A.1:</b>	Solubility study at 25 °C and a concentration of 1 mg/mL (+ soluble, +/- partial soluble, - insoluble).....	100
<b>Table A.2:</b>	Solubility study at 40 °C and a concentration of 1 mg/mL (+ soluble, +/- partial soluble, - insoluble).....	101
<b>Table A.3:</b>	Solubility study at 40 °C and a concentration of 0.5 mg/mL (+ soluble, +/- partial soluble, - insoluble).....	102
<b>Table A.4:</b>	Solubility study at 40 °C and a concentration of 0.5 mg/mL in the presence of a salt (+ soluble, +/- partial soluble, - insoluble).....	102
<b>Table B.1:</b>	Description of the dn/dc values used for molar mass determination.....	104

## List of Abbreviations

Ace	Acetone
ACN	Acetonitrile
ADH	Adipic Acid Dihydrazide
AMA	Ammonium Acetate
ATR	Attenuated Total Reflectance
Bu	Butanone
C*	Critical Overlap Concentration
CA	Cellulose Acetate
CAC	Critical Aggregation Concentration
CC	Chemical Composition
CCD	Chemical Composition Distribution
DCM	Dichloromethane
DMAc	Dimethyl Acetamide
DMF	Dimethyl Formamide
DMSO	Dimethyl Sulfoxide
DMSO-d <sub>6</sub>	Deuterated Dimethyl Sulfoxide
D <sub>p</sub>	Degree of polymerization
DP <sub>w</sub>	Weight-Average Degree of Polymerization
DS	Degree of Substitution
DS <sub>ve</sub>	Degree of Substitution from Elution Volume
ELSD	Evaporative Light Scattering Detector
EtOH	Ethanol
FIFFF	Flow Field-Flow Fractionation
FT-IR	Fourier Transform Infrared Spectroscopy
GAG	Glucosaminoglycan
GlcA	β-(1-4)-D-glucuronic acid
GlcNAc	β-(1-3)-N-acetyl-D-glucosamine
HA	Hyaluronic Acid
HAM	Modified Hyaluronic Acid
Hex	Hexane
HPLC	High Performance Liquid Chromatography
I.D.	Internal Diameter
IR	Infrared Spectroscopy
Isoprop	Isopropanol
LAC	Liquid Adsorption Chromatography
LC	Liquid Chromatography
LC-CC	Liquid Chromatography at Critical Conditions
LS	Light Scattering
m	Medium intensity
M	Molar
MAA	Methacrylic Anhydride
MALDI-MS	Matrix-Assisted Laser Desorption/Ionization Mass Spectroscopy
MALLS	Multi-Angle Laser Light Scattering
MeOH	Methanol
MM	Molar Mass
MMD	Molar Mass Distribution
NMR	Nuclear Magnetic Resonance Spectroscopy
NP	Normal Phase
OLA	Oligomers of Lactic Acid

PLA	Polylactic Acid
RC	Regenerated Cellulose
RI	Refractive Index Detector
RMS	Root Mean Square
RP	Reversed Phase
rpm	Revolutions per Minute
s	Strong intensity
SEC	Size Exclusion Chromatography
S/N	Signal-To-Noise Ratio
THF	Tetrahydrofuran
TOL	Toluene
UV	Ultraviolet Spectroscopy
w	Weak intensity
2D-LC	Two-Dimensional Liquid Chromatography



## List of Symbols

$\alpha$	Attenuation Constant
$\text{\AA}$	Angstrom
$A_2$	Second Virial Coefficient
$c$	Concentration
$C_{MP}$	Concentration of Analyte in Mobile Phase
$C_{SP}$	Concentration of Analyte in Stationary Phase
$\bar{D}$	Dispersity Index
$\Delta G$	Change in Gibbs Free Energy
$\Delta H$	Change in Enthalpic Interactions
$dn/dc$	Refractive Index Increment
$dn/dv$	change in refractive index with change in voltage
$\Delta S$	Change in Entropic Interactions
$\eta$	Intrinsic Viscosity
$F$	Flow Rate Value
$G$	Gibbs Free Energy
$I_o$	Incident Light Intensity
$I_\theta$	Intensity of Scattered Light at a Given Angle
$K$	Polymer Optical Constant
$K_d$	Distribution Coefficient
$K_{LAC}$	Distribution Coefficient as a Function of Enthalpic Interactions
$K_{SEC}$	Distribution Coefficient as a Function of Entropic Interactions
$L_p$	Persistence Length
$\lambda$	Wavelength of the Incident Light in the Solvent
$\lambda_o$	Incident Wavelength
$M_i$	Molar Mass of Given Chain Length
$M_n$	Number-Average Molar Mass
$M_w$	Weight-Average Molar Mass
$N_i$	Number of Molecules
$n_o$	Refractive Index of Solvent
$\omega$	Refractive Index Function
$P_\theta$	Dependence of Scattered Light Intensity on the Angle of Scattering
$R$	Universal Gas Constant
$R_g$	Radius of Gyration
$R_\theta$	Rayleigh Constant
$T$	Absolute Temperature
$t_R$	Retention Time
$\theta$	Angle
$V_e$	Retention Volume/ Elution Volume
$V_i$	Interstitial Column Volume
$V_p$	Pore Volume of Packing Material
$\delta$	Chemical Shift

# Chapter 1

## Introduction and Objectives

*In this chapter, the importance of hyaluronic acid, a natural polymer classified as a polysaccharide, will briefly be discussed followed by a summary of the objectives of the study. A layout of the thesis is also provided.*

### 1.1 Introduction

The use of natural polymers such as hyaluronic acid, cellulose and starch has increased in the last decade, due to their versatility in formulations as well as their sustainability.<sup>1-4</sup> However, there is limited information in published literature regarding the characterization of these natural polymers, rendering the characterization of them still a challenge. The natural polymer of interest in this study is hyaluronic acid (HA, also known as hyaluronan), which is a linear polysaccharide. It consists of a repeating disaccharide unit comprising of  $\beta$ -(1-4)-D-glucuronic acid (GlcA) and  $\beta$ -(1-3)-N-acetyl-D-glucosamine (GlcNAc). Natural polymers, with reference to HA, find extensive application in the medical and cosmetic industries.<sup>5, 6</sup> These polymers are obtained from different sources, in order to obtain polymers that present wide ranges of different properties.<sup>5</sup> Due to its physicochemical properties HA has become attractive for a variety of medical and aesthetic applications such as viscosupplementation therapy for osteoarthritis and tissue augmentation. HA is generally modified to improve its mechanical and physical properties for desired applications. Unmodified HA is completely soluble in water, however, after modification with non-polar groups its water solubility decreases, thus making the complete solvation of modified HA a challenging task. The chemical composition and molar mass of hyaluronic acid has a direct correlation to its application.<sup>7-11</sup> In order to obtain information on the chemical structure, molar mass and chemical composition of modified HA to enable the determination of structure-property correlations, an appropriate solvent system in combination with suitable characterization techniques is required.

Natural polymers, like synthetic polymers, are heterogeneous with regard to their molar mass and chemical composition. The relationship between polymer microscopic and macroscopic properties are defined through structure-property correlations. In order to establish the desired application of these natural polymers, the structure-property correlations have to be well understood. This requires the necessary molecular

characterization to be performed. For the characterization of macromolecules, separation techniques are highly relevant, particularly High Performance Liquid Chromatography (HPLC).<sup>12-14</sup> For the determination of the chemical composition or molar mass of a polymer, gradient liquid adsorption chromatography (LAC), liquid chromatography at critical conditions (LC-CC) and size exclusion chromatography (SEC) are the methods of choice.<sup>12-16</sup>

The focus of this study was to develop chromatographic techniques for the characterization of HA modified with acrylate groups, over a degree of acrylate substitution ranging from 0 (no substitution) to 4 (complete substitution). To our knowledge, no separations for polysaccharides bearing acrylate functionalities have been reported in literature. Thus, the comprehensive characterization of the HA's in terms of molar mass and chemical heterogeneity is a challenging task. The information would provide more fundamental insight into the influence of the structure of HA on its application, and in turn the materials' performance. The methods would shed light on the molecular heterogeneity of both unmodified and modified HA. An investigation of these parameters would lead to a better understanding of the structure-property correlations of these molecules.

## 1.2 Objectives

The main objectives of this study were to:

- I. Carry out a comprehensive solubility study on the unmodified and modified HA samples. Here the aim was to:
  - find a suitable solvent system that will completely dissolve the unmodified and modified hyaluronic acid, regardless of the degree of substitution and with minimal sample degradation.
- II. Investigate the HA's using bulk analytical techniques, which include Fourier transform infrared (FT-IR) and nuclear magnetic resonance (NMR) spectroscopy. The main focus was to:
  - determine the average degree of substitution of the HA's and obtain information regarding the chemical nature of the samples.
- III. Develop a SEC method that will enable the determination of the molar mass and molar mass distribution of the HA's.
- IV. Develop an HPLC method that would enable the separation of the HA's according to chemical composition and/or the degree of substitution, as well as determination of the substituent distribution and chemical composition distribution.

- V. Couple liquid chromatography with an information rich detector such as FT-IR to obtain information on the HA's degree of substitution as a function of either molar mass and/or chemical composition.

### **1.3 Layout of Thesis**

#### **Chapter 1**

Chapter 1 provides a short introduction to the topic of the research as well as the objectives of the study and a layout of the thesis.

#### **Chapter 2**

Chapter 2 is dedicated to the historical and theoretical aspects of the work, and gives an overview of the reported characterization techniques for the analysis of polysaccharides. The presented literature review focuses on structure, properties and characterization of modified and unmodified hyaluronic acid. A theoretical background of the analytical techniques employed for the characterization of hyaluronic acid is also given.

#### **Chapter 3**

Chapter 3 is divided into two sections, the first section presents an in-depth solubility study conducted on the hyaluronic acid samples, to try and establish the most suitable solvent system. The second part covers the bulk analysis of the samples, giving insight into the chemical structures of the samples. For the bulk analysis of the samples, NMR and FT-IR spectroscopy were employed.

#### **Chapter 4**

In Chapter 4 a SEC method was developed for investigating the molar mass and molar mass distribution of the HA samples. The modified and unmodified HA samples were analysed via SEC coupled to a MALLS detector, to obtain absolute molar mass information on the samples. In addition, MALLS in conjunction with an RI detector enabled the determination of the extent of aggregation for the HA samples dissolved in the newly developed solvent system.

#### **Chapter 5**

A gradient HPLC method for the separation of the HA's according to chemical composition was developed in Chapter 5. The approaches used to separate the modified from the unmodified HA's, as well as to separate the modified HA's according to their degree of substitution with the aid of gradient liquid adsorption chromatography are described.

**Chapter 6**

Finally, Chapter 6 is a summary of the results obtained from this research study as well as concluding remarks and also recommendations for future work.

## References

- [1] Alvarez-Lorenzo, C.; Blanco-Fernandez, B.; Puga, A. M.; Concheiro, A. *Adv. Drug. Del. Rev.* **2013**, *65* (9), 1148–1171.
- [2] Lapasin, R.; Pricl, S. *Rheology of industrial polysaccharides: theory and applications*. Blackie Academic & Professional, London, **1995**.
- [3] Buschmann, M. D.; Merzouki, A.; Lavertu, M.; Thibault, M.; Jean, M.; Darras, V. *Adv. Drug. Deliv. Rev.* **2013**, *65* (9), 1234–1270.
- [4] Varma, A. J.; Kennedy, J. F.; Galgali, P. *Carbohydr. Polym.* **2004**, *56* (4), 429–445.
- [5] Rinaudo, M. *Polym. Int.* **2008**, *57* (3), 397–430.
- [6] Bulpitt, P.; Aeschlimann, D. *J. Biomed. Mater. Res.* **1999**, *47* (2), 152–169.
- [7] Yu-Jin, J.; Ubonvan, T.; Kim, D. *J. Pharm. Invest.* **2010**, *40*, 33–43.
- [8] Balazs, E. A.; Leshchiner, A. U.S. Patent No. 4,582,865. 15 Apr. **1986**.
- [9] Illum, L.; Farraj, N. F.; Fisher, A. N.; Gill, I.; Miglietta, M.; Benedetti, L. M. *J. Controlled Release.* **1994**, *29* (1), 133-141.
- [10] Luo, Y.; Kirker, K. R.; Prestwich, G. D. *J. Controlled Release.* **2000**, *69* (1), 169-184.
- [11] Hahn, S. K.; Jelacic, S.; Maier, R. V.; Stayton, P. S.; Hoffman, A. S. *J. Biomater. Sci. Polymer Edition.* **2004**, *15* (9), 1111–1119.
- [12] Pasch, H.; Trathnigg, B. *HPLC of Polymers*. Springer, Berlin, Germany, **1998**.
- [13] Striegel, A.; Yau, W. W.; Kirkland, J. J.; Bly, D. D. *Modern size-exclusion liquid chromatography: practice of gel permeation and gel filtration chromatography*. John Wiley & Sons, Hoboken, New Jersey, USA, **2009**.
- [14] Pasch, H.; Trathnigg, B. *Multidimensional HPLC of Polymers*. Springer, Berlin, Germany, **2013**.
- [15] Chang, T. *J. Polym. Sci. Pol. Phys.* **2005**, *43*, 1591.
- [16] Mori, S.; Taziri, H. *J. Liq. Chromatogr. Rel. Technol.* **1994**, *17* (14–15), 3055–3068.

## Chapter 2

### Historical and Theoretical Perspectives

*This chapter will provide an overview of polysaccharides in general and then focus more specifically on hyaluronic acid, with regard to its structure and properties, functionalization and finally the characterization of hyaluronic acid after functionalization. The chapter is also dedicated to the theoretical and experimental aspects pertaining to the analytical techniques employed in this work.*

#### 2.1 Polysaccharides

In the last few decades there has been a worldwide focus on the utilization of sustainable polymeric materials, particularly polymers based on carbohydrates. Naturally derived mono-, di-, oligo- and polysaccharides can provide the necessary raw materials for the production of a large variety of industrial materials in a much more sustainable manner. Polysaccharides are defined as complex, high molecular weight carbohydrate structures, consisting of monosaccharide repeat units bound by glycosidic linkages.<sup>1, 2</sup> The general structural formula of polysaccharides is  $C_n(H_2O)_m$ , where  $n$  is between 200 and 2500. Polysaccharides possess unique properties which makes them highly attractive for a wide range of applications in different fields, e.g. biomedical, pharmaceutical (drug delivery systems) and in cosmetics. Some of their properties include: (1) they can be obtained from natural resources in a well characterized and reproducible fashion;<sup>3</sup> (2) they can undergo a wide range of modifications via chemical and enzymatic reactions to produce different materials<sup>4</sup> and (3) they have improved biocompatibility, biodegradability, lower toxicity and immunogenicity.<sup>5, 6</sup> There is a wide variety of polysaccharides available and they can be classified according to their biological functions, i.e. (1) storage polysaccharides, which include starches and glycogen, (2) structural polysaccharides, which can be classified as cellulose and chitin polysaccharides; (3) acidic polysaccharides, which are polysaccharides that contain carboxyl-, phosphate-, and/or sulphuric ester groups, and (4) bacterial polysaccharides, which include peptidoglycan and lipopolysaccharides to name a few.<sup>7, 8, 9</sup>

##### 2.1.1 Hyaluronic Acid: Structure and Properties

The naturally derived polysaccharide that will be the focus of this dissertation is hyaluronic acid (also known as HA, hyaluronan or hyaluronate). HA has excellent biocompatibility as

well as biodegradability, and has received widespread attention in the biomedical and cosmetic industries. The reason for the interest in HA is that it occurs naturally in human tissue and promotes cell motility and differentiation and allows for accelerated wound healing.<sup>10, 11</sup> From a cosmetic point of view HA plays an important role due to its moisture retention capabilities.<sup>10</sup> From a formulation point of view unmodified HA is a good polysaccharide to work with since it is 100% water soluble.<sup>10, 12</sup>

The word hyalos is derived from Greek, which means vitreous. The first extraction of HA was achieved in 1934 by Meyer and Palmer when they discovered it in the vitreous humour of cattle eyes.<sup>13, 14</sup> Hyaluronic acid, a glucosaminoglycan (GAG), is a linear polysaccharide with alternating disaccharide units of  $\beta$ -(1–4)-D-glucuronic acid (GlcA) and  $\beta$ -(1–3)-N-acetyl-D-glucosamine (GlcNAc)<sup>13, 15, 16</sup> (see **Figure 2.1**). These repeat units are  $\beta$ -linked in the polymer backbone, because of the stereochemistry of the acetal group formed when joining the GlcA unit with the GlcNAc unit. The  $\beta$  position refers to the position of the –OH group (of the individual disaccharide units) in relation to the anomeric carbon. The anomeric carbons in the HA repeat unit are labelled as position 4 of the GlcA unit and position 1 of the GlcNAc unit (**Figure 2.1**). As can be seen from **Figure 2.1**, the glycoside linkage is in the equatorial position, hence its known as a  $\beta$  linkage.<sup>17</sup> The average molar mass (MM) of naturally occurring HA is fairly high and varies between about  $10^5$ – $10^7$  g/mol, which relates to its random-coil conformation, occupying a large hydrodynamic volume in solution.<sup>13, 18–21</sup> HA also has the tendency to form a vast hydrogen bond network structure in aqueous media, which is due to the strong affinity between the alcohol (–OH), acetamido (–CO–NH–) and carboxyl (–COOH) groups and water molecules (see **Figure 2.2**).<sup>19</sup>

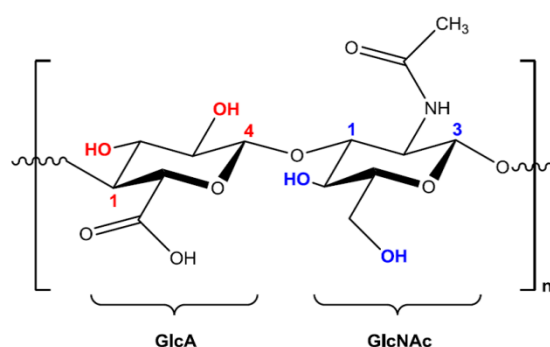


**Figure 2.1:** Schematic illustration of the repeat unit in hyaluronic acid (HA).

HA is generally extracted from rooster combs, bovine vitreous or umbilical cords. However, the extraction of HA from these sources is an expensive procedure and is not a viable option from an economical and ethical point of view. It also has the drawback that it is associated



with some undesirable proteins, which could have negative effects on certain applications. This has led to the exploration of alternative ways to produce HA. It is being produced on an industrial scale at a lower price with good yield and high purity by the bacteria *Streptococcus zooepidemicus* and *Streptococcus equi*.<sup>10</sup>

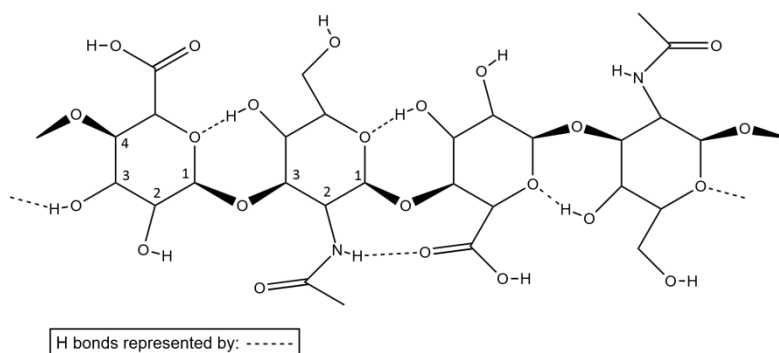


**Figure 2.2:** Schematic illustration of the hydrogen bonds of HA in water.

Taking a closer look at the solubility of the HA molecule, one needs to consider the electrostatic interactions and conformations of charged molecules. These interactions play a pivotal role in polymer conformations due to electrostatically induced stiffening and swelling. Furthermore, the strength and range of these interactions can be controlled by changing the salt concentration of the solution. Salt ions screen long-range electrostatic repulsion between ionized groups on the polymer backbone, reducing chain swelling and bending rigidity. One of the most widely used measures to describe/quantify conformations of a polymer in solution is the persistence length ( $L_p$ ), since it lends insight into the polymer's functional properties. Rinaudo<sup>10</sup> found the intrinsic persistence length of HA at 25 °C to be 7.5 nm. Rinaudo has also shown that the chain rigidity is described by the  $L_p$ , and decreases at elevated temperatures due to the disruption of the hydrogen bond network.<sup>10, 22</sup> It has also been found by Balazs<sup>23</sup> that when progressively decreasing the pH of a HA solution, a gel is formed at a pH of around 2.5 as a result of decreased carboxylate dissociation, which in turn favours hydrogen bond formation. If the pH is then further decreased it causes a gel-sol transition; this transition may possibly be ascribed to the protonation of the acetamido groups, which then causes electrostatic repulsion.<sup>10, 22, 23</sup> The conformation and network structure of HA directly influences the rheological properties, which are important for applications such as viscosupplementation and viscosurgery.<sup>11</sup>

### 2.1.2 Hyaluronic Acid Derivatization

Unmodified HA has a modest application range. Derivatizing/modifying HA can yield new

products with different properties, and in turn expand the application range of HA. For the development of new biomaterials, HA is a good candidate due to its unique physicochemical properties, biodegradability and excellent biocompatibility, as mentioned before. HA is also unique among the glycosaminoglycan group, since it is non-sulfated and not covalently bound to a polypeptide (depending on the source). Some strategies for the modification of HA include esterification, acrylation and crosslinking using divinylsulfone and/or glycidyl ether.<sup>11, 24–30</sup> Esterification reactions with benzylic acid result in an increased hydrophobicity of the HA molecule and have been used to produce a variety of different materials such as sponges, films and micro-perforated films.<sup>10, 31</sup> When derivatizing HA, the general reaction route is that of an esterification reaction on the GlcA and GlcNAc monosaccharide units, where the –COOH or –OH groups are targeted. In a fairly recent publication by Mravec et al.<sup>32</sup> the authors specifically targeted the secondary hydroxyls of the GlcA and GlcNAc monosaccharide units. This modification left all the –COOH groups free, and enabled a higher degree of substitution (DS) to be achieved.<sup>32</sup> However, when modifying HA the physical properties are also altered, which generally results in a decreased water solubility. The introduction of certain functional groups onto the HA molecule, such as amino groups, has also received great interest, since it enables further crosslinking or coupling reactions under relatively mild physiological conditions.<sup>11</sup> Another important chemical modification of HA is the carbodiimide modification with adipic acid dihydrazide (ADH). This modification provides multiple pendant hydrazide groups, which can then be further functionalized by different molecules such as crosslinking agents or alkyl chains.<sup>10, 33–36</sup> In a publication by Creuzet et al.,<sup>37</sup> they developed a new method for the chemical modification of HA-ADH by alkylation. This modification led to an amphiphilic polymer which, in the presence of an aqueous solution, associates to form a physical gel.<sup>37</sup> A detailed discussion of the different chemical modifications of HA can be found in the review article by Schanté et al.<sup>38</sup>

In literature the crosslinking reaction of HA gets a significant amount of attention, since it provides for a relatively simple development of biomaterials and plays a pivotal role in biomedical applications. Some of the first crosslinkers used to produce hydrogels are divinylsulfone, bisepoxide and glutaraldehyde. In a study carried out by Burdick et al.<sup>39</sup> HA was modified with methacrylic anhydride (MAA), which was then followed by the photopolymerization of the MAA to form a covalent network structure.<sup>39</sup> Highly crosslinked HA is generally used in dermatology and wrinkle folding as a filler, whereas linear HA is generally used in cosmetics to preserve tissue hydration and to facilitate ion, solute as well as nutrient transport.<sup>10</sup> The polysaccharides in this dissertation are linear HA.

The derivatized HA samples used in this work were synthesized by L'Oréal (Paris, France). For the derivatization of HA, L'Oréal performed the chemical modifications on the –OH groups. Looking at the HA molecular structure, it has four possible –OH groups available for chemical modification via esterification (see **Figure 2.1**). The degree to which chemical modification can take place on the HA repeat unit is defined as the degree of substitution (DS), which is governed by the average number of substituted –OH groups per repeat unit (**Equation 2.1**):

$$DS = \frac{\text{Number of Substituted -OH Groups}}{\text{Number of HA Repeat Units}} \dots \text{Equation 2.1}$$

Thus, the DS values for HA can have values of 0–4. For example, if a modified HA molecule has a DS of 2, then half of –OH groups are functionalized while the other half remain unsubstituted.

The suitability of HA for a given application is predominantly governed by its properties, which depend on the type of substituents and the DS. Palumbo et al.<sup>40</sup> linked HA to polylactic acid (PLA) and showed how the average DS influences the physicochemical properties of the HA–PLA derivatives. In one case they had a HA–PLA derivative with a low DS of 1.5 mol%, which in an aqueous medium showed a clear tendency to form more compact coils than HA. This was ascribed to the strong hydrophobic interaction of the PLA chains. On the other hand they had a HA–PLA with a higher DS of 7.85 mol% which showed a decreased affinity towards an aqueous medium, the sample was insoluble in the aqueous medium due to strong ionic interactions, and behaved like a gel when dispersed in water. However, it was soluble in dimethyl sulfoxide (DMSO).<sup>40</sup>

Taking the –OH groups on the HA repeat unit into consideration, they consist of one primary alcohol and three secondary alcohols. The rate of –OH group substitution is then as follows: the primary alcohol will normally be substituted first, since it is more reactive as a result of lower electron density, followed by the sterically hindered more electron-dense secondary alcohols. When derivatizing HA, the reaction sites on the HA repeat unit have different degrees of accessibility. This results in differences in the substitution distribution on the polymer microstructure. The substitution distribution can be classified into two groups: (1) first order heterogeneity, which refers to the substitution distribution among the polymer chains and (2) second order heterogeneity, which refers to the substitution distribution along the polymer chain (see **Figure 2.3**).

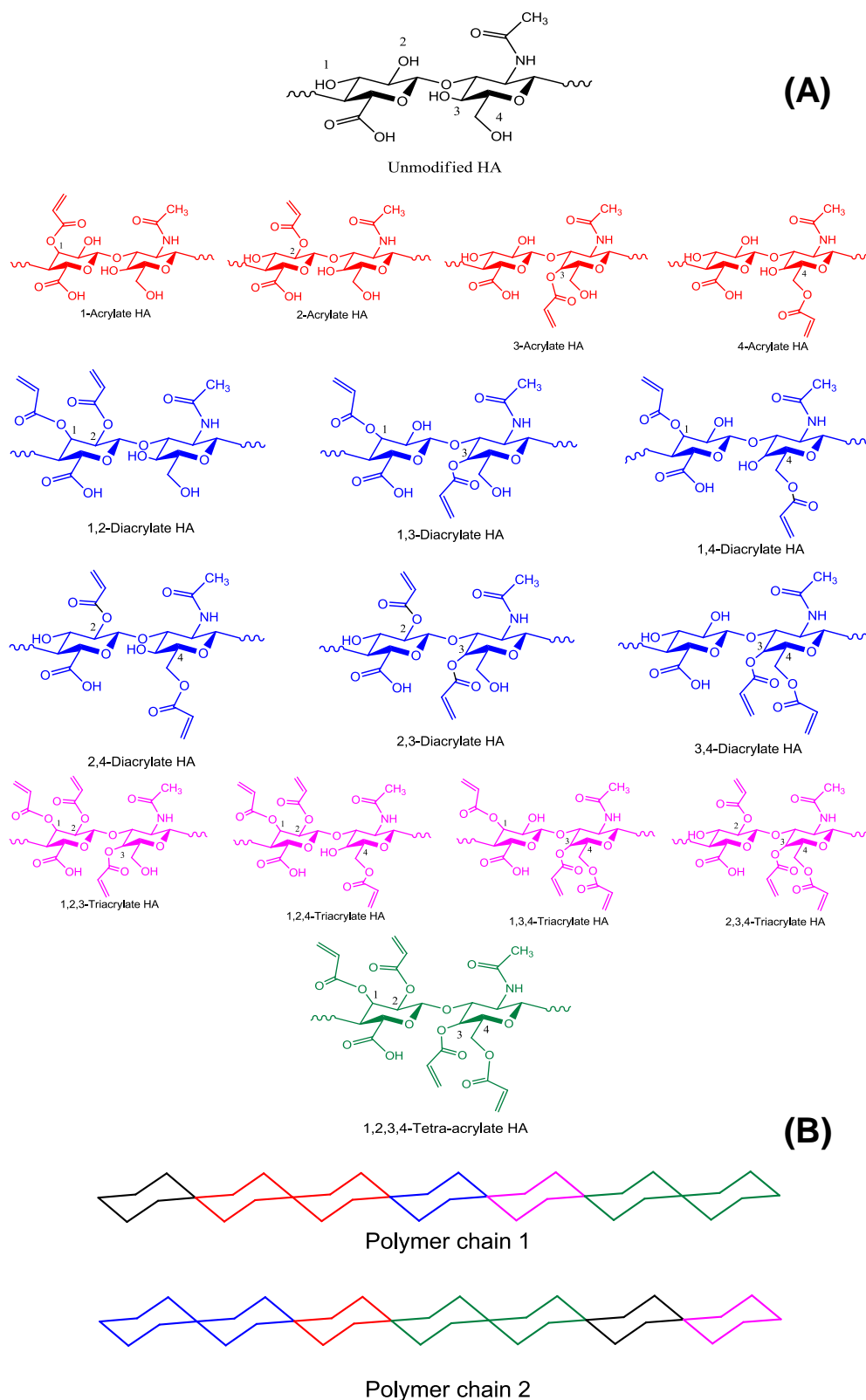


**Figure 2.3:** Illustration of the (A) sixteen different substitution patterns of HA and (B) chemical heterogeneity among polymer chains (1<sup>st</sup> order) and along the polymer chain (2<sup>nd</sup> order).

Derivatized HA, like all synthetic polymers, consists of a mixture of molecules with different chain lengths. The variation of the molar mass of derivatized HA has an influence on the material properties, for instance high molar mass derivatized HA can be used as a hydrogel, whereas low molar mass derivatized HA can be used as a drug delivery system.<sup>24, 25, 27–29</sup> Therefore, the molar mass (MM) and molar mass distribution (MMD) need to be investigated. Kim et al.<sup>41</sup> showed that the apparent average MM of the sodium salts of HA (Na-Ha) increased as the ionic strength of the Na-HA solution was decreased. They ascribed this to enhanced entanglement (aggregation) of the HA molecule. They achieved this conclusion using flow field-flow fractionation coupled to multi-angle laser light scattering (FIFFF-MALLS).<sup>41</sup>

However, derivatized HA obtained from the same parent material with the same MM and chemical composition (CC) can vary significantly in performance when being applied to a specific application. Thus, the influence of the substituent distribution (chemical heterogeneity) and its correlation to the MM need to be investigated. Therefore, from a product development point of view, it is crucial to understand the structure/property correlations of derivatized HA to establish its applications. Thus a comprehensive characterization needs to be conducted on the samples to retrieve three vital pieces of information, which are (1) molar mass distribution, (2) DS and (3) chemical composition and/or heterogeneity.

### **2.1.3 Hyaluronic Acid Derivative Characterization**

Polysaccharides are highly complex natural polymers that are distributed with regard to molar mass, degree of substitution and type of substituents on the monomeric, oligomeric as well as on the polymeric microstructure level.

HA derivatives are mainly characterized in terms of MM, MMD, average DS and chemical composition distribution (CCD). The average DS can be determined by a variety of methods, which include elemental and functional group analysis,<sup>32</sup> NMR<sup>42</sup> and MALDI-MS<sup>43</sup>. The method utilized for the determination of the average DS depends on the nature of the substituents. Size exclusion chromatography (SEC) is the routine technique employed for the determination of MM and MMD and is also applied to HA derivatives, since it is a fairly straightforward and a relatively fast analytical procedure.

As shown by Mravec et al.,<sup>32</sup> a higher DS is possible when modification is performed on the secondary hydroxyl groups. In their study they conducted a comprehensive analysis on the aggregation behaviour of sodium hyaluronate and its novel alkyl derivatives with the aid of a fluorescence probe. These derivatives show surfactant-like aggregation behaviour in aqueous solution and the critical aggregation concentration (CAC) depends on the MM and DS of the derivatized HA.<sup>32</sup>

Oudshoorn et al.<sup>42</sup> synthesized methacrylated hyaluronic acid with a tailored DS. Because of overlapping peaks in the <sup>1</sup>H-NMR spectra they used reversed phase (RP) high performance liquid chromatography (HPLC) to determine the DS. They hydrolysed the polymer-bound methacrylate groups under alkaline conditions and successfully determined the DS of the attached methacrylate moieties.<sup>42</sup>

Furthermore, Zawko et al.<sup>43</sup> determined the DS of HA functionalized with  $\beta$ -cyclodextrin with the aid of matrix-assisted laser desorption/ionization mass spectrometry (MALDI-MS) and <sup>1</sup>H-NMR spectroscopy.<sup>43</sup>

SEC is being coupled more frequently with light scattering detection, e.g. the multi-angle laser light scattering (MALLS) detector, to gain more reliable MM values. The major advantage of coupling SEC with MALLS is that absolute molar masses can be determined. These values are not dependent on a change in the hydrodynamic volume which occurs after HA functionalization, and in turn do not lead to inaccurate data interpretation.<sup>38</sup>

Intensive studies have been conducted on finding an appropriate solvent system that would fully dissolve the supramolecular structure for both unmodified and modified HA, depending on the substituent used for derivatization.<sup>38</sup> As mentioned before, HA forms a vast hydrogen bond network in aqueous solutions, so analysis in solution as with chromatographic techniques, especially SEC, is problematic. The aggregation of the polymer backbone causes inaccurate measurements regarding qualitative and quantitative information. In addition, when derivatizing HA with polylactic acid, it tends to become less soluble in aqueous media as shown by Palumbo et al.<sup>40</sup> A variety of solvents and/or solvent systems have been established to fully dissolve unmodified HA. The majority of these solvent systems consist of pure water in the presence of a salt, typically sodium chloride (NaCl), since the salt acts as a hydrogen bond disrupter and inhibits hydrogen bond networks.<sup>40</sup> However, challenges still remain in finding appropriate solvent systems when HA are being functionalized with certain moieties, since HA modification mainly results in a decreased water solubility.<sup>44–46</sup>

Pravata et al.<sup>47</sup> utilized SEC-MALLS to determine the conformational structure of amphiphilic lactic acid oligomer-hyaluronan conjugates in an aqueous medium. Their solvent system consisted of a phosphate buffer containing 0.15M NaCl and sodium azide (NaN<sub>3</sub>) to eliminate aggregation. They showed that Na-HA adopts a random coil conformation in aqueous solutions. They also verified that HA functionalized with oligomers of lactic acid (OLA) had a decreased affinity towards water. The hydrophobic interactions of the OLA chains led to the formation of aggregates, causing compact conformations to occur.<sup>47</sup>

When combining SEC with light scattering (LS) detectors it also allows for the retrieval of more information with regard to aggregation of polymers in solution, especially the degree of aggregation, which is not always possible when using just a concentration sensitive detector such as RI. Chang et al.<sup>48</sup> separated polysaccharides according to their MM and MMD with the aid of size exclusion chromatography in conjunction with a MALLS detector (SEC-MALLS). The MALLS detector allowed for the direct analysis of the MM of the polysaccharides. They also showed with the hyphenated technique used, that the polysaccharides are prone to aggregation.<sup>48</sup> It is also possible to determine, in parallel with MM and MMD determinations, the chemical composition of macromolecules in SEC. Several studies have demonstrated this by using nuclear magnetic resonance (NMR) spectroscopy and Fourier-transform infra-red (FTIR) spectroscopy as opposed to ultraviolet (UV) spectroscopy.<sup>49-51</sup>

Gradient HPLC is well known for its ability to separate (co)polymers according to chemical composition and to allow the determination of the chemical composition distribution.<sup>52, 53</sup> Only few successful attempts to separate HA itself, different derivatives thereof or derivatives according to the DS have been reported in literature. One rare example is the study of Finelli et al.<sup>54</sup> who employed HPLC/fluorimetry in their study on the gel-like structure of a hexadecyl derivative of HA. They used a method with a mobile phase consisting of MeOH/H<sub>2</sub>O (95/5) to determine the degree of amide substitution on their derivatized HA's.<sup>54</sup>

In the forthcoming sections, a detailed description will be given regarding the theoretical aspects of liquid chromatography.

## **2.2 High Performance Liquid Chromatography (HPLC)**

HPLC is one of the most powerful fractionation tools for modern polymer analysis. This is ascribed to its high throughput, accuracy and versatility. Different operational modes allow the characterization of many desired polymer properties, such as molar mass, chemical

composition, functionality or molecular architecture. HPLC is mainly employed as a separation tool, and the fundamental principles for separation in any liquid chromatographic (LC) technique are based on the selective distribution of analytes between the stationary and mobile phases. Separation results in different retention times for the components in a given sample. An analytes' retention time is governed by its adsorption or partition equilibria between the mobile and stationary phases. This distribution is defined by the distribution (or partition) coefficient,  $K_d$ :<sup>55</sup>

$$K_d = \frac{c_{SP}}{c_{MP}} \dots\dots\dots \text{Equation 2.2}$$

where  $c_{SP}$  and  $c_{MP}$  are the concentrations of the analyte in the stationary and mobile phases, respectively. In liquid chromatography the separation process can be described by the following equation:

$$V_e = V_i + V_p K_d \dots\dots\dots \text{Equation 2.3}$$

where  $V_e$  describes the retention volume of the solute,  $V_i$  the interstitial column volume,  $V_p$  is the pore volume of the packing, better defined as the stationary phase volume. The analyte, in both the mobile and stationary phases, is thermodynamically related to the difference in the Gibbs free energy ( $\Delta G$ ) and the distribution coefficient ( $K_d$ ).<sup>52, 53</sup> The change in the Gibbs free energy can be caused both by the change in the enthalpic ( $\Delta H$ ) and entropic ( $\Delta S$ ) contributions, due to interaction of the analyte with the stationary phase and limited pore dimension not allowing the analyte to occupy all possible conformations, respectively. The dependence of the distribution coefficient on these contributions can be expressed as follows:

$$\Delta G = \Delta H - T\Delta S = -RT \ln K_d \dots\dots\dots \text{Equation 2.4}$$

After mathematical rearrangement,  $\ln K_d$  can be expressed as follows:

$$\ln K_d = \frac{\Delta G}{-RT} = \frac{\Delta S}{R} - \frac{\Delta H}{RT} \dots\dots\dots \text{Equation 2.5}$$

where  $\Delta G$  is the difference in Gibbs free energy,  $\Delta H$  and  $\Delta S$  are the changes in enthalpy and entropy, respectively. T is the absolute temperature and R the universal gas constant. The change in the Gibbs free energy may be a result of the following: (1) the pores of the



stationary phase, having limited dimensions, cannot occupy all the possible conformations of the macromolecule, and as a result will decrease the conformational entropy ( $\Delta S$ ), and (2) when the analytes enter the pores of the stationary phase, they may have an affinity for the pore walls, and result in a change in the enthalpy ( $\Delta H$ ).<sup>56, 57</sup> Depending on the choice of the chromatographic system and chemistry of the analyte, either entropic or enthalpic interactions or even both may be at work. The general case for the distribution coefficient can be expressed as follows:

$$K_d = K_{SEC}K_{LAC} \dots\dots\dots\text{Equation 2.6}$$

Where  $K_{SEC}$  and  $K_{LAC}$  refer to entropic and enthalpic interactions, respectively. If the contribution of either the entropic or enthalpic interactions overrides the other, the overriding interaction will determine the operational mode for example, if entropic contributions are the dominating factor, the size exclusion mode will dominate the separation mechanism. It is also possible to express the retention volume in a time scale instead of a volume, since the retention time,  $t_R$ , is related to the retention volume,  $V_e$ , by the flow rate value of the mobile phase,  $F$ , as shown in **Equation 2.7**:

$$t_R = \frac{V_e}{F} \dots\dots\dots\text{Equation 2.7}$$

Even though both the retention time and retention volume can be used in analyte retention determination, it is more convenient to use the retention volume ( $V_e$ ) because the retention volume enables the direct comparison of results obtained on the same chromatographic system but at different flow rates. This becomes particularly useful when comparing results obtained from a one-dimensional chromatographic system with a two-dimensional chromatographic system.

The different operation modes in HPLC consist of **Size Exclusion Chromatography (SEC)**, **Liquid Adsorption Chromatography (LAC)** and **Liquid Chromatography at Critical Conditions (LC-CC)**, which all depend on the choice of the mobile and stationary phases as well as the temperature. The modes differ with regard to their dependence of the elution volume on molar mass (see **Figure 2.4**).

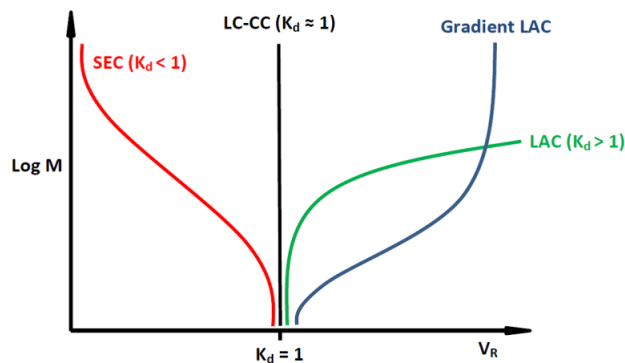


**Figure 2.4:** Schematic illustration of the chromatographic behaviour of elution volume dependence on the molar mass in SEC, LC-CC, LAC and gradient LAC mode.

In the forthcoming sections each HPLC operational mode will be discussed with regard to their basic principles and as potential polymer analysis tools.

### 2.2.1 Size Exclusion Chromatography (SEC)

SEC enables the separation of molecules according to their size in solution (hydrodynamic volume). The hydrodynamic volume of a given molecule is related to its radius of gyration ( $R_g$ ), which can differ with regard to the shape and hydration, and is directly related to the molar mass and molar mass distribution. The stationary phase consists of a rigid structure containing porous particles with a defined pore size distribution. The separation of a given molecular size range is governed by the pore size and pore size distribution of the packed particles. The mobile phase should be a thermodynamically good eluent for the polymer in order to avoid non-exclusion effects e.g. avoiding any form of enthalpic interaction between the stationary phase and the analyte.<sup>58</sup> The separation mechanism in SEC is governed by entropic contributions.

In ideal SEC, the only contributing factor in the separation mechanism would be the entropic contribution and no enthalpic contributions, thus, separation will only be governed by the hydrodynamic volume of the molecules with no additional interaction between the stationary phase and the polymer molecules (i.e.  $\Delta H = 0$ ). **Equation 2.8** describes the distribution coefficient,  $K_d$ , in ideal SEC separations:

$$K_{SEC (ideal)} = \exp \left[ \frac{(\Delta S)}{R} \right] \dots \dots \dots \text{Equation 2.8}$$

The distribution coefficient ranges from  $0 < K_{SEC} < 1$ , due to  $\Delta S < 0$ . The retention in 'ideal' SEC is also temperature independent. Therefore, the smaller the molecules separated in SEC, the more pore volume they can penetrate and the longer they are retained in the porous stationary phase (due to less severe change/loss in conformational entropy and easier re-establishment of thermodynamic equilibrium). Thus, from the distribution coefficient, it is clear that larger molecules will not be retained as much as their smaller counterparts, and in some cases will be excluded from the porous particles, due to a more severe change in conformational entropy and unfavourable thermodynamic equilibria and would, therefore, be eluted first, followed by the smaller molecules.<sup>59</sup> The retention volume for ideal SEC can be described by the following equation:

$$V_e = V_i + V_p K_{SEC} \dots \dots \dots \text{Equation 2.9}$$

To measure the MM, SEC is normally calibrated with well defined, narrowly distributed polymer samples (calibration standards). From the resulting chromatograms, two unique types of average molar masses are calculated; the number-average molar mass ( $\overline{M}_n$ ) and the weight-average molar mass ( $\overline{M}_w$ ).  $\overline{M}_n$  is related to the ordinary arithmetic MM of the polymeric chains and  $\overline{M}_w$  is related to the average MM of the polymeric chains, and are defined by **Equations 2.10** and **2.11**, respectively. The MMD, referring to the relationship between the number of moles of each polymer species ( $N_i$ ), and the molar mass ( $M_i$ ) of that species, is generally described by the dispersity index ( $\mathfrak{D}$ ), which is calculated from the two unique molar masses obtained by SEC. A  $\mathfrak{D}$  equal to 1, related a monodispersed sample (e.g. proteins), would mean that all the polymer chains are of the same length and MM, which is related to uniformity. It is not possible to obtain a value lower than 1 for  $\mathfrak{D}$ , since  $\overline{M}_w$  is always  $\geq \overline{M}_n$ , therefore  $\mathfrak{D} \geq 1$ . Thus, the higher the  $\mathfrak{D}$ , the broader the MMD. The following equations describe how the  $\overline{M}_n$ ,  $\overline{M}_w$  and  $\mathfrak{D}$  are determined mathematically:

$$\overline{M}_n = \sum_i N_i M_i / \sum_i N_i \dots \dots \dots \text{Equation 2.10}$$

$$\overline{M}_w = \sum_i N_i M_i^2 / \sum_i N_i M_i \dots \dots \dots \text{Equation 2.11}$$

$$\mathfrak{D} = \frac{\overline{M}_w}{\overline{M}_n} \dots \dots \dots \text{Equation 2.12}$$

where  $N_i$  is the number of molecules and  $M_i$  is the molar mass of a given chain length.

In order to avoid the use of a calibrant to extrapolate MM data, a molar mass sensitive detector e.g. a multi-angle laser light scattering detector (MALLS) can be employed to determine the absolute MM's and MMD's. SEC-MALLS will be explained in section 2.3.2.

SEC offers a variety of benefits as a separation tool, making it an attractive method for both preparative and analytical applications. However, certain limitations are also associated with SEC. It has three major drawbacks as analytical tool: (1) its separation ability is fairly modest when compared to that of LAC or LC-CC; (2) SEC has a low capacity with regard to volume- and mass-loading; (3) SEC has limited (shorter) column lifetime, especially for silica-based columns compared to interactive chromatography.<sup>60-62</sup>

### 2.2.2 Liquid Adsorption Chromatography (LAC)

In LAC the separation mechanism is based on adsorptive interactions of the analyte molecules with the stationary phase, i.e. the affinity of the analyte towards the given functional groups on the stationary phase. Since the separation mechanism in LC is mainly governed by  $G$ , the so-called interaction or affinity is related to that of the enthalpic contribution. LAC was originally developed for the separation of smaller molecules; however, it is now being employed regularly for the separation of macromolecules according to their chemical composition distribution. In LAC the involvement of the entropic term in the separation mechanism is over-powered by the adsorptive interaction forces associated with  $\Delta H$ . In this mode of HPLC, it allows only certain types of molecules (with specific chemical compositions) are susceptible to adsorption to the stationary phase depending on the conditions.<sup>54</sup>

In ideal LAC separations, only the  $\Delta H$  contribution plays a role, since it is assumed that the pores in the stationary phase are of sufficient size to accommodate all polymeric substances, therefore the entropic contributions are neglected ( $\Delta S = 0$ ). **Equation 2.13** describes the distribution coefficient,  $K_d$ , in ideal LAC separations:

$$K_{LAC (ideal)} = \exp \left[ \frac{(-\Delta H)}{RT} \right] \dots \dots \dots \text{Equation 2.13}$$

The values of the distribution coefficient is  $K_{LAC} > 1$ , due to  $\Delta H < 0$ .

The retention factor associated with the separation mechanism is sometimes described by Martin's rule.<sup>55</sup> Martin's rule states that an increasing number of repeat units of a certain

chemical composition, showing affinity for the stationary phase, will result in an exponential increase in the retention factor.

LAC is mainly used for the separation of smaller molecules, however, when compared to macromolecules, their retention behaviour differs significantly. In the analysis of chemically homogeneous macromolecules, with reference to Martin's rule, retention increases with the number of interacting repeat units along the polymer backbone. Therefore, if a certain functional group on the repeat unit shows an affinity toward the column, an increase in the number of repeat units will increase the  $K_d$  value significantly, and will result in increased retention volumes. This behaviour can better be defined as a multiple attachment mechanism.<sup>63–65</sup> Thus, higher molar mass species will be retained longer on the chromatographic column as opposed to smaller molar mass species with the same chemical composition, if the repeat unit has an affinity towards the column. Therefore, the inverse separation mechanism is observed for LAC when compared to SEC (**Figure 2.4**). In addition to adsorptive interactions, macromolecules can undergo large conformational variations, which allows for the existence of entropic contributions. With the latter being mentioned, the effective enthalpic contribution remains the overriding factor in the separating mechanism ( $\Delta H \gg T\Delta S$ ). Therefore, the overall  $K_d > 1$ .<sup>53</sup>

When performing isocratic LAC separations on high molar mass species, it is only possible to achieve effective separation in a very small window of interaction strength. In other words, repeat units with weak column interactions can result in very high retention volumes for high MM species, and a minute deviation in the mobile phase composition can have a tremendous effect, i.e. it can cause the polymeric species to go from complete retention to complete desorption with respect to the chromatographic column. This does not occur readily for low MM species. As a result isocratic LAC is generally used for the analysis according to chemical composition of lower molar mass (oligomeric) polymers.<sup>66, 67</sup>

Since isocratic LAC is not the recommended analytical approach for the analysis of high molar mass species according to their chemical composition, it led to the development of gradient LAC, which is more suited for the separation of macromolecules according to their CC. Gradient LAC will be discussed in section 2.2.4.

### **2.2.3 Liquid Chromatography at Critical Conditions (LC-CC)**

The separation mechanism in LC-CC is based on selectively separating molecules with the same chemical composition, irrespective of their molar mass (MM). This can only be

achieved if the gain in enthalpic contributions ( $\Delta H$ ), as a result of adsorption, can exactly be compensated by that of the loss in entropic contributions ( $\Delta S$ ), as a result of exclusion from the porous particles on the stationary phase ( $\Delta H = T\Delta S$ ) (**Figure 2.5**).<sup>53, 68</sup> At the so-called critical adsorption point in LC-CC  $\Delta G = 0$  and the distribution coefficient approaches unity ( $K \approx 1$ ), irrespective of the pore size volume of the stationary phase and the MM of the given polymeric material. The distribution coefficient in LC-CC is expressed in **Equation 2.14**:

$$K_{LC-CC} = \exp\left(\frac{\Delta S}{R} - \frac{\Delta H}{RT}\right) \dots\dots\dots \text{Equation 2.14}$$

At the critical point of adsorption the MMD of polymeric materials becomes so-called 'chromatographically invisible' and the separation mechanism is governed by the different types of chain heterogeneities (e.g. the number and type of functional groups, their geometric positioning on the chain, and chain topology).<sup>69-74</sup>

The LC-CC mode is based on the feature of polymer adsorption, which occurs as a second-order phase transition (which refers to the number of stationary phase binding sites that are limited), that take place in systems in which the monomer units are connected together as a flexible chain.  $\Delta S$  losses related to the chain arise from the imposed restrictions on the degree of freedom of the monomer units near the pore walls of the stationary phase, as well as the change in the  $\Delta G$  as a result of monomer interaction with the surface of the pores of the stationary phase.

The theory behind this mechanism was developed by Gorbunov and Skvortsov.<sup>75</sup> If critical conditions are used in non-functionalized homopolymers, the polymer molecules will elute at the same elution volume, regardless of their molar mass and chain length. To obtain the critical conditions for a given polymeric species is a difficult process, since this depends on the nature of the stationary phase, the temperature, flow rate as well as the eluent composition.<sup>76</sup> LC-CC is a very powerful separation tool if the correct conditions can be found for a given polymer species. Extensive research has been done on the establishment of critical conditions for a variety of polymeric species.<sup>77</sup> However, the application of LC-CC is often limited due to difficulties in establishing critical conditions for very complex polymeric species. Reproducibility is another challenge, because a slight variation of the eluent composition can have a crucial effect on the retention mode of separation (i.e. can change to either SEC or LAC mode).

### 2.2.4 Gradient LAC

In gradient LAC the mobile phase composition is changed as a function of time. Gradient LAC separates polymeric species by reducing the influence of the molar mass on the separation.<sup>78</sup> Gradient LAC works as follows; the polymeric species to be analysed are adsorbed onto the stationary phase, then polymeric species of similar chemical composition are eluted in the same separation slice by gradually increasing the mobile phase strength i.e. increasing polymer-mobile phase interactions and decreasing polymer-stationary phase interactions (**Figure 2.5**). In gradient LAC, smaller molecules elute before larger molecules due to less repeat units adsorbing to the stationary phase.<sup>79, 80</sup> Chang et al.<sup>81</sup> applied a temperature gradient, producing high resolution separations, which in turn increases the separation strength of gradient LAC when working with high molar mass species.<sup>81, 82</sup>

LAC can also be subdivided into two unique chromatographic modes namely normal-phase (NP) and reversed-phase (RP) chromatography. The combination of a polar stationary phase and a non-polar mobile phase is called NP chromatography. RP chromatography, however, uses a non-polar stationary phase and is employed with a polar mobile phase such as water and ethanol. The latter is more widely used nowadays since it allows for the separation of many samples of biological origin, pharmaceutical and/or medical interest (i.e. more complex molecules).<sup>55</sup>

Following the method for thin layer chromatography developed by Kamide et al.<sup>83</sup> to separate cellulose acetates (CA's) according to MM and DS, Ghareeb et al.<sup>84</sup> conducted a study on the separation of CA's by degree of substitution with NP chromatography. The separation was based on an adsorption-desorption mechanism and used a bare silica column as stationary phase and dichloromethane (DCM) and methanol (MeOH) in a multi-step gradient solvent system. The developed system allowed for the separation of CA's over a relatively wide DS range of DS = 1.5–2.9 which is more than reported for previous methods. The method developed by Ghareeb et al. was also able to allow for the determination of the DS distribution in which the CA chains are still intact over a wide DS range, which makes it one of the first results reported to have the CA chains intact in the DS determination.<sup>84</sup>

### 2.2.5 Detectors

The detection of a sample subjected to LC is one of the most crucial parts in the separation set-up, since without any means of detection, separation is of no use. The main qualities of a

good detector include: (1) it must have a high sensitivity, (2) respond to all the analytes or have a predictable preference, (3) must be reliable and versatile, (4) have a linearly increasing response with an increasing solute concentration, and (5) should preferably be non-destructive with regard to the solute.<sup>85</sup>

There are a variety of different instruments available for the detection of the analytes as they exit the chromatographic column. The detectors utilized in the identification of polymers can be subdivided into two main categories; (1) concentration sensitive detectors and (2) molar mass sensitive detectors (see **Table 2.1**).

**Table 2.1:** Categorization of LC detectors with regard to their applicability.<sup>53</sup>

Concentration sensitive detectors		Molar mass sensitive detectors
Selective detectors	Universal detectors	Viscometers:
UV detector	RI detector	Single capillary viscometer
IR detector	Conductivity detector	Differential viscometer
Fluorescence detector	Density detector	<b>Light scattering detectors:</b>
Electrochemical detector	Evaporative light scattering detector	LALLS, MALLS, MALLS3, TALLS, RALLS
<sup>1</sup> H-NMR detector		

Concentration sensitive detectors function on the basis of producing a signal (response) which is determined by the concentration of a given solute (analyte) in the mobile phase. In general, these types of detectors consist of spectroscopic detectors, which enable the detection of specific functional groups present in a polymeric substance. There are two main subdivisions of concentration sensitive detectors; selective and universal detectors (**Table 2.1**). When considering these two subdivisions, selective detectors only detect a certain property of the solute (analyte), whereas universal detectors generally detect a bulk property of a given mobile phase. It's of high importance to choose the appropriate detector when analysing polymeric substances. There are two major requirements when using concentration sensitive detectors: (1) the polymeric substance must contain certain functional groups for which these detectors are sensitive towards and (2) the functional groups of the polymeric substance should not absorb in the same wavelength region as mobile phase (solvent system).<sup>53</sup> The concentration sensitive detectors used in this work are RI and ELSD detectors. The RI detector will be explained in more detail in section 2.3.2.



Evaporative detectors such as the evaporative light scattering detector (ELSD) are widely used in LC and are very useful in gradient LAC. The ELSD operates on the following basis: it nebulizes the mobile phase exiting the column, followed by the evaporation of the solvent, any non-volatile product remaining, then becomes a particle which is driven through a light beam by a carrier gas. These particles will be detected by their scattering of a light beam, and the intensity of scattered light holds a direct relation to the detector signal, see **Figure 2.5**.<sup>86–89</sup> Because of the influence of several factors on the ELSD response, such as analyte structure and concentration, mobile phase composition and temperature, the signal is not directly proportional to concentration. Therefore, quantification is not always reliable and the data need to be interpreted with care.<sup>89–93</sup>

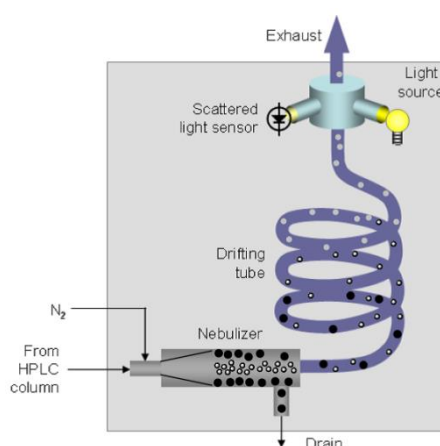


**Figure 2.5:** Schematic illustration of an ELSD (modified from reference 94).<sup>94</sup>

Molar mass sensitive detectors function on the basis of producing a signal (response), which relates to the molar mass as well as the concentration of a given solute in the mobile phase. Therefore, molar mass sensitive detectors have to be combined with concentration sensitive detectors. Light scattering (LS) detectors allow for the direct determination of the absolute molar mass (MM) of a polymeric species.<sup>95</sup> Molar mass sensitive detectors (see **Table 1**) are applied more frequently with SEC instruments, since concentration sensitive detectors require calibration (with calibration standards of known molar mass) to determine molar masses. However, this is a relative method and a degree of error is always associated with the obtained molar masses.<sup>53, 95</sup> The molar mass sensitive detector of choice for this work is the MALLS detector and will be explained in more detail in section 2.3.2.

### **2.3 Hyphenated Liquid Chromatography Techniques: Coupling with Chemically Selective or Molar Mass Sensitive Detectors**

When polymer molecules exit the column after separation according to a certain molecular parameter, they can be analysed by various detection methods, depending on the information required. The detection methods can be used in different modes, i.e. on-line detection as they exit the column, or off-line, where fractions are collected and analysed. Depending on the information required regarding the polymer molecules, they can be either chemically selective or molar mass sensitive detectors. For the purpose of hyphenating specific detectors with liquid chromatography in this study, the chemically selective and molar mass sensitive detectors of choice are an infrared (IR) and MALLS detector, respectively.

#### **2.3.1 Liquid Chromatography–Infrared Spectroscopy (LC-IR)**

In order to analyse complex molecules after separating them either according to molar mass or chemical composition, their bulk chemical properties must be known. A fast and reliable way to determine these properties is with IR spectroscopy. IR spectroscopy is a (chemically) selective method that enables the analysis of a large variety of molecules. It is a quantized process of the infrared radiation interaction between molecules, showcasing the molecular stretching and bending vibrational transitions and in turn providing characteristic information on the molecular structure.<sup>96</sup> IR spectroscopy can be used before the establishment of a suitable separation technique, such as gradient LAC, to determine the bulk chemical properties, and can then be used as a hyphenated technique after the separation of molecules as a means of specific detection and/or identification. It is also used to validate an established separation technique. LC-IR can be used in either on-line or off-line mode. However, when using it on-line it poses certain problems, such as poor signal-to-noise (S/N) ratio's, and poor IR transparency of most solvents.<sup>61, 95</sup> In order to avoid solvent interference in IR analysis, the use of off-line detection is the preferred choice. In off-line mode a two-step process is used: (1) a solvent elimination step with a LC-Transform interface is used to evaporate the solvent from the fractions collected after separation allowing for the deposition of the separated molecules in the form of a continuous film on a collection interface (e.g. an IR transparent Germanium disc), and (2) independent IR analysis of the fractionated samples.<sup>60</sup>

The solvent elimination process works as follows: the eluent exiting the LC column is directed to a heated nebulizer nozzle, which then sprays a fine mist of solvent onto a heated rotating interface (e.g. Germanium disc), which allows for the solvent to be evaporated and the polymer fractions to be deposited.<sup>95, 96</sup> The off-line IR analysis of the fractions then follows, where spectra can be obtained from any location on the collection interface (see **Figure 2.6**).

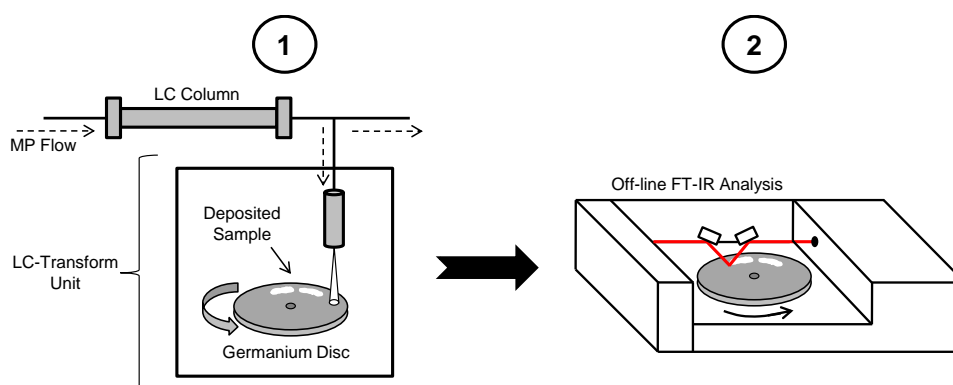


**Figure 2.6:** Schematic illustration of an LC-Transform coupling.

### 2.3.2 Size Exclusion Chromatography–Multi-Angle Laser Light Scattering (SEC-MALLS)

The use of calibration standards to estimate the MM of a given polymeric material is the so-called standard operating procedure in most laboratories. The reason is that it is relatively cheap and straightforward to use. However it has the intrinsic drawback that it is only a relative method, resulting in greater uncertainty with respect to the obtained molar mass and in effect does not represent the true/absolute molar mass of a given polymeric material.

This is where light scattering (LS) detectors play a major role in state-of-the-art laboratories, since they allow for the absolute MM and MMD determination of macromolecules over a relatively large molar mass range ( $10^3$ – $10^9$  g/mol). Taking the use of calibration standards into account, the chemical structure of the calibrant needs to be more or less equivalent to that of the sample being analysed to obtain more accurate results. However, this is not always possible with complex samples (with specific mention to natural samples), and LS detectors allow the determination of the MM and MMD without the need of a calibrant. There is a wide variety of LS detectors available; however, for the purpose of this study the LS detector of interest is the MALLS detector (see 'HPLC of Polymers' ref 37 pages 31–38 for a detailed description on the different detectors available). The MALLS detector can provide

reliable information on the root mean square (RMS) or radius of gyration ( $R_g$ ) of a polymer as well as information with respect to branching and polymer structure.<sup>61, 97–99</sup>

A MALLS detector is generally used in on-line mode, although, batch mode is also a possibility. In on-line mode the analyte passes through a light beam after the elution of the polymeric species from the SEC column into the MALLS detector. This results in the scattering of light, the intensity of light scattered is then measured at different angles ( $\theta$ ) simultaneously (see **Figure 2.7**). The measuring angles generally vary from about  $30^\circ$ – $150^\circ$ . The intensity of the scattered light at a given angle ( $\theta$ ), ( $I_\theta$ ) compared to the incident light ( $I_0$ ), for Rayleigh light scattering is given by the following equation:

$$\frac{I_\theta}{I_0} = \alpha\omega R_\theta \dots \dots \dots \text{Equation 2.15}$$

where  $\alpha$  is defined as the attenuation constant,  $\omega$  is the refractive index function and  $R_\theta$  is the Rayleigh constant.<sup>97</sup>

The molar mass ( $M_w$ ) of an analyte is related to  $R_\theta$  and is expressed as follows:

$$M_w = \frac{R_\theta}{c(K - 2A_2R_\theta)} \dots \dots \dots \text{Equation 2.16}$$

where  $c$  is the concentration of the analyte,  $A_2$  is the second virial coefficient defined as the polymer-solvent interaction and  $K$  is the polymer optical constant.

The MALLS detector sensitivity is defined as the minimum detectable excess Rayleigh ratio, which relates to the minimum detectable concentration of the analyte. The relationship between the scattered light intensity, scattering angle and the molecular properties of the analyte can be given by the following equation:

$$\frac{cK}{R_\theta} = 2cA_2 + \frac{1}{M_w P(\theta)} \dots \dots \dots \text{Equation 2.17}$$

where ( $P_\theta$ ) is defined as the dependence of the scattered light intensity on the angle of scattering. For small molecules, with a particle diameter of  $< \lambda/20$ , the intensity of the scattered light is independent of the scattering angle. The  $P_\theta$  value is then equal to 1. In the case where the particle diameter is  $> \lambda/20$ , the intensity of the scattered light is dependent on the scattering angle, and  $P_\theta \neq 1$ . Therefore when measuring analytes with a particle

diameter  $> \lambda/20$ , the scattering angle has to be considered. The radius of gyration ( $R_g$ ) of an analyte can be determined from the following equation where  $P_\theta$  can be given at a certain angle:

$$P(\theta) = 1 - \frac{16\pi^2}{3\lambda^2} \langle R_g^2 \rangle \frac{\sin^2\theta}{2} \dots \text{Equation 2.18}$$

where  $\lambda$  is the wavelength of the incident light in the solvent, which can be defined as the ratio of the incident wavelength and the refractive index of the solvent ( $\lambda = \lambda_0/n_0$ ).<sup>61, 97-99</sup>

The intensity of the scattered light holds a direct correlation to the concentration of the fractions, and in order to extrapolate the response of the LS detector into useable MM information a suitable concentration sensitive detector is also required to measure the concentration of each chromatographic fraction.<sup>61, 97-99</sup> The concentration sensitive detector utilized in this work is a refractive index (RI) detector, which is generally employed with a MALLS detector, since it enables the molar mass extrapolation of a given polymeric species. The detection principle of a RI detector is primarily based on the change in the refractive index ( $n$ ) between the mobile phase and the mobile phase containing polymeric analytes during the course of a chromatographic run. Another important feature is the refractive index increment ( $dn/dc$ ) of the polymeric analyte, which holds a direct correlation of the refractive index and concentration of the given analyte. The following equation describes the linear relationship between the refractive index and the concentration of the polymeric analyte:

$$\frac{dn}{dc} = \lim_{c \rightarrow 0} \left( \frac{n - n_0}{c} \right) \dots \text{Equation 2.19}$$

Looking at **Equation 2.19**,  $n$  is defined as the refractive index,  $n_0$  is defined as the refractive index of the solvent (mobile phase),  $c$  is the analyte concentration (g/mL) and  $dn/dc$  is the refractive index increment of the analyte.  $dn/dc$  is expressed as mL/g and has to be known in order to calculate absolute molar mass information of a given polymeric sample from the MALLS detector.<sup>97</sup>

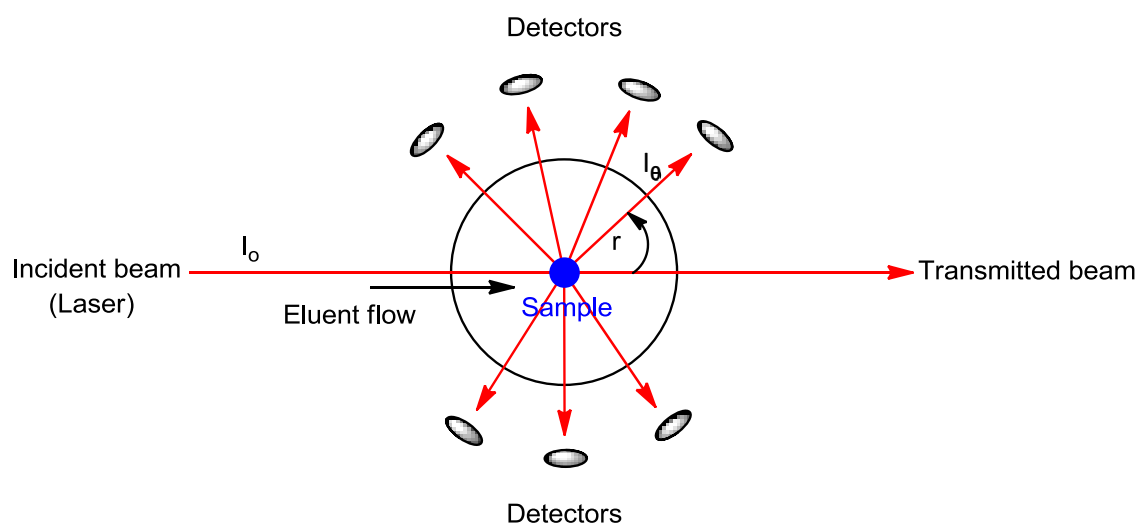


**Figure 2.7:** A simplified schematic illustration of a MALLS detector.

## References

- [1] Posocco, B.; Dreussi, E.; de Santa, J.; Toffoli, G. *Materials*. **2015**, *8* (5), 2569–2615.
- [2] Raemdonck, K.; Martens, T. F.; Braeckmans, K.; Demeester, J.; De Smedt, S. C. *Adv. Drug Deliv. Rev.* **2013**, *65* (9), 1123–1147.
- [3] Alvarez-Lorenzo, C.; Blanco-Fernandez, B.; Puga, A. M.; Concheiro, A. *Adv. Drug Del. Rev.* **2013**, *65* (9), 1148–1171.
- [4] Lapasin, R.; Prici, S. *Rheology of industrial polysaccharides: theory and applications*. Blackie Academic & Professional, London, **1995**.
- [5] Buschmann, M. D.; Merzouki, A.; Lavertu, M.; Thibault, M.; Jean, M.; Darras, V. *Adv. Drug. Deliv. Rev.* **2013**, *65* (9), 1234–1270.
- [6] Varma, A. J.; Kennedy, J. F.; Galgali, P. *Carbohydr. Polym.* **2004**, *56* (4), 429–445.
- [7] [www.newwordencyclopedia.org/entry/polysaccharide \(08/04/2015\)](http://www.newwordencyclopedia.org/entry/polysaccharide%20(08/04/2015))
- [8] Sutherland, I. W. *Biopolym.* **2002**, *5*, 1–19.
- [9] Ullrich, M. *Bacterial polysaccharides: Current innovations and future trends*. Caister Academic Press, Norfolk, UK, **2009**.
- [10] Rinaudo, M. *Polym. Int.* **2008**, *57* (3), 397–430.
- [11] Bulpitt, P.; Aeschlimann, D. *J. Biomed. Mater. Res.* **1999**, *47* (2), 152–169.
- [12] Maeda, N.; Miao, J.; Simmons, T. J.; Dordick, J. S.; Linhardt, R. J. *Carbohydr. Polym.* **2014**, *102*, 950–955.
- [13] Kupská, I.; Lapčík, L.; Lapčíková, B.; Žáková, K.; Juříková, J. *Colloids Surf., A.* **2014**, *454*, 32–37.
- [14] Meyer, K.; Palmer, J. W. *J. Biol. Chem.* **1934**, *107* (3), 629–634.
- [15] Orviský, E.; Šoltés, L.; Chabreček, P.; Novák, I.; Stančíková, M. *Chromatographia.* **1993**, *37* (1–2), 20–22.
- [16] Podzimek, S.; Hermannova, M.; Bilerova, H.; Bezakova, Z.; Velebny, V. *J. Appl. Polym. Sci.* **2010**, *116* (5), 3013–3020.
- [17] Clayden, G.; Warren, W.; Greeves, N.; Wothers, P. *Organic Chemistry*. Oxford University Press, New York, USA, **2001**, 1367.
- [18] Garg, H. G.; Hales, C. A. *Chemistry and biology of hyaluronan*. Elsevier, Oxford, UK, **2004**.
- [19] Haxaire, K.; Marechal, Y.; Milas, M.; Rinaudo, M. *Biopolymers.* **2003**, *72* (1), 10–20.
- [20] Maréchal, Y. *Faraday Discuss.* **1996**, *103*, 349–361.
- [21] Balazs, E. A.; Watson, D.; Duff, I. F.; Roseman, S. *Arthritis. Rheum.* **1967**, *10* (4), 357–376.
- [22] Gatej, I.; Popa, M.; Rinaudo, M. *Biomacromolecules.* **2005**, *6* (1), 61–67.
- [23] Balazs, E. A. *Fed. Proc.* **1965**, *25* (6), 1817–1822.
- [24] Yu-Jin, J.; Termsarasab, U.; Dae-Duk, K. *J. Pharm. Invest.* **2010**, *40*, 33–43.
- [25] Balazs, E. A.; Leshchiner, A. U.S. Patent No. 4,582,865. 15 Apr. **1986**.
- [26] Kuo, J. W.; Swann, D. A.; Prestwich, G.D. *Bioconjugate Chem.* **1991**, *2.4*, 232–241.
- [27] Illum, L.; Farraj, N. F.; Fisher, A. N.; Gill, I.; Miglietta, M.; Benedetti, L. M. *J. Controlled Release.* **1994**, *29* (1), 133–141.
- [28] Luo, Y.; Kirker, K. R.; Prestwich, G. D. *J. Controlled Release.* **2000**, *69* (1), 169–184.
- [29] Hahn, S. K.; Jelacic, S.; Maier, R. V.; Stayton, P. S.; Hoffman, A. S. *J. Biomater. Sci. Polymer Edition.* **2004**, *15* (9), 1111–1119.
- [30] Ohri, R.; Hahn, S. K.; Hoffman, A. S.; Stayton, P. S.; Giachelli, C. M. *J. Biomed. Mater. Res. Part A*, **2004**, *70* (2), 328–334.

- [31] Benedetti, L.; Cortivo, R.; Berti, T.; Berti, A.; Pea, F.; Mazzo, M.; Abatangelo, G. *Biomaterials*. **1993**, *14* (15), 1154–1160.
- [32] Mravec, F.; Pekař, M.; Velebný, V. *Colloid. Polym. Sci.* **2008**, *286* (14–15), 1681–1685.
- [33] Luo, Y.; Ziebell, M. R.; Prestwich, G. D. *Biomacromolecules*. **2000**, *1* (2), 208–218.
- [34] Prestwich G, Luo Y, Kirker K, Ziebell M, Shelby J. *Hyaluronan biomaterials for targeted drug delivery and wound healing*. In: Kennedy J, Phillipps G, Williams P, Hascall V, editors. *Hyaluronan: biomedical, medical, and clinical aspects*. Woodhead Publishing Limited, Cambridge, UK, **2002**, 277–284.
- [35] Davidson, J. M.; Nanney, L. B.; Broadley, K. N.; Whitsett, J. S.; Aquino, A. M.; Beccaro, M.; Rastrelli, A. *Clin. Mater.* **1991**, *8* (1), 171–177.
- [36] Kurisawa, M.; Chung, J. E.; Yang, Y. Y.; Gao, S. J.; Uyama, H. *Chem. Commun.* **2005**, (34), 4312–4314.
- [37] Creuzet, C.; Kadi, S.; Rinaudo, M.; Auzély-Velty, R. *Polymer*. **2006**, *47* (8), 2706–2713.
- [38] Schanté, C. E.; Zuber, G.; Herlin, C.; Vandamme, T. F. *Carbohydr. Polym.* **2011**, *85* (3), 469–489.
- [39] Burdick, J. A.; Chung, C.; Jia, X.; Randolph, M. A.; Langer, R. *Biomacromolecules*. **2005**, *6* (1), 386–391.
- [40] Palumbo, F. S.; Pitarresi, G.; Mandracchia, D.; Tripodo, G.; Giammona, G. *Carbohydr. Polym.* **2006**, *66* (3), 379–385.
- [41] Kim, B.; Woo, S.; Park, Y. S.; Hwang, E.; Moon, M. H. *Anal. Bioanal. Chem.* **2014**, 1–8.
- [42] Oudshoorn, M. H.; Rissmann, R.; Bouwstra, J. A.; Hennink, W. E. *Polymer*. **2007**, *48* (7), 1915–1920.
- [43] Zawko, S. A.; Truong, Q.; Schmidt, C. E. *J. Biomed. Mater. Res. Part A*, **2008**, *87* (4), 1044–1052.
- [44] Vermonden, T.; Censi, R.; Hennink, W. E. *Chemical Reviews*. **2012**, *112* (5), 2853–2888.
- [45] Zhao, C.; Sun, Y. L.; Amadio, P. C.; Tanaka, T.; Ettema, A. M.; An, K. N. *The Journal of Bone & Joint Surgery*. **2006**, *88* (10), 2181–2191.
- [46] Sadozai, K. K.; Kuo, J. W.; Sherwood, C. H. *U.S. Patent No. 6,548,081*. Washington, DC: U.S. Patent and Trademark Office, **2003**.
- [47] Pravata, L.; Braud, C.; Boustta, M.; El Ghzaoui, A.; Tømmeraas, K.; Guillaumie, F.; Vert, M. *Biomacromolecules*. **2007**, *9* (1), 340–348.
- [48] Chang, Y. W., Lu, T. J. *J. Food. Drug. Anal.* **2004**, *12* (1), 59–67.
- [49] Albrecht, A.; Brüll, R.; Macko, T.; Sinha, P.; Pasch, H. *Macromol. Chem. Phys.* **2008**, *209*, 1909–1919.
- [50] Kok, S.J.; Wold, C.A.; Hankemeier, T.H.; Schoenmakers, P.J. *J. Chromatogr. A*, **2003**, *1017*, 83–96.
- [51] Hatada, K.; Kitayama, T. *NMR Spectroscopy of Polymers*, Springer-Verlag, Berlin-Heidelberg, Germany, **2004**.
- [52] Glöckner, G. *Gradient HPLC of copolymers and chromatographic cross-fractionation*, Springer-Verlag: Berlin, Germany, **1991**.
- [53] Pasch, H.; Trathnigg, B.; *HPLC of Polymers*, Springer-Verlag: Berlin-Heidelberg, Germany, **1998**.
- [54] Finelli, I.; Chiessi, E.; Galesso, D.; Renier, D.; Paradossi, G. *Macromol. Biosci.* **2009**, *9* (7), 646–653.



- [55] Snyder, L.R.; Kirkland, J.J.; Dolan, J.W. *Introduction to Modern Liquid Chromatography*, Ed. 3; Wiley, New York, USA, **2010**.
- [56] Entelis, S.G.; Evreinov, V.V.; Gorshkov, A.V. *Adv. Polym. Sci.* **1986**, *76*, 129–175.
- [57] Raust, J. A. Development of multidimensional Chromatography for complex (METH) Acrylate-based Copolymers used in cosmetic Applications (Doctoral dissertation, Deutsches Kunststoff-Institut-TU Darmstadt), **2008**.
- [58] Barth, H. G.; Boyes, B. E.; Jackson, C. *Anal. Chem.* **1998**, *70* (12), 251–278.
- [59] Radke, W. *Macromol. Theory. Simul.* **2001**, *10* (7), 668–675.
- [60] Striegel, A.; Yau, W. W.; Kirkland, J. J.; Bly, D. D. *Modern size-exclusion liquid chromatography: practice of gel permeation and gel filtration chromatography*. John Wiley & Sons, Hoboken, New Jersey, USA, **2009**, 277–280.
- [61] Wu, Chi-San, ed. *Handbook Of Size Exclusion Chromatography And Related Techniques: Revised And Expanded*. Vol. 91. Marcel Dekker, Inc. New York, USA, **2003**.
- [62] Berek, D. *J. Sep. Sci.* **2010**, *33* (3), 315–335.
- [63] Glöckner, G.; van den Berg, J.H.M. *J. Chromatogr.* **1991**, *550*, 629–638.
- [64] Skvortsov, A.; Trathnigg, B. *J. Chromatogr. A*, **2003**, *1015* (1–2), 31–42.
- [65] Glöckner, G. *Adv. Polym. Sci.* **1986**, *79*, 159–214.
- [66] Trathnigg, B. *Encyclopedia of Anal. Chem.* John Wiley & Sons, Chichester, UK, **2000**.
- [67] Raust, J.-A.; Brüll, A.; Sinha, P.; Hiller, W.; Pasch, H. *J. Sep. Sci.* **2010**, *33* (10), 1375–1381.
- [68] Entelis, S.G.; Evreinov, V.V.; Kuzaev, A.I. *Reactive Oligomers*, Khimiya, Moscow, **1985**.
- [69] Gorshkov, A.V.; Much, H.; Becker, H.; Pasch, H.; Evreinov, V.V.; Entelis, S.G. *J. Chromatogr.* **1990**, *523*, 91–102.
- [70] Mengerink, Y.; Peters, R.; van der Wal, S.; Claessens, H.A.; Cramers, C.A. *J. Chromatogr. A*, **2002**, *949* (1–2), 337–349.
- [71] Berek, D.; Janco, M.; Hatada, K.; Kitayama, T.; Fujimoto, N. *Polym. J.* **1997**, *21* (12), 1029–1033.
- [72] Kitayama, T.; Janco, M.; Ute, K.; Niimi, R.; Hatada, K.; Berek, D. *Anal. Chem.* **2000**, *72* (7), 1518–1522.
- [73] Pasch, H.; Rode, K. *Polymer.* **1998**, *39* (25), 6377–6383.
- [74] Esser, K.E.; Braun, D.; Pasch, H. *Angew. Makromol. Chem.* **1999**, *271*, 61–67.
- [75] Skvortsov, A. M.; Gorbunov, A. A. *J. Chromatogr. A*, **1990**, *507*, 487–496.
- [76] Macko, T.; Hunkeler, D.; Berek, D. *Macromolecules*, **2002**, *35*, 1797.
- [77] Macko, T.; Hunkeler, D. *Adv. Polym. Sci.* **2003**, *163*, 61–136.
- [78] Philipsen, H.J.A. *J. Chromatogr. A*, **2004**, *1037*, 329–350.
- [79] Quarry, M. A.; Stadalius, M. A.; Mourey, T. H.; Snyder, L. R. *J. Chromatogr. A*, **1986**, *358*, 1–16.
- [80] Stadalius, M. A.; Quarry, M. A.; Mourey, T. H. Snyder, L. R. *J. Chromatogr. A*, **1986**, *358*, 17–37.
- [81] Cho, D.; Park, S.; Chang, T.; Avgeropoulos, A.; Hadjichristidis, N. *Eur. Polym. J.* **2003**, *39* (11), 2155–2160.
- [82] Ryu, J.; Park, S.; Chang, T. *J. Chromatogr., A*, **2005**, *1075* (1–2), 145–150.
- [83] Kamide, K.; Kunihiro, O. *Polym. J.* **1981**, *13* (2), 127–133.
- [84] Ghareeb, H. O.; Radke, W. *Polymer.* **2013**, *54* (11), 2632–2638.
- [85] Zhang, B.; Li, X.; Yan, B. *Anal. Bioanal. Chem.* **2008**, *390* (1), 299–301.

- [86] Lafosse, M.; Elfakir, L.; Morin-Allory, L.; Dreux, M. *J. High Res. Chromatogr.* **1992**, *15*, 312.
- [87] Rissler, R.; Fuchslueger, U.; Grether, H.J. *J. Liq. Chromatogr.* **1994**, *17*, 3109.
- [88] Brossard, S.; Lafosse, M.; Dreux, M. *J. Chromatogr.* **1992**, *591*, 149.
- [89] Oppenheimer, L.E.; Mourey, T.H. *J. Chromatogr.* **1985**, *323*, 297–304.
- [90] Dreux, M.; Lafosse, M.; Morin-Allory, L. *LC-GC Int.* **1996**, *9*, 148.
- [91] Vandermeeren, P.; Vandermeeren, J.; Baert, L. *Anal. Chem.* **1992**, *64*, 1056.
- [92] Hopia, A.I.; Ollilainen, V.M. *J. Liq. Chromatogr.* **1993**, *16*, 2469.
- [93] Trathnigg, B.; Kollroser, M.J. *J. Chromatogr.* **1997**, *768*, 223.
- [94] [www.sielc.com](http://www.sielc.com) (17/06/2015)
- [95] Pasch, H.; Trathnigg, B. *Multidimensional HPLC of Polymers*. Springer, Berlin, Germany, **2013**, 183–188.
- [96] Lampman, G.M.; Pavia, D.L.; Kriz, G.S.; Vyvyan, J.R. *Spectroscopy*. 4th Ed. Brooks/Cole, Belmont, CA, USA, **2010**, 16–25.
- [97] Scott, Raymond PW. *Liquid chromatography detectors*. Chrom-Ed Book Series, book 5, Library4Science, USA, **2003**, 81–88.
- [98] Ciric, J.; Oostland, J.; De Vries, J. W.; Woortman, A. J. J.; Loos, K. *Anal Chem.* **2012**, *84* (23), 10463–10470.
- [99] Fischer, K.; Krasselt, K.; Schmidt, I.; Weightman, D. *Macromol. Symp.* **2005**, *223* (1), 109–120.

## Chapter 3

### Solubility Studies and Spectroscopic Analysis

*This chapter is divided into two sections. The first section will elaborate on the solubility results obtained for the HA's in the DS range investigated. The second section covers the spectroscopic analysis of the HA's by means of  $^1\text{H-NMR}$  and Fourier transform infrared/attenuated total reflectance (FTIR/ATR) spectroscopy. Each section will be subdivided into a brief introductory, experimental, results and discussion as well as conclusion part.*

#### 3.1 Solubility Studies of Hyaluronic Acid with Respect to DS

##### 3.1.1 Introduction

One of the objectives of this work was to characterize HA's according to their molar mass and chemical composition with the aid of chromatographic techniques. The major problem with complex polysaccharides such as HA, is that of solvating them properly (random coil/ $\Theta$  conditions) in order to conduct quantitative analysis on them. In order to obtain MM and CC information a suitable solvent system is required in order to fully dissolve these samples to obtain the most accurate and representative information on the HA's. Thus, the starting point of this research endeavour was an in-depth solubility study in order to try and establish a suitable solvent system for the given polysaccharide samples. The solvent system has a few requirements: it must be of such nature that it can be applied in aqueous SEC and HPLC, should not degrade the samples, and should solvate the calibration standards used, which consist of Pullulan standards.

The samples consisted of both unmodified (HA) and modified hyaluronic acid (HAM). The modified hyaluronic acid (HAM) samples have a DS range of 0.4–3.4. The analyses of the samples are mainly conducted in order to obtain structure-property relations with the aim of better understanding these polysaccharides on a molecular level and to determine their applications.

### 3.1.2 Experimental Procedure

#### Solvents and Chemicals

The solvents used were all of HPLC-grade and consisted of: acetone (Ace) (Sigma-Aldrich), acetonitrile (ACN) (Merck), butanone (Bu) (Sigma-Aldrich), chloroform (CHCl<sub>3</sub>) (Merck), dichloromethane (DCM), 1,4-dioxane (Sigma-Aldrich), dimethyl acetamide (DMAc) (Sigma-Aldrich), dimethyl formamide (DMF) (Merck), dimethyl sulfoxide (DMSO) (Sigma-Aldrich), ethanol (EtOH) (Merck), ethyl acetate (Merck), hexane (Hex) (Merck), methanol (MeOH) (Romil-SPS™), 2-propanol (Isoprop) (Sigma-Aldrich), Toluene (TOL) (Sigma-Aldrich), tetrahydrofuran (THF) (Sigma-Aldrich) and water (H<sub>2</sub>O) (Sigma-Aldrich). The chemicals used in addition to the solvents consisted of: ammonium acetate (AMA) (Fluka), disodium phosphate (Na<sub>2</sub>HPO<sub>4</sub>) (Riedel-de Haën), lithium bromide (LiBr) (Riedel-de Haën), monopotassium phosphate (KH<sub>2</sub>PO<sub>4</sub>) (Riedel-de Haën), sodium azide (NaN<sub>3</sub>) (Riedel-de Haën), sodium chloride (NaCl) (Scienceworld), sodium hydroxide (NaOH) and sodium nitrate (NaNO<sub>3</sub>) (Riedel-de Haën). The solvents and chemicals were used as received.

#### Samples and Sample Preparation

All the samples were used as received from L'Oréal (Paris, France). Sample preparation varied according to the results obtained for the given solvent system. Parameters that changed during sample preparation included sample concentration, temperature and the addition of a salt. The initial starting point of the sample preparation for the HA's being subjected to different solvents was as follows: a mass of 1 mg of each sample was weighed, followed by the addition of 1 mL of the desired solvent system (listed in **Table 3.1**) at ambient temperature (23-25 °C) under agitation (500 rpm) for a dissolution period of 24 hours. The next step was to test the samples at an elevated temperature (40 °C) and observe if any changes occur. Note that the temperature elevation cannot be too significant, since it would result in the cross-linking/degradation of the polysaccharides, which would not be favoured for sample dissolution and analysis (see **Figure 4.5** in section 4.3.2).

In cases where solvents showed partial dissolution for the polysaccharides, the sample concentration was halved (0.5 mg/mL) for a dissolution period of 24 hours at a temperature of 40 °C. In some cases a salt was added, to break up aggregates. [See **Appendix A** for a complete description of the results obtained for the solubility studies under different experimental conditions. **Tables A.1–A.4** depict the different solvent systems used under different conditions].

### 3.1.3 Results and Discussion

The solubility of polysaccharides in general is mainly determined by their degree of substitution (DS). The DS of polysaccharides also governs their solubility in organic solvents.<sup>1, 2</sup> For example, the solubility of a certain polysaccharide may decrease in a given solvent as the DS is increased, due to a change in the polarity or chemistry of that given polysaccharide.<sup>1, 2</sup>

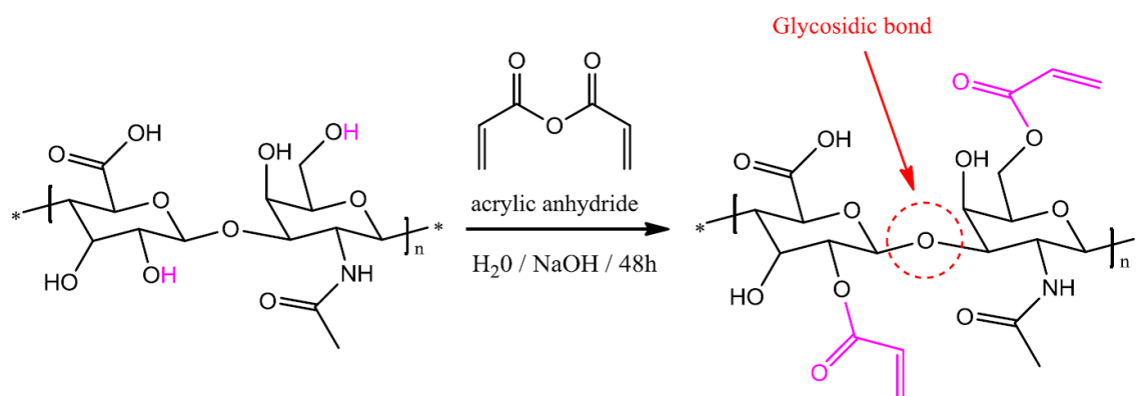
Due to the novel nature of the acrylic modified HA's, limited information was available in literature on certain properties such as their solubility in solvents. Therefore, a wide variety of solvents and solvent mixtures were explored and tested in order to establish the most suitable solvent system. In order to conduct qualitative liquid chromatography on these polysaccharides, a suitable solvent or solvent mixture is required that would dissolve all the samples irrespective of their acrylate content (DS). The solvent must also allow for adequate detection of the solute in the eluent and not degrade samples during dissolution. To identify suitable solvents for sample dissolution, all the samples, with a possible DS range of 0–4, were tested (sample preparation was carried out as mentioned in the experimental section). The solubilities of the samples were evaluated by visible inspection (see **Appendix A**). It was found that most of the solvents (or even solvent mixtures) were not capable of fully dissolving all the samples or were only able to dissolve samples of a certain DS range. An example of sample degradation was observed for solvent 20 in **Table 3.1**. After a visible test was performed it seemed like the sample was solvated, however, when proton nuclear magnetic resonance (<sup>1</sup>H-NMR) spectroscopy was conducted it revealed that the solvent had in fact hydrolysed the sample. In **Table 3.1** a description of all the solvent systems tested on the HA's is represented.

From theoretical aspects in literature<sup>3–6</sup> on the solubility of macromolecules it seems fairly straightforward to evaluate solubility, if certain parameters such as solubility parameters ( $\delta$ ) and degree of polymerization ( $D_p$ ) are known; however, this is not the case for polysaccharides. The solubility parameters of HA are far more complex than first anticipated. One of the most challenging parameters of polysaccharides is the hydrogen bond networks formed by these compounds. The fact that these polymers form vast hydrogen bond networks, which result in aggregate formation, makes it a really difficult task to dissolve them properly. The formation of aggregates makes the analysis of these samples rather difficult and can lead to misleading information with regard to structure-property relations, which is crucial in understanding these polymers on a molecular level.<sup>7</sup>

**Table 3.1:** Description of different solvent systems tested on the HA's.

Solvent systems tested		
1. DMSO	13. Toluene	25. 0.02% NaN <sub>3</sub>
2. CHCl <sub>3</sub>	14. H <sub>2</sub> O: MeOH (70:30)	26. 0.1M NaNO <sub>3</sub>
3. H <sub>2</sub> O	15. 2-Propanol	27. 0.1M Ammonium acetate
4. Acetone	16. Ethanol	28. PBS
5. DCM	17. 0.1M NaCl + H <sub>2</sub> O and MeOH (50:50)	29. Toluene: MeOH (50:50)
6. DMAc	18. 0.2M NaCl + H <sub>2</sub> O and MeOH (50:50)	30. 0.02M PB: MeOH (90:10)
7. DMF	19. 0.3M NaCl + H <sub>2</sub> O and MeOH (50:50)	31. H <sub>2</sub> O: 1,4-Dioxane (50:50)
8. THF	20. 0.5M NaOH	32. ACN: H <sub>2</sub> O (50:50)
9. MeOH	21. DMSO: H <sub>2</sub> O (50:50)	33. ACN: H <sub>2</sub> O (20:80)
10. Hexane	22. DMSO: H <sub>2</sub> O (60:40)	34. 0.1M NaCl + 300 mg/L NaN <sub>3</sub>
11. Ethyl Acetate	23. DMSO: H <sub>2</sub> O (70:30)	35. DMSO: H <sub>2</sub> O (60:40) + 0.1M Ammonium acetate
12. Butanone	24. DMSO: H <sub>2</sub> O (80:20)	

The solubility tests on the HA samples were trial-and-error based, due to the novel nature of the samples modified with an acrylic moiety and the scarcity of information in literature on their solubility parameters.

**Figure 3.1:** Hyaluronic acid before and after modification ( $DS = 2$ ).

The major drawback in finding a suitable solvent system, is that the unmodified samples are relatively polar molecules while the modified HA samples are relatively non-polar molecules (**Figure 3.1**). With this being said, it seemed highly improbable that a 'universal' single solvent could be obtained, since a single solvent would not allow for the dissolution of both the unmodified and modified samples, due to the polarity variations in the HA's. Therefore, only a binary or even ternary solvent system would allow for the dissolution of the HA's

across the entire DS range, since the polarity of the solvent system can be adjusted to favour dissolution.

The solvent systems showing the most promising results are listed in **Table 3.2**. As can be seen from **Table 3.2**, a given solvent system only works effectively if the right ratio of solvents is used. In some of the cases, like solvent systems 3 and 4, it works either for the unmodified samples or for the modified samples but not for both. Note that all the samples are soluble to a certain degree in both solvents 3 and 4, the major difference being that the extent of their solubility in the solvents is dependent on their DS. For instance, in solvent 3 good recoveries (performed gravimetrically) were obtained for the unmodified samples, while for the modified samples the recoveries were all below 30 %. The inverse case was observed for solvent 4. The major advantage we get from solvent systems 3 and 4 is the possibility of using it in gradient LAC and separating the polysaccharide molecules according to their DS (CCD separation).

**Table 3.2:** Description of most effective solvent systems.

<b>Solvent system</b>	<b>Sample</b>
<b>1.</b> H <sub>2</sub> O:DMSO (80:20)	For both un- and modified samples
<b>2.</b> H <sub>2</sub> O:DMSO (40:60)	For both un- and modified samples
<b>3.</b> H <sub>2</sub> O:ACN (80:20)	Only unmodified samples
<b>4.</b> H <sub>2</sub> O:ACN (50:50)	Only modified samples

In order to confirm that the different solvent systems listed in **Table 3.2** are 'good' solvents for the HA samples, preliminary recovery test were conducted after filtration. The solubility tests were evaluated by doing visible tests. Visible solubility tests work on the following basis: after the dissolution period of the samples under the desired conditions, the samples were evaluated by physically looking at them in order to determine whether the sample plus solvent system provides a clear solution or not. If the solution was clear, the assumption was made that the solvent system used was 'good' and the sample was then classified as solvated. However, visible test are not sufficient to determine whether the solvent system is in fact a 'good' solvent system for the samples. For example, when nanogels are formed upon dissolution of a given sample, according to a visible test the solvent system 'looks good', but upon filtration of the sample or when performing SEC on the sample the results vary significantly.

**Table 3.3**, contains the sample information as obtained from L'Oréal. The samples named HA in the table refer to unmodified HA and do not all originate from the same parent materials, HAM refers to modified hyaluronic acids which differ with regard to their DS.

**Table 3.3:** Sample information as obtained from L'Oréal.

Sample Code (SU)	Sample Code (L'Oréal)	Composition	Expected rate of grafting (%)	Expected DS	$\overline{M}_n$ (g/mol)	$\overline{M}_w$ (g/mol)
HA 01	DGA 1340144 (79544)	unmodified	–	–	–	–
HA 02	DGA 1350354 (79544)		–	–	–	–
HA 03	ES 83501190 (79544)		–	–	–	–
*HA 1	HA 1		–	–	–	–
**HA 2	HA 1		–	–	–	–
HAM 01	R0076848 A001 L002	modified with acrylic moiety	60	2.4	22 700	78 700
HAM 02	R0076848 A002 L001		60	2.4	24 600	68 100
HAM 03	R0076848 A001 L003		60	2.4	30 000	137 400
HAM 04	R0076848 A003 L001		80	3.2	–	–
HAM 05	R0077309 A001 L001		50	2.0	28 700	108 400
HAM 06	R0077308 A001 L001		18	0.7	35 200	61 700
HAM 07	R0077310 A001 L001		12.5	0.5	40 700	109 600
*HAM 08	R0076583 A005 L002		50	2.0	–	–
*HAM 09	R0076583 A005 L003		50	2.0	–	–
*HAM 10	R0076583 A005 L004		42.5	1.7	–	–
**HAM 11	R0076583 A005 L005		38	1.5	–	–

\*Sample HAM 08, 09 and 10 were modified from HA 1. \*\*Sample Ham 11 were modified from HA 2.

In **Figure 3.2** the schematic illustration of the recoveries after filtration of the samples with the four different solvent systems listed in **Table 3.2** is depicted.

From the preliminary solubility studies conducted on the samples it is clear (taking the sample recoveries into consideration) that the desired solvent systems were dissolving the samples relatively well. However, this was still not effective enough in completely solvating the samples, and required some more attention. As mentioned before, the addition of a salt can also aid in the dissolution of polysaccharides. However, when adding a salt, one should take care with regard to salt concentration, since there is a very fine line between adding too little or too much salt.<sup>8,9</sup> In the case where too little salt is added, it would have no effect on breaking up aggregates. However, when adding too much salt it can significantly increase the solution viscosity.<sup>1,8,9</sup>





The next step was to test these samples in the presence of a salt, and the salt of choice preferably had to be ELSD compatible in order to allow for the use on an HPLC instrument. The salt used in this case was ammonium acetate. The recoveries after filtration of the samples conducted in the presence of ammonium acetate are depicted in **Figure 3.3**.

**Figure 3.3** illustrates the results obtained for only the most representative solvent system, (DMSO:H<sub>2</sub>O (60:40) (v/v%)), in the presence of ammonium acetate. The comparison of the results of **Figures 3.2** and **3.3** showed that there is no major difference in the recoveries of the given samples. In some cases the recoveries increase and in some they decrease, the reason for that is still unclear mainly due to the complex nature of these samples. The sample recoveries after filtration have a direct correlation to the solubility of the samples in a given solvent system, however, this can only be verified with the aid of a light scattering detector, which will be presented in Chapter 4.

When comparing the results obtained in **Figure 3.2** with the results obtained for a well-known solvent system for unmodified HA in **Figure 3.4**, it can be seen that the solvent systems presented in **Figure 3.2** are a major improvement with regard to the recoveries after filtration. The recoveries after filtration hold a direct correlation to the solubility of the samples in the desired solvent system. The solvent system depicted in **Figure 3.4** works exceptionally well for unmodified HA's but not as well for modified HA's.

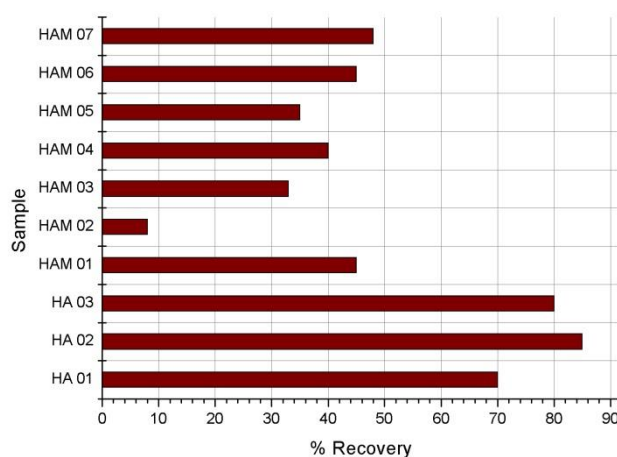


**Figure 3.4:** Sample recoveries after filtration using a 0.1M NaCl + NaN<sub>3</sub> solution solvent system.

From **Figure 3.4** it is clear that the 0.1 M NaCl and NaN<sub>3</sub> solvent system used was not suitable to solvate all the samples. Since HA dissolves 100% in H<sub>2</sub>O, this system works for

the unmodified HA samples. However it does not solvate the modified HA samples properly and, therefore, a more effective solvent system was required for the modified HA samples.

The ELSD-compatible salt used (ammonium acetate) did improve the solubility of certain samples slightly, however, ammonium acetate is not sufficient for the purpose of this study. We therefore explored more salts which, according to literature, would be more suited for the given samples and solvents. These salts were sodium chloride (NaCl)<sup>2</sup> and lithium bromide (LiBr), respectively.<sup>10, 11</sup> The different behaviours of the samples in NaCl and LiBr were compared to ammonium acetate. Unfortunately, these are non-volatile salts rendering them non-ELSD-compatible. The sample recoveries obtained for the samples dissolved in DMSO:H<sub>2</sub>O/NaCl are tabulated in **Table 3.4**. The results obtained were promising for the NaCl modified solvent system. No sample recoveries for the LiBr modified solvent system are presented due to problems arising from the hygroscopic nature of the LiBr salt. The effect that NaCl and LiBr have on the samples when combined with DMSO:H<sub>2</sub>O will be explained in more detail in Chapter 4.

**Table 3.4:** Recoveries after filtration using DMSO:H<sub>2</sub>O/NaCl as solvent.

Sample Code (SU)	% Recovery
1. HA 01	70
2. HA 02	90
3. HA 03	90
4. HAM 01	50
5. HAM 02	40
6. HAM 03	50
7. HAM 04	90
8. HAM 05	50
9. HAM 06	80
10. HAM 07	80
11. HA 1	90
12. HA 2	100
13. HAM 08	50
14. HAM 09	80
15. HAM 10	90
16. HAM 11	90

From the results obtained for the solubility tests a clear trend was observed. The solubility of the HA samples in organic solvents is primarily dependent on the acrylate content, since the acrylate content determines the overall polarity of the HA's. By increasing the acrylate content (DS) on the HA backbone, the polymers tend to become less polar, which in turn results in decreased solubility in polar solvents and increased solubility in less polar solvents. We also know from literature that the solubility of polysaccharides is a complex

function.<sup>12</sup> For example, the solubility of neutral polysaccharides is generally low due to the presence of a large number of hydrogen bonds. These hydrogen bonds stabilize intra- and inter-chain interactions.<sup>13</sup> The solubility is not only dependent on the average DS of a given polysaccharide but also on the distribution of the substituents along the polymer backbone, i.e. minor differences in the substituent distribution pattern can have a major effect on the solubility.<sup>12</sup>

## **3.2 Spectroscopic Analysis of HA Polysaccharides**

### **3.2.1 Introduction**

Following the solubility studies, bulk analyses were performed on the HA's to obtain information regarding their chemical structure i.e. chemical composition, architecture and end-group functionality. The bulk analyses of the samples were conducted on <sup>1</sup>H-NMR and FT-IR/ATR instruments, respectively. Bulk analyses were also conducted in order to determine the degree of substitution of the HA's.

### **3.2.2 Experimental**

#### **Solvents and Chemicals**

In the bulk analysis of the HA's deuterated solvents were used to conduct <sup>1</sup>H-NMR spectroscopy. The solvents consisted of deuterated dimethyl sulfoxide (DMSO-d<sub>6</sub>) and deuterated water (D<sub>2</sub>O), and were used as received.

#### **Samples and Sample Preparation**

All the samples were analysed with the aid of <sup>1</sup>H-NMR and FT-IR/ATR spectroscopy. For <sup>1</sup>H-NMR analyses, 10 mg per sample were weighed off and dissolved in 0.7 mL of either D<sub>2</sub>O or in a mixture of DMSO-d<sub>6</sub>:D<sub>2</sub>O (60:40 (v/v%)) depending on the degree of substitution of the sample. A dissolution period of 24 hours at ambient temperatures with agitation (500 rpm) was employed.

#### **Analytical Techniques**

##### **NMR Experiments**

The spectra were acquired on a Varian INOVA 400 MHz Liquid State NMR spectrometer with an acquisition time of 2.0 s, relaxation delay of 1.0 s and a PRESAT pulse sequence at 25 °C with more than 256 scans. <sup>1</sup>H NMR spectra for all the samples were recorded either

dissolved in 100% deuterated water ( $D_2O$ ) or in a mixture of DMSO- $d_6$ : $D_2O$  (50:50 (v/v%)) solvent. The NMR data were processed using MestReNova software version 6.0.2  $^1H$ -NMR processor.

### FT-IR/ATR Spectroscopy

Attenuated total reflectance (ATR) measurements of the bulk HA's were acquired on a Thermo Scientific Nicolet iS10 Spectrometer (Thermo Scientific, Waltham, MA) equipped with a Smart iTR ATR accessory. Spectra were recorded from 4000–600  $cm^{-1}$  from a collection of 64 scans at a resolution of 8  $cm^{-1}$ , with automatic background subtraction. FT-IR spectra were obtained on the samples in their solid as well as film forms. Films were produced by dissolving the samples in pure water and then allow the solvent to evaporate. On each film 5 scans at different positions were taken to ensure that the data retrieved are representative of the entire sample. Data acquisition was performed on Thermo Scientific OMNIC software (version 8.1).

### 3.2.3 Results and Discussion

After the establishment of a suitable solvent system for the HA samples, the average DS was determined for the modified HA samples by quantitative  $^1H$ -NMR spectroscopy.  $^1H$ -NMR spectroscopy is the most commonly used tool to characterize HA derivatives, as shown in earlier studies,<sup>14, 15, 16</sup> since it shows the presence of the isolated compounds and makes it possible to determine the DS of the modified HA's.<sup>17</sup> As mentioned before, the maximum DS that each HA repeat unit can have is four, as illustrated by **Figure 3.5**.

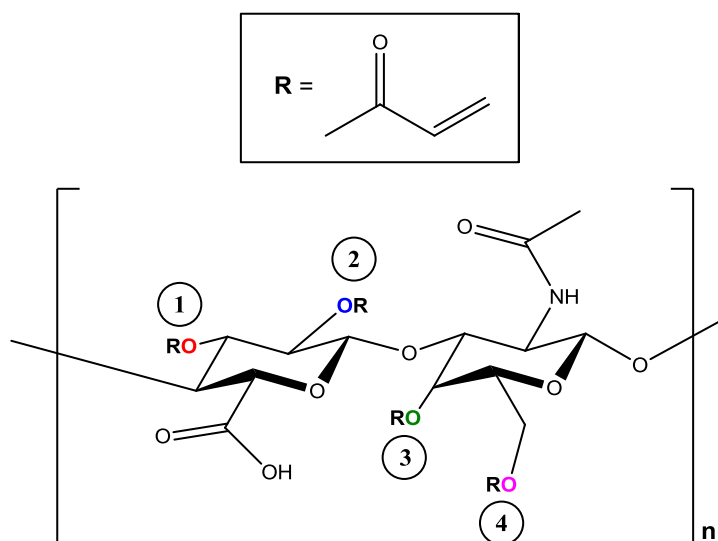


**Figure 3.5:** Schematic illustration of the maximum DS of each HA repeat unit.

Figure 3.6 shows the  $^1\text{H-NMR}$  spectrum of a modified HA with an average DS of 2.6. The resonance peak of the  $\text{CH}_3$ -protons of the acetyl group can be seen at a chemical shift ( $\delta$ ) = 1.95–2.1 ppm, which is generally used as the reference peak to calculate the DS of modified HA's. The signals for the acrylate protons can be seen at  $\delta = 6.0$ –7.0 ppm. Both sets of resonance peaks are nicely separated from the HA backbone protons, which can be seen at  $\delta = 3.0$ –4.5 ppm. It is difficult to assign each of the protons on the HA backbone individually, since the resonance protons are superimposed. The broad doublet situated at  $\delta = 4.2$ –4.5 ppm corresponds to the anomeric protons which are attached to the carbons adjacent to the two oxygen atoms. The  $^1\text{H-NMR}$  spectrum obtained for the sample (HAM 04, DS = 2.6) presents slightly broader signals than for an unmodified HA sample, which can possibly be ascribed to the molar mass and dispersity as well as the high viscosity of the solution.

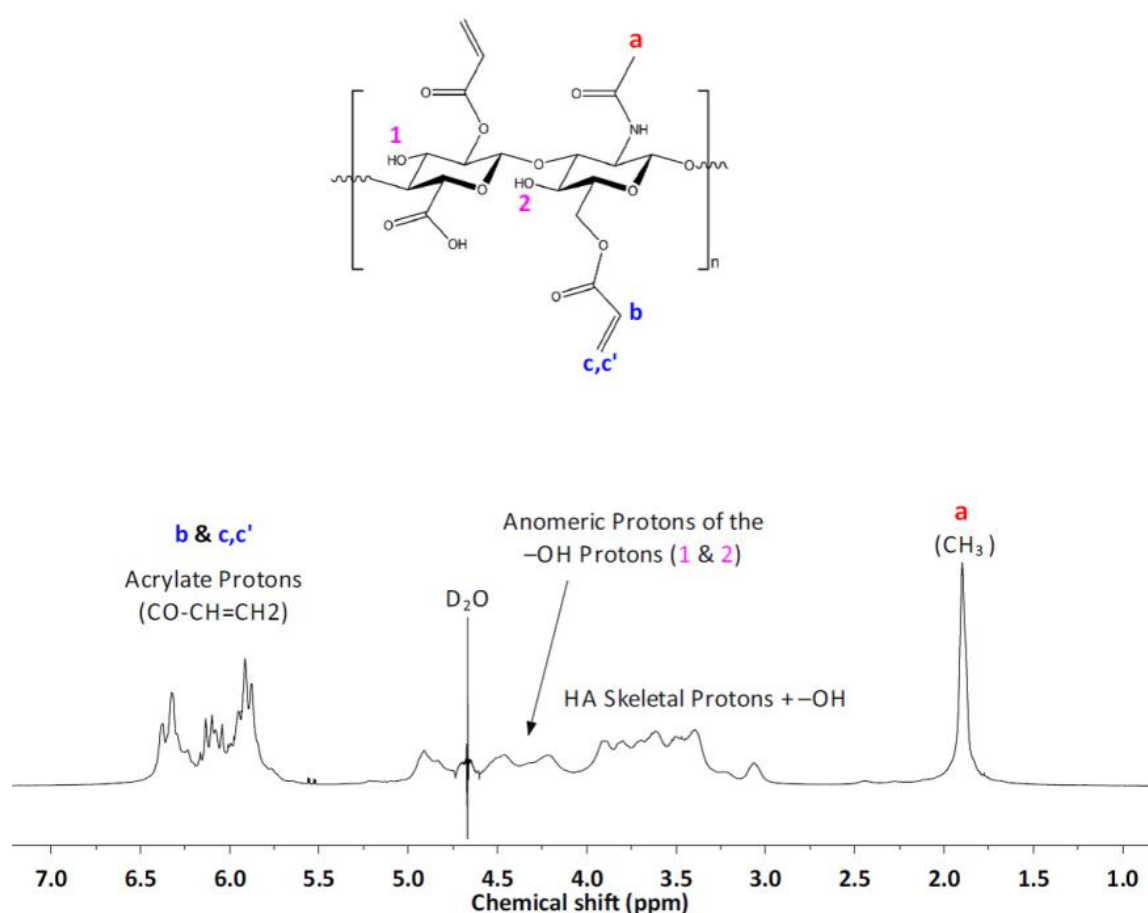


Figure 3.6:  $^1\text{H-NMR}$  spectrum of sample HAM 04 (DS = 2.6) in  $\text{D}_2\text{O}$ .

The grafting ratio of the modified HA samples was estimated using  $^1\text{H-NMR}$  data by comparing the integrated acrylate protons ( $\text{CO-CH=CH}_2$ ) to the integrated methyl protons ( $\text{CH}_3$ ) of the acetyl group. This ratio gives the number of acrylate functions per polymer

repeat unit. The average DS of the modified HA samples was determined using the following equation:

$$DS = \frac{\int c, c' + b}{\int a} \dots \dots \dots \text{Equation 3.5}$$

where  $c$ ,  $c'$  and  $b$  are the protons attributed to the acrylate moiety and  $a$  the methyl protons of the acetyl group. The results obtained for the modified HA's can be seen in **Table 3.5**.

**Table 3.5:** Summary of the DS for the modified polysaccharides as obtained from  $^1\text{H-NMR}$  spectroscopy.

Sample Code	Expected Grafting Ratio (mol %)	Expected DS	Actual Grafting Ratio (mol %)	Actual DS
HAM 01	60	2.4	78	3.1
HAM 02	60	2.4	85	3.4
HAM 03	60	2.4	73	2.9
HAM 04	80	3.2	65	2.6
HAM 05	50	2.0	55	2.2
HAM 06	18	0.7	20	0.8
HAM 07	12.5	0.5	10	0.4
HAM 08	50	2.0	65	2.6
HAM 09	50	2.0	63	2.5
HAM 10	42.5	1.7	38	1.5
HAM 11	38	1.5	40	1.6

NMR spectroscopy is a valid asset, since it is a direct method for the determination of the DS. However, it has the inherent drawback that it requires large amounts of sample to produce a spectrum of high signal-to-noise ratio (S/N ratio). This is a problem due to the fact that the modified HA samples are limited with respect to their solubility.

Infra-red (IR) spectroscopy was explored as an alternative route for the determination of the average DS. It is also a means to obtain additional information in conjunction with NMR spectroscopy and is also used frequently for this purpose.<sup>18–20</sup> Due to the sensitivity of IR spectroscopy, smaller quantities of the sample are required for analysis (also no solvent is required for FTIR/ATR). The differences between the FT-IR/ATR spectra for an unmodified HA and modified HA can be seen in **Figure 3.7**, where sample HA 1 (no substituents) and sample HAM 09 (DS = 2.5) are used to show the observable differences. From the stacked FT-IR spectra of these two samples, a clear difference can be seen in the region of 1800–1500  $\text{cm}^{-1}$ , where two main peaks are observed in the modified spectrum where there is only one main peak in the spectrum of the unmodified HA. The second peak observed (due to the

C=O stretch) in the modified sample is as a result of the acrylic ester group. This information also supports the information obtained from  $^1\text{H-NMR}$  spectroscopy. In the  $^1\text{H-NMR}$  spectra of the modified samples, a clear indication of the acrylate functionalities can be observed at  $\delta = 6.0\text{--}7.0$  ppm (as represented in **Figure 3.6**). In the FT-IR spectra of the modified HA's the acrylate functionalities are observed at frequencies of  $1500\text{--}1700\text{ cm}^{-1}$  (refer to **Table 3.5**). This proves that the HA's have been successfully modified with the acrylic moiety. **Figure 3.8** is an overlay of FT-IR spectra of all the modified HA samples with a DS range of 0.4–3.4.

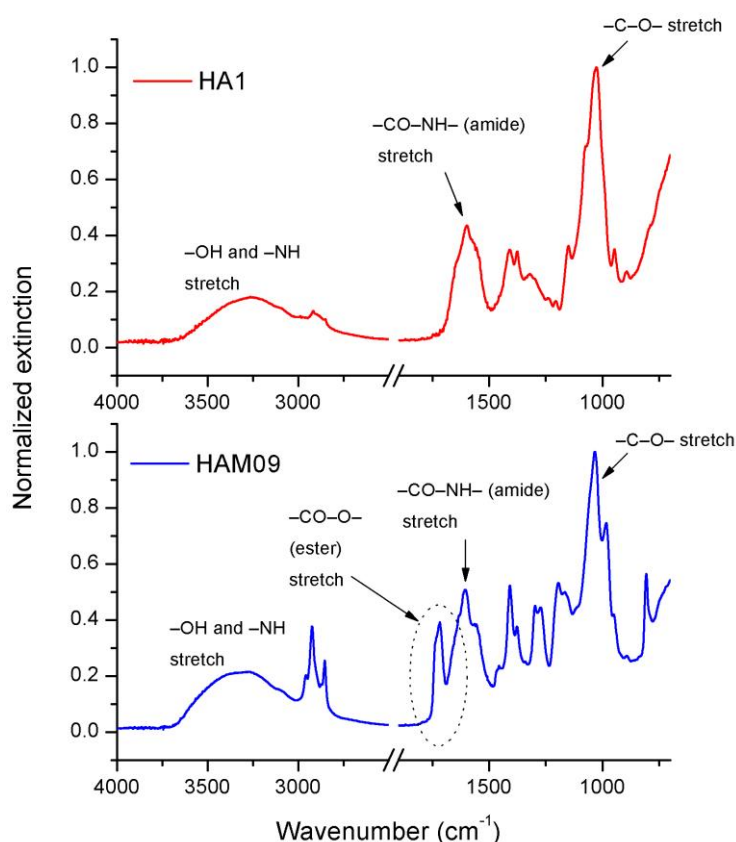


**Figure 3.7:** Stacked IR spectra of unmodified (HA 1) and modified (HAM 09, DS = 2.5) HA samples.

It is of the utmost importance that the samples are thoroughly dried, since IR spectroscopy is highly sensitive to hydrogen bonds and residual water. Using it without carefully drying of the samples unavoidably leads to having saturated bands that lead to the destruction of all the qualities of the IR spectra, since the presence residual water will interfere/overlap with the region of interest at  $1780\text{--}1690\text{ cm}^{-1}$ , where the ester absorption band is observed.<sup>7</sup> This would also make quantification of the DS a challenge and unreliable.



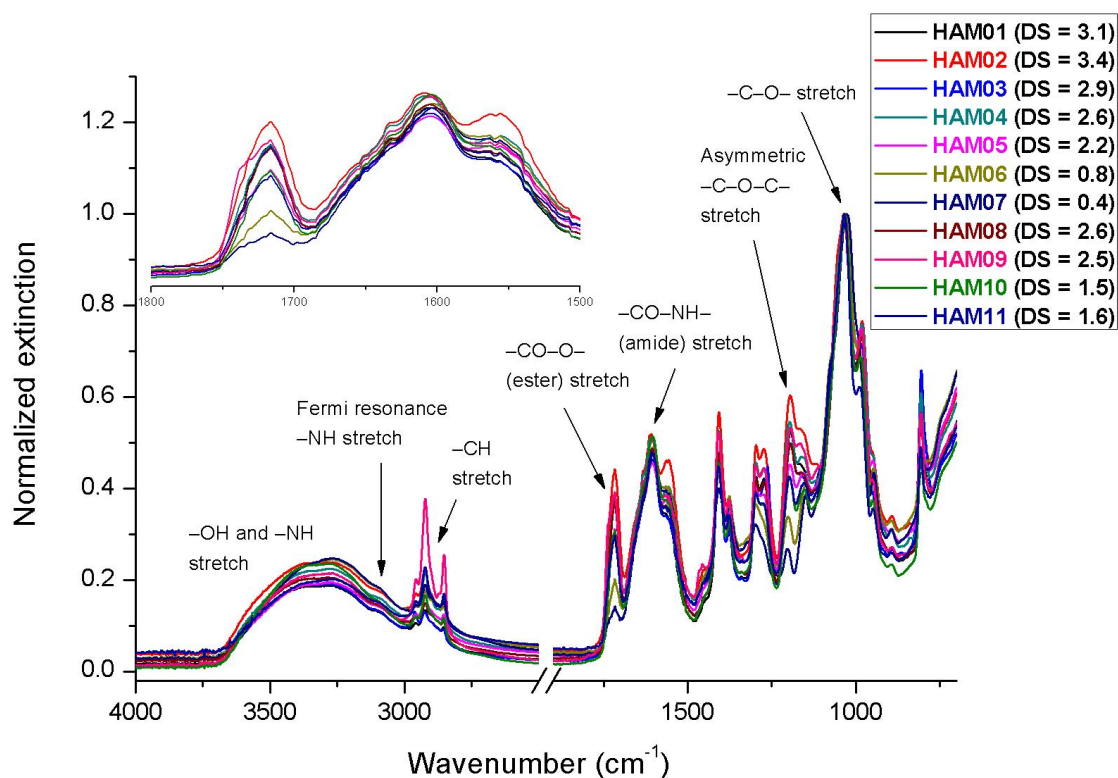


**Figure 3.8:** Overlaid FTIR spectra of the modified HA samples (DS range of 0.4–3.4). The inset represents an expansion of the frequency range 1500–1800  $\text{cm}^{-1}$ .

The spectral assignments of **Figure 3.8** are tabulated in **Table 3.6**. In the table all the major absorption peaks which are observed in **Figure 3.8** are identified and assigned accordingly. This information gives an in-depth picture of the modified HA's chemical structure.

**Table 3.6:** FT-IR spectral assignments for the modified HA's.<sup>7, 21, 22</sup>

Type of Vibration	Frequency (cm <sup>-1</sup> )	*Intensity
• Liberation band ( $\delta_L$ ) of residual H <sub>2</sub> O molecules (Rotational vibrations of the entire H <sub>2</sub> O molecule)	600	m-s
• C–O stretching vibrations ( $\nu_{C-OH}$ ) of alcohols	950–1200	s
• Asymmetric $\nu_{C-O-C}$ stretching corresponding to that of the glycosidic groups (observable shoulder on the main C–O peak).	1160	m-s
• Symmetric stretching of the carboxylate group ( $\nu_{COO^-}^s$ ).	1400	m
• Superposition of the amide bending bands and of some of the carbonyl and carboxyl ( $\nu_{C=O}$ ) bands	1500–1700	m
• Stretching band of $\nu_{C-H}$ (–CH stretch).	2900	m
• Broad band is related to that of the –NH and –OH groups engaged in hydrogen bonds.	2800–3600	m
• Fermi resonance of $\nu_{N-H}$ with a slight overtone of the amide stretching band.	3100	w

\*The signal intensities are classified as weak (w), medium (m) and strong (s).

The FT-IR data obtained for all the modified HA samples (**Figure 3.8**) are in good agreement with what is observed from <sup>1</sup>H-NMR spectroscopy, with reference to the acrylate moieties. These results validate that all the modified HA's in fact contain the acrylate moiety. What is also apparent from **Figure 3.8** is that, when the DS of the modified HA's increases, there is an observable increased trend in the C=O (carbonyl stretch due to the acrylate ester, as labelled on **Figure 3.8**) peak area. This increase in C=O peak area is ascribed to the increase in number of acrylate moieties present, which is directly related to the DS. The change in the peak areas for the C=O (carbonyl stretch due to the acrylate ester) and the DS values was used to show their interrelationship.

In **Figure 3.9** the relation between the band ratios obtained by FT-IR and the DS determined by <sup>1</sup>H-NMR is represented. From **Figure 3.9** it is clear that the relationship between the DS values and the corresponding band ratios of the modified HA samples is directly proportional, although some points deviate slightly from the fitted linear regression line.

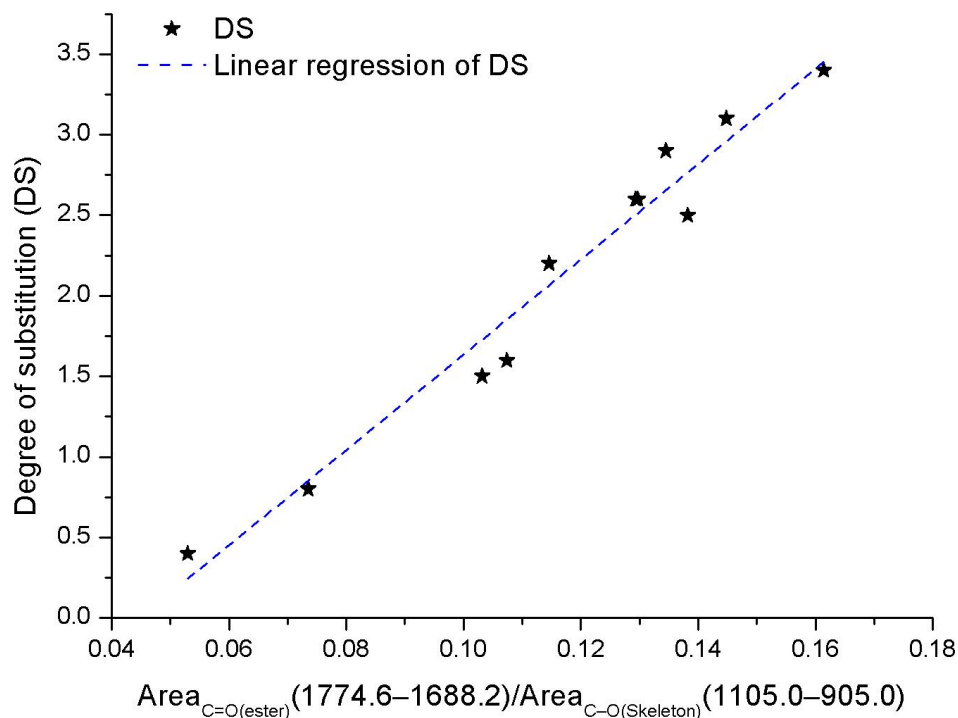


**Figure 3.9:** Interrelationship of specific FT-IR signal area ratios (C=O ester and C–O skeleton) with the DS values obtained by <sup>1</sup>H-NMR spectroscopy of the modified HA samples.

The calibration curve can be described by the following equation:

$$DS = -1.32 + 29.6 \times \left( \frac{Area_{(C=O, ester)}}{Area_{(C-O, skeleton)}} \right) \dots \dots \dots \text{Equation 3.6}$$

where Area, refers to the FT-IR peak areas of the specific spectral bands, consisting of the ester groups (1774.6–1688.2 cm<sup>-1</sup>) and the C–O skeleton groups (1105.0–905.0 cm<sup>-1</sup>) of the HA polymer backbone.

**Equation 3.6** enables the direct calculation of the average DS of any unknown HA sample modified with the acrylate moiety within a DS range of 0–4 (with a relative standard deviation of 14.6%) once the FT-IR spectrum is available. The FT-IR correlation is a very effective alternative in determining the average DS, especially when compared to <sup>1</sup>H-NMR spectroscopy, since this can be acquired with very small amounts of sample and without the use of a solvent in a very short analysis time frame.

### 3.3 Conclusions

In conclusion, from the solubility studies conducted on the HA's it is evident that a single solvent will not allow for the complete dissolution of the HA's across the entire DS range, but rather only for HA's with certain DS ranges. Therefore, the only logical way in which the HA's can be completely dissolved over the entire DS range (0–4) is with the aid of a binary or even ternary solvent system. A binary and/or a ternary solvent system makes it possible to adjust the polarity of the solvent system, and in doing so allows for the dissolution of the HA's over the entire DS range. The adjustment of the polarity of the solvent system is rather crucial, since the polarity of the HA's changes with changing acrylate content on the polymer backbone.

The chemical structure of the HA's was successfully confirmed with the aid of  $^1\text{H-NMR}$  and FT-IR spectroscopy. As seen from the results, FT-IR spectroscopy provides an alternative method to obtain the chemical composition (DS) of the HA's, and is also a means to obtain additional information compared to  $^1\text{H-NMR}$  spectroscopy.

## References

- [1] Creuzet, C.; Kadi, S.; Rinaudo, M.; Auzély-Velty, R. *Polymer*. **2006**, *47* (8), 2706–2713.
- [2] Palumbo, F. S.; Pitarresi, G.; Mandracchia, D.; Tripodo, G.; Giammona, G. *Carbohydr. Polym.* **2006**, *66* (3), 379–385.
- [3] Sariban, A.; Binder, K. *J. Chem. Phys.* **1987**, *86* (10), 5859–5873.
- [4] Sperling, L. H. *Introduction to physical polymer science*. John Wiley & Sons, Hoboken, New Jersey, USA, **2015**.
- [5] Pesci, A. I.; Freed, K. F. *J. Chem. Phys.* **1989**, *90* (3), 2017–2026.
- [6] Warren, P. B. *Macromolecules*. **2007**, *40* (18), 6709–6712.
- [7] Haxaire, K.; Marechal, Y.; Milas, M.; Rinaudo, M. *Biopolymers*. **2003**, *72* (1), 10–20.
- [8] Rinaudo, M. *Macromol. Biosci.* **2006**, *6* (8), 590–610.
- [9] Haxaire, K.; Braccini, I.; Milas, M.; Rinaudo, M.; Pérez, S. *Glycobiology*. **2000**, *10* (6), 587–594.
- [10] Coppola, G.; Fabbri, P.; Pallesi, B.; Bianchi, U. *J Appl. Polym. Sci.* **1972**, *16* (11), 2829–2834.
- [11] Hann, N. D. *J. Polym. Sci., Polym. Chem. Ed.* **1977**, *15* (6), 1331–1339.
- [12] Rinaudo, M. *Polym. Int.* **2008**, *57* (3), 397–430.
- [13] Rinaudo, M. *Food Hydrocolloid.* **2001**, *15* (4), 433–440.
- [14] Pouyani, T.; Harbison, G. S.; Prestwich, G. D. *J. Am. Chem. Soc.* **1994**, *116* (17), 7515–7522.
- [15] Pouyani, T.; Prestwich, G. D. *Bioconjugate Chem.* **1994**, *5* (4), 339–347.
- [16] Bulpitt, P.; Aeschlimann, D. *J. Biomed. Mater. Res.* **1999**, *47* (2), 152–169.
- [17] Schanté, C. E.; Zuber, G.; Herlin, C.; Vandamme, T. F. *Carbohydr. Polym.* **2011**, *85* (3), 469–489.
- [18] Schneider, A.; Picart, C.; Senger, B.; Schaaf, P.; Voegel, J. C.; Frisch, B. *Langmuir*. **2007**, *23* (5), 2655–2662.
- [19] Young, J. J.; Cheng, K. M.; Tsou, T. L.; Liu, H. W.; Wang, H. J. *J. Biomater. Sci., Polym. Ed.* **2004**, *15* (6), 767–780.
- [20] Zhao, X. *J. Biomater. Sci., Polym. Ed.* **2006**, *17* (4), 419–433.
- [21] Haxaire, K.; Marechal, Y.; Milas, M.; Rinaudo, M. *Biopolymers*. **2003**, *72* (3), 149–161.
- [22] Maréchal, Y.; Milas, M.; Rinaudo, M. *Biopolymers*. **2003**, *72* (3), 162–173.

## Chapter 4

### Development of a SEC Method for Modified and Unmodified HA

*This chapter reports the development of a SEC method for determining the molar mass and molar mass distribution of the HA samples. In this chapter information regarding the following aspects will be provided: (1) the molar mass determination of the HA's with a mobile phase that is fairly well known in literature and (2) a detailed discussion on the molar mass determination of the HA's with a newly developed mobile phase. Chapter 4 will be subdivided into the following sections: introduction, experimental, results and discussion, and finally a conclusion part for clarification purposes.*

#### 4.1 Introduction

One of the most important molecular parameters influencing the application of HA is the molar mass.<sup>1-3</sup> Molar mass characterization provides information that enables the better understanding of the structure-property correlations of HA. The MMD characterization of natural polymers is difficult due to solubility problems, degradation during dissolution and size separation, the broadness of size distributions and shear scission, to name a few problems.<sup>4-6</sup> Thus, a comprehensive characterization of the HA's in terms of molar mass is required, since it would provide the fundamental understanding of the influence of the structure of the HA's on application and performance properties. In this chapter, the aim is to discuss the approaches taken to systematically develop a method for the determination of the molar masses by means of SEC-MALLS.

#### 4.2 Experimental

##### Solvents and Chemicals

Water (H<sub>2</sub>O) (Sigma-Aldrich) and dimethyl sulfoxide (DMSO) (Sigma-Aldrich) were of HPLC-grade and used as received. The salts used included: LiBr (Riedel-de Haën), ammonium acetate (Fluka) and NaCl (Scienceworld) were used as received. Narrow molar mass distributed Pullulan polymer standards were used as received from Polymer Standards Service (PSS GmbH, Mainz, Germany).

**Size exclusion chromatography (SEC)**

The molar mass and molar mass dispersity of the HA samples were determined on an Agilent 1260 Infinity series HPLC instrument (Agilent Technologies) consisting of the following components: an on-line degasser, quaternary pump, auto-sampler, thermostatted column compartment, variable wavelength (UV) detector and differential refractometer (RI) detector. The Agilent 1260 infinity series was also connected to a Wyatt DAWN® Heleos™ II, 8 angle laser light scattering detector. Two sets of stationary phases were employed in the MM determination of the HA's: (1) a PSS Suprema column set (guard column, 10 µm particle size, 50 x 8 mm I.D.; 2 x 1000 Å 10 µm particle size, 300 x 8 mm I.D.; 1 x 30 Å 10 µm particle size, 300 x 8 mm I.D.) (PSS GmbH (Mainz, Germany)) and (2) a PSS GRAM column set (guard column, 10 µm particle size, 50 x 8 mm I.D.; 2 x 1000 Å 10 µm particle size, 300 x 8 mm I.D.; 1 x 100 Å 10 µm particle size, 300 x 8 mm I.D.) (PSS GmbH, Mainz, Germany).

The experimental procedure for the analysis of the HA's according to their molar mass was as follows, unless stated otherwise: the HA samples (1 – 1.5 mg) were dissolved in 1 mL of either (1) 0.1 M NaCl solution in water with 300 mg/L NaN<sub>3</sub>, (2) DMSO:H<sub>2</sub>O (60:40) [v/v%] or (3) DMSO:H<sub>2</sub>O/0.05M LiBr (60:40) [v/v%] for a dissolution period of 16 hours at ambient temperature with agitation at 500 rpm. The samples were covered with aluminium foil, due to the possibility of light degrading the samples. After the dissolution period the samples were filtered through a 0.45 µm regenerated cellulose (RC) filter to ensure that no unwanted insoluble parts end up on the SEC column. An injection volume of 100 µL at an operating temperature of 40 °C with a flow rate of 0.30 or 0.35 mL/min was used for all the HA's. In the case where the entire column set was used for separations an injection interval of 120 min/sample was used. In cases where only a guard column plus one analytical column were employed an injection interval of 80 min/sample was used.

**[NOTE:** Sample injections were performed at low flow rates due to the high viscosity of DMSO at low temperatures. In the present case the use of high temperatures to decrease the viscosity of DMSO is not possible, because the HA's are not thermally stable at temperatures exceeding 40 °C.<sup>7</sup> Higher flow rates are also not an option, since higher flow rates result in higher backpressures and might possibly damage the packing materials of the columns and can also lead to shear degradation of the HA samples.]

**Determination of Refractive Index Increment (dn/dc)**

To our knowledge there is no information in published literature on the dn/dc values for the HA's under investigation in DMSO:H<sub>2</sub>O (60:40)/0.05M LiBr at 40 °C. Therefore, the dn/dc values for all the HA's were determined as follows:

A batch/stand-alone instrument approach was used for the dn/dc determinations, since it is the most accurate method and is not influenced by chromatographic parameters.<sup>8-11</sup> The first step was to determine the RI detector calibration constant (dn/dv). This was performed using a series of aqueous NaCl solutions of varying concentrations consisting of 0.2, 0.4, 0.6, 0.8, 1.0 and 1.2 mg/mL. Since the dn/dc value of NaCl in water (0.174 mL/g at a wavelength of 658 nm) as well as the concentrations are known, we can calculate the dn/dv, the change in refractive index with respect to change in voltage. The dn/dv value for the RI detector is extrapolated in the same way as will be described for the determination of the dn/dc values. After the establishment of the RI detector constant, a series of six different concentrations in DMSO:H<sub>2</sub>O/LiBr solutions of 0.3, 0.6, 0.9, 1.2, 1.5 and 1.8 mg/mL for each sample was prepared. Each concentration and a blank before the lowest and after the highest concentration were injected into the RI detector with the aid of a syringe pump. This resulted in a "staircase" profile, with each flat plateau corresponding to a concentration of the HA sample (see **Figure 4.1**). A flow rate of 0.50 mL/min was used with an injected volume of 1000 µL, to ensure that the flow cell of the RI detector is completely saturated with the given sample concentration to ensure flat plateaus. After this was achieved, Astra 6.0 software was incorporated to extrapolate the dn/dc value from the different sample concentrations used (see **Figure 4.2**); a linear fit of the concentrations, with R<sup>2</sup> as close to 1 as possible, is required to obtain the most accurate dn/dc value. A linear fit value of R<sup>2</sup> = 0.9994 was obtained for the illustrated sample.



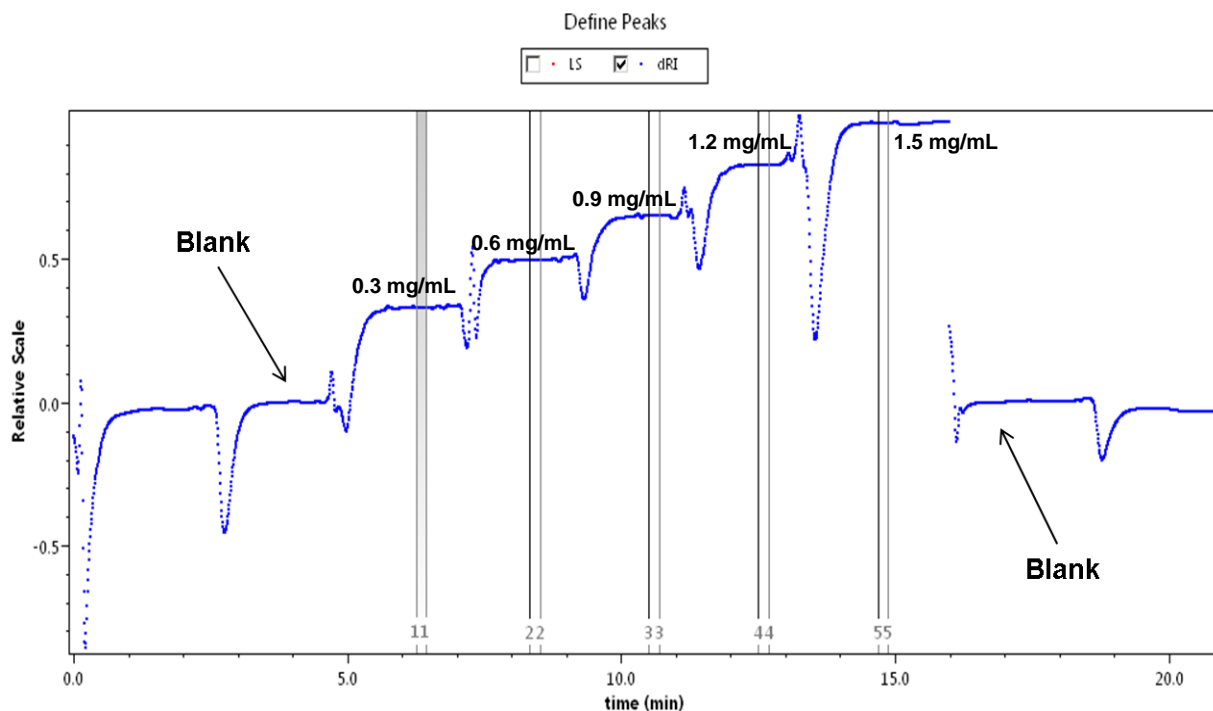
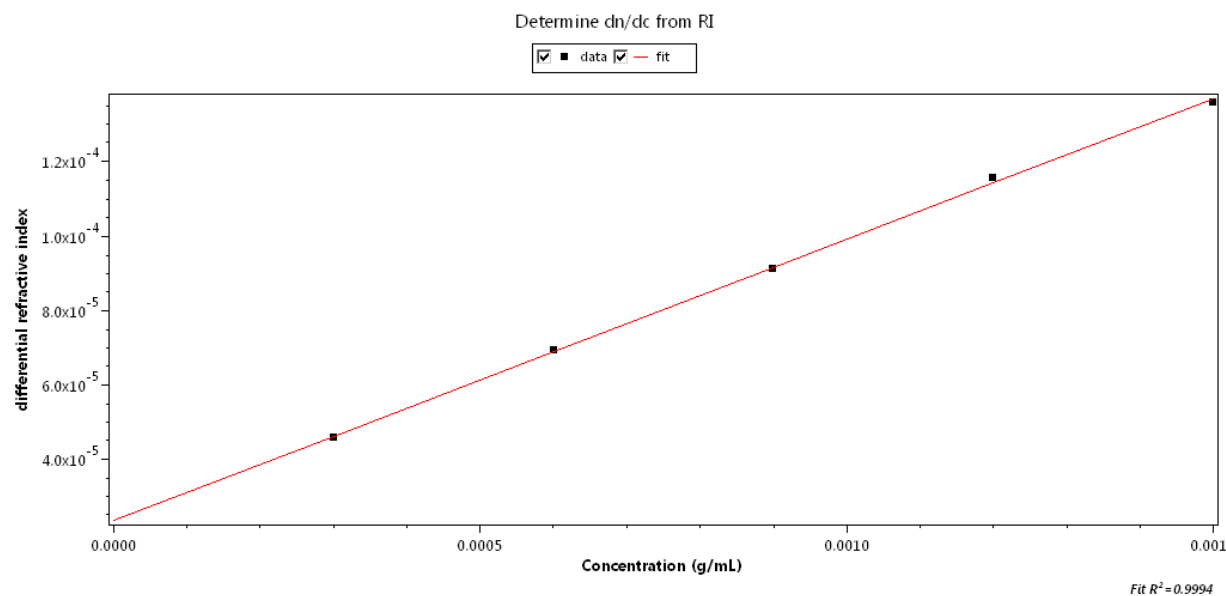


**Figure 4.1:** “Staircase” profile obtained on RI at different sample concentrations, used to obtain  $dn/dc$  value, sample HAM 04 ( $DS = 2.6$ ) is used as illustration, solvent DMSO:H<sub>2</sub>O/LiBr at 40 °C.



	Value
dn/dc	0.0756 ± 0.0011 mL/g
Fit Degree	1
Percentage To Keep	100
Enabled Peaks	

**Figure 4.2:** Linear fit performed by ASTRA 6.0 software after the different concentrations have been defined to produce the  $dn/dc$  value. HAM 04 ( $DS = 2.6$ ) is used as illustration, solvent DMSO:H<sub>2</sub>O/LiBr at 40 °C.

## LC-FTIR and FTIR Spectroscopy

### Analyte Deposition by LC-Transform Interface.

An LC-Transform series model 303 (Lab Connections) was coupled to the HPLC system and the eluate (flow rate of 0.35 mL/min) from the column was deposited on a rotating germanium disk at a speed of 10°/min. The disk stage, nozzle and transfer line temperatures of the LC-Transform were set at 160, 130 and 40 °C, respectively. An operating pressure of 100 torr was used.

### FTIR Analyses of the Deposited Analytes.

FTIR analysis was performed on a Thermo Nicolet iS10 spectrometer (Thermo Scientific, Waltham, MA), equipped with the LC-transform FTIR interface connected to a standard transmission baseplate. Spectra were recorded at a disk speed of 3°/min and resolution of 8 cm<sup>-1</sup> with 16 scans being recorded for each spectrum. Thermo Scientific OMNIC software (version 8.1) was used for data collection and processing.

## 4.3 Results and Discussion

### 4.3.1 Molar Mass Determination of HA's

The HA samples were first analysed using a mobile phase that is well known in literature for unmodified HA. The mobile phase consisted of an aqueous 0.1 M NaCl solution with 300 mg/L NaN<sub>3</sub>. It is clear from literature that the addition of an inorganic salt (e.g. NaCl, LiCl and LiBr) aids in the prevention of aggregate formation.<sup>4, 12-15</sup> As seen from the solubility studies and known from literature<sup>7</sup>, HA's form vast hydrogen bond networks in aqueous solutions, and the addition of a hydrogen bond disrupter is required. Furthermore, the addition of NaN<sub>3</sub> is to destroy any form of bacterial growth that might occur. This investigation was conducted as initial starting point in the method development for the SEC characterization of the HA's. **Figure 4.3** shows the chromatograms of HA samples with varying DS i.e. HA 03 (DS = 0), HAM 01 (DS = 3.1), HAM 03 (DS = 2.9) and HAM 06 (DS = 0.8). The SEC characterization was performed on the PSS Suprema column set due to the nature of the mobile phase.

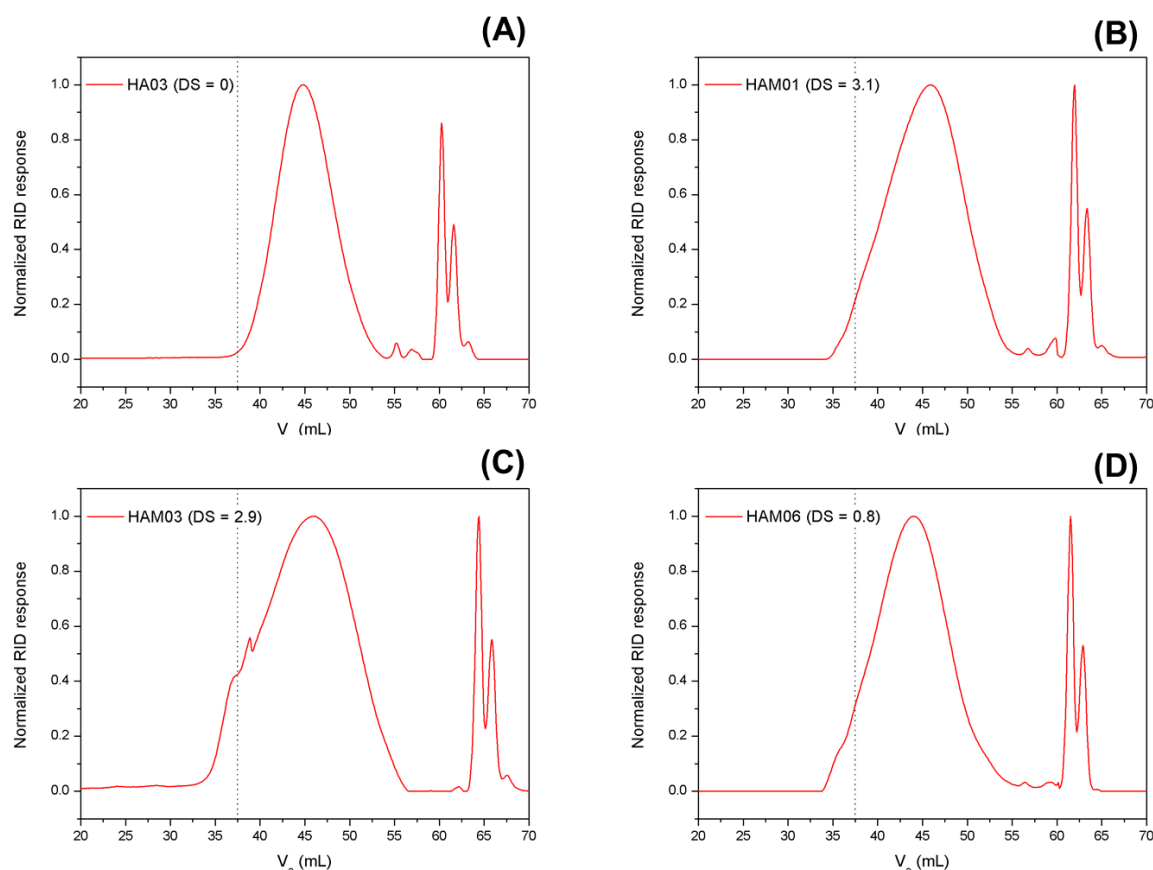


**Figure 4.3:** SEC-RI traces of the HA samples dissolved in 0.1 M NaCl eluent; injection volume: 100  $\mu$ L (conc. = 1.5 mg/mL); Eluent: aqueous 0.1 M NaCl solution with 300 mg/L  $\text{NaN}_3$ ; column: PSS-Suprema set at 40  $^{\circ}\text{C}$ ; RI temperature: 40  $^{\circ}\text{C}$ ; Flow rate: 1.0 mL/min; Detector: RI; Samples: (A) HA03 (unsubstituted), (B) HAM01 (DS = 3.1), (C) HAM03 (DS = 2.9) and (D) HAM 06 (DS = 0.8). The dotted line at 37.5 mL represents the exclusion limit of the column set.

From the figures it is evident that the mobile phase works fairly well for the unmodified HA, since there is no observable aggregation or any form of bimodality present in the RI traces. What is clear from **Figures 4.3 B–D** is that parts of the samples are eluting at the exclusion limit of the column set, which was determined to be 37.5 mL. Although no clear bimodality or shoulders are observed (except for image **C**), it is evident that some aggregation is still present for the modified HA's. This can be ascribed to the low water solubility of modified HA's. From the resulting chromatograms it is apparent that the present mobile phase is not the most effective regarding the modified samples.

To obtain molar mass information, a pullulan calibration was used. The use of pullulan as calibration standard was due to its chemical structure being close to the samples under investigation.

The elution in SEC is a function of the hydrodynamic volume/size of the analyte in solution, rather than on the actual molar mass. Therefore, the use of a calibration standard, e.g. pullulan, with a molecular structure different than that of the HA molecular structure, will only allow for the determination of relative molar masses. In order to obtain true molar mass information, well characterized standards of the same type as the analyte are required for calibration, or alternatively the use of a light scattering detector to enable the analysis of the absolute molar masses of the analytes. Pullulan has an inherent drawback, since it tends to overestimate MM's and MMD's of the present samples.<sup>16</sup> The data obtained therefore had a certain degree of uncertainty. The MM data obtained for the present mobile phase are reported in **Table 4.1**.

**Table 4.1:** Average molar masses and molar mass dispersities as determined by SEC with the HA's dissolved in 0.1M NaCl water solution and 300 mg/L NaN<sub>3</sub> on a PSS Suprema column set using a pullulan calibration.

Sample Code	Composition	DS	Mn (g/mol)	Mw (g/mol)	Đ
HA 01	Unmodified hyaluronic acid	–	188 100	290 000	1.54
HA 02		–	133 200	197 800	1.49
HA 03		–	66 500	126 100	1.90
HAM 01	Modified hyaluronic acid	3.1	34 300	129 700	3.79
HAM 02		3.4	15 100	67 900	4.48
HAM 03		2.9	15 600	264 800	17.0
HAM 04		2.6	3 800	82 800	21.6
HAM 05		2.2	61 400	137 200	2.23
HAM 06		0.8	324 400	3 964 600	12.2
HAM 07		0.4	568 400	7 808 200	13.7

It is evident from the MM results obtained that the present mobile phase is not the best choice, especially for modified HA, since they are not completely soluble in water. In SEC the resolution at the column exclusion limit (very high molar mass species) tends to decrease and as a result the dispersity index is also likely to increase. Therefore, a factor contributing to the increased dispersity index, indicating broad molar mass distributions for the NaCl mobile phase, may be the presence of fractions exceeding the exclusion limit of the SEC columns (aggregates).<sup>17</sup> The present method is quite suitable for unmodified HA, see **Table 4.1**, since the dispersities in those cases are relatively low and according to expected values, indicating that the unmodified HA's are well solvated by the mobile phase. This is also clear when looking at **Figure 4.3 (A)**, since the unmodified sample elutes within the exclusion limits of the column set. Nonetheless, method development with regard to the mobile phase had to be conducted, seeing that the mobile phase was not very effective for the modified HA's. As seen in **Figure 4.3 (B, C and D)** the modified HA's all elute at the

exclusion limit of the column set (37.5 mL). This is indicative of very high molar mass species, which can be ascribed to aggregates (occupying a large hydrodynamic volume in solution). Looking at the results obtained in **Table 4.1**, the dispersity index values for the modified HA's vary from moderate (HAM 05, DS = 2.2,  $\bar{M}_w/\bar{M}_n = 2.23$ ) to very high (HAM 04, DS = 2.6,  $\bar{M}_w/\bar{M}_n = 21.6$ ), which indicates that these samples are not solvated properly. It is, therefore, obvious from the result that the NaCl mobile phase is not the recommended choice for the modified HA's.

### 4.3.2 SEC Method Development for HA's in DMSO-Water

After establishing that aqueous 0.1 M NaCl solution with 300 mg/L  $\text{NaN}_3$  is not well suited for the modified HA's, results obtained from the solubility studies (refer to Chapter 3, **Table 3.2**) were exploited to find an appropriate solvent system for the samples under investigation. It was clear that the use of an organic modifier was required to dissolve the HA's irrespective of their DS. Therefore, the next approach was to analyse the samples with the binary solvent appearing to be the most promising, DMSO:H<sub>2</sub>O (60:40) (v/v%). Since an organic modifier was incorporated, an appropriate stationary phase was required for this purpose. The PSS GRAM column set was employed since it is compatible with DMSO. **Figure 4.4** shows the analysis of HA samples with varying degrees of substitution i.e. (A) HA 1 (DS = 0), HAM 10 (DS = 1.5) and HAM 09 (DS = 2.5) on this column. In this approach SEC was also hyphenated with a MALLS detector, in order to obtain a more descriptive picture on the degree of aggregation of the samples. One of the reasons for the hyphenation with MALLS is because the RI detector on its own was not capable of fully showing the extent of aggregation for the HA's due to the difference in detection principles for the detectors.

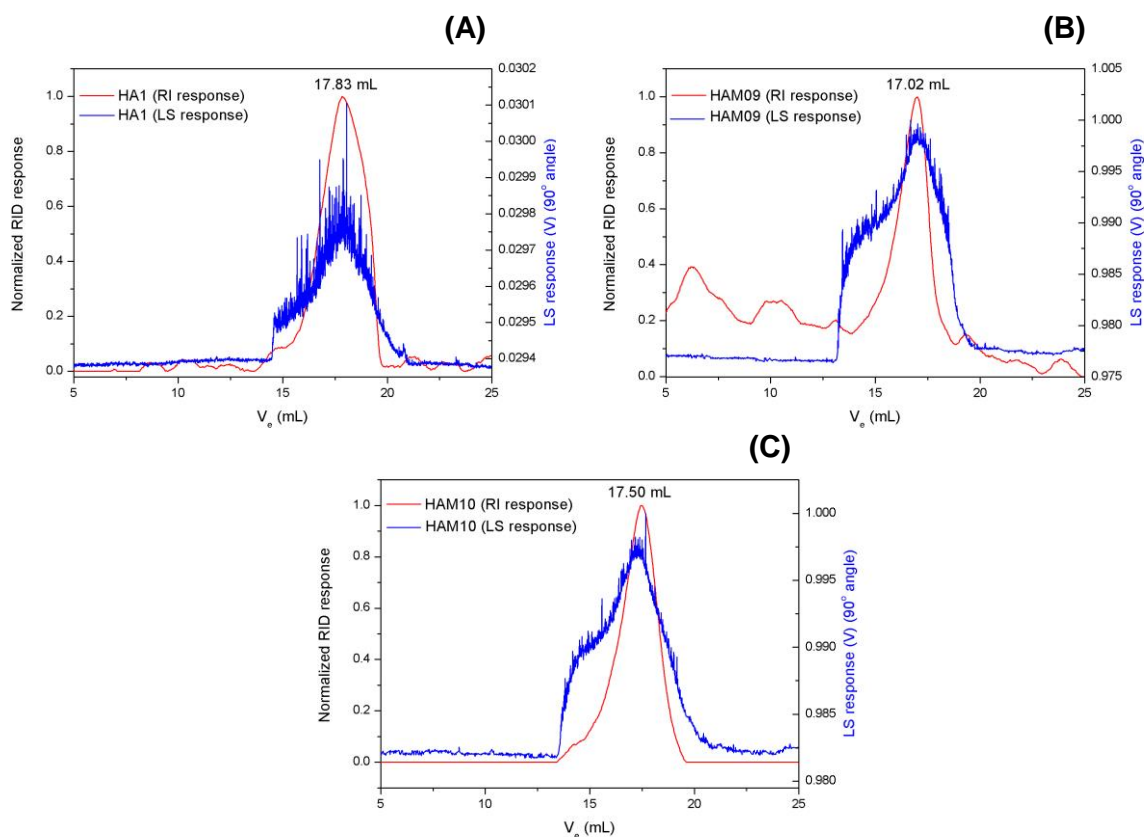


**Figure 4.4:** RI- (solid red line) and corresponding LS-traces (blue star-lines) of the HA samples dissolved in DMSO:H<sub>2</sub>O; injection volume: 100  $\mu$ L (conc. = 1.5 mg/mL); Eluent: DMSO:H<sub>2</sub>O (60:40)(v/v%); column: PSS-GRAM set at 40  $^{\circ}$ C; RI temperature: 40  $^{\circ}$ C; Flow rate: 0.30 mL/min; Detectors: MALLS and RI; Samples: (A) HA1 (unsubstituted), (B) HAM09 (DS = 2.5) and (C) HAM10 (DS = 1.5).

It is evident from the figure that DMSO:H<sub>2</sub>O (60:40) alone was not sufficient in breaking up aggregates, since the samples also eluted at the exclusion limit of the columns (which was determined to be 17.5 mL for the GRAM column set). The RI peaks of the three samples contain small pre-peaks at an elution volume of 13–15 mL at the base of the main peaks (higher molar masses) with a somewhat odd peak shape. These pre-peaks at lower elution volumes are possibly a result of aggregation between the polymer chains (as mentioned before). The higher the number of –OH groups, the higher the probability of H-bond formation (aggregation). Therefore, the lower the DS is the higher the probability of intermolecular interactions. The assumption of aggregation is supported by the corresponding LS-traces of the samples. From the LS-traces shoulders can be seen at the same elution volume as the RI-traces ( $V_e$  = 13–15 mL), which is indicative of very high molar mass species. In order to determine accurate molar mass data from light scattering

detection, suppression of aggregate formation is a prerequisite.<sup>18</sup> An increase in the temperature can aid in the solubility of the samples as well as decrease hydrogen bond formation. Therefore, the next approach was the analysis of samples at different temperatures in order to establish if a temperature increase would aid in the solubility of the samples and/or decrease aggregation. The temperature test would also give an indication as to what a suitable temperature for the effective separation of the samples according to their size in solution would be. Four different temperatures were investigated; 30 °C, 40 °C, 50 °C and 55 °C (the samples were dissolved at ambient temperature prior to analysis at variable temperatures). We were restricted regarding the maximum operating temperature, since the RI detector in our set-up has an upper temperature limit of 55 °C. Examples of the chromatograms obtained for HAM 10 (DS = 1.5) are illustrated in **Figure 4.5**.

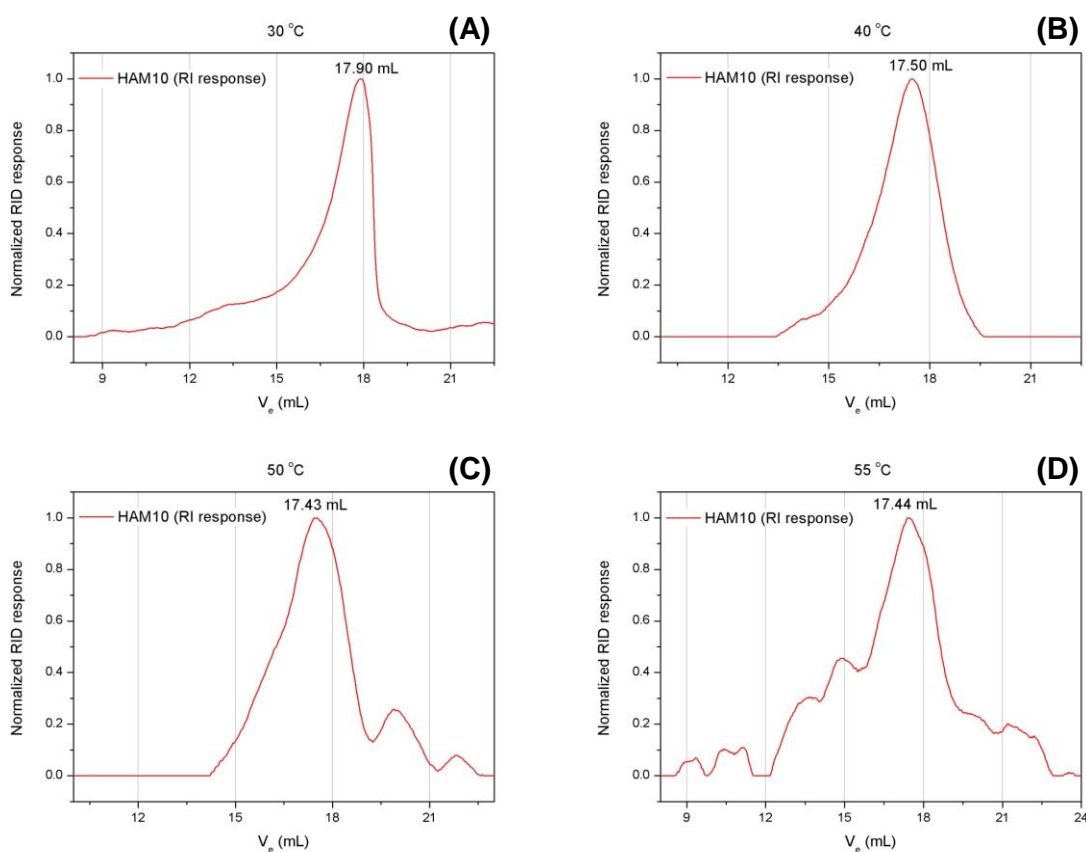


**Figure 4.5:** RI traces of sample HAM 10 (DS = 1.5) in DMSO:H<sub>2</sub>O (60:40) at (A) 30 °C, (B) 40 °C, (C) 50 °C and (D) 55 °C. Experimental conditions were the same as in **Figure 4.4**.

The effect that the temperature has on the separation of the samples was clear from the resulting RI traces. At 30 °C (image **A**) there is severe peak fronting that occurs, the reason for this is still unknown. Furthermore, the presence of aggregation can be seen at the base

of the main RI peak at an elution volume of 12–15 mL. At 40 °C (image **B**) the peak shape is improved compared to that at 30 °C with less peak fronting occurring, but the presence of aggregates is still an issue as can be observed around an elution volume of 13–15 mL. Looking at image **C** and **D**, the RI peak shapes start to look multimodal, with shoulders now also appearing after the main RI peak. The small peaks appearing before the main RI peak at an elution volume of 9–12 mL at 55 °C (image **D**), are not a result of aggregates, since no peaks were observed in the MALLS traces (not presented) at these elution volumes. These small peaks are possibly a result of detector noise caused by the DMSO, due to its high viscosity. The observable shoulder after the main RI peak is representative of smaller polymer species (since it elutes at higher elution volumes of 19–22 mL). This observation supports our hypothesis that the samples degrade at elevated temperatures. It would be advisable to work at higher temperature when working with DMSO in order to decrease the viscosity and the backpressure, however, in this case this is not possible due to sample degradation. Therefore, it is clear from the results that the operating temperature cannot exceed 40 °C or be below 40 °C. Thus, 40 °C was chosen as the most effective operating temperature for the given mobile phase to ensure that no sample degradation occurs.

After establishing a suitable operating temperature, the next step was to try and further improve the mobile phase, by decreasing the formation of aggregates. In order to obtain qualitative and quantitative MM information from light scattering it is crucial to completely suppress the formation of aggregates.<sup>18</sup> The commonly used solvent for the characterization of polysaccharides is DMSO with lithium salts or its combination with water for widely known reasons, such as good solvation without degradation at moderate temperatures and prevention of aggregation and adsorption of the material on the column.<sup>4, 19</sup> Therefore, experiments with different salts and salt concentrations were conducted in order to establish whether the addition of salt has a positive effect on breaking up aggregates in the samples under investigation, and if so to determine the amount of salt required to completely suppress aggregation. From literature, the two most frequently used salts with hyaluronic acid and DMSO to screen hydrogen bonds are NaCl and LiBr, respectively.<sup>4</sup> Due to the use of NaCl in literature to screen hydrogen bonds of HA in solution, the salt of choice to start with was NaCl. A concentration of 0.1 M NaCl was used. The samples were dissolved in the salt-modified mobile phase and then tested for their recoveries after filtration as a preliminary test. The results obtained were promising, with the exception of a few samples (see **Table 3.3** in section 3.1.3). However, when performing SEC on the samples with the DMSO:H<sub>2</sub>O/0.1M NaCl mobile phase, very poor signal-to-noise ratios were obtained for the samples. We assume that the salt decreased the polymer-polymer interactions, but not the polymer-stationary phase interactions and resulted in unfavourable adsorption of the analyte



on the SEC column. This could possibly be ascribed to solubility issues of NaCl in DMSO, since NaCl has a solubility of 0.4g/100 mL of DMSO at 25 °C. Even though it dissolves fully in water, the solubility limit in DMSO may cause undesirable interaction when the samples are dissolved in it. Thus, NaCl was ruled out as an option, which then led to the investigation of the LiBr salt. The solubility of LiBr in DMSO is 31.4 g/100 mL at 25 °C, which is much higher than that of NaCl. It is evident from literature that the addition of LiBr minimizes interaction with the column and hydrogen bonding as well as prevention of retrogradation problems for linear polysaccharides.<sup>20</sup>

Again the sample recoveries were tested after filtration, using a 0.05M LiBr salt concentration. The recovery tests were difficult to quantify, since LiBr is highly hygroscopic, and performing gravimetry on the recovered samples was challenging due to the recovered sample mass containing moisture. However, we continued with the study, and tested the LiBr mobile phase with SEC-MALLS. The resulting RI and LS traces are depicted for two samples, consisting of an unmodified sample (HA 02) and a modified sample (HAM 11, DS = 1.6) in **Figure 4.6**. The results obtained were promising since not only polymer-polymer interactions were minimized but also polymer-stationary phase interactions. An additional modification was made to the GRAM column set, only a guard column and one 1000 Å column was employed.

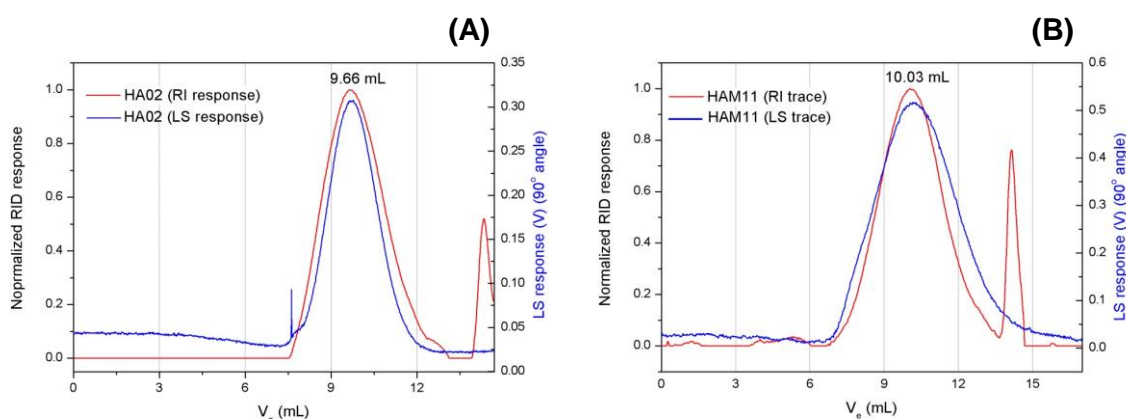


**Figure 4.6:** Overlays of the RI and LS traces of (A) HA 02 (unsubstituted) and (B) HAM 11 (DS = 1.6) in DMSO:H<sub>2</sub>O/LiBr; Injection volume: 100  $\mu$ L (conc. = 1.5 mg/mL); Sample solvent and eluent: DMSO: H<sub>2</sub>O (60:40, v/v%) + 50 mmol/L LiBr; Columns: PSS-GRAM guard column and one 1000 Å (300 mm x 80 mm I.D., 10  $\mu$ m) analytical column at 40 °C; RI temperature, 40 °C; Flow rate: 0.350 mL/min; Detectors: MALLS and RI.

From **Figure 4.6** it is evident that the addition of the LiBr aids in breaking up the aggregates, since in the LS traces of the samples (**A**) HA 02 (unsubstituted) and (**B**) HAM 11 (DS = 1.6) the bimodality has been suppressed. It is also apparent from the RI traces of the samples that the salt has a positive effect since the RI peak shapes are more Gaussian with no observable peak fronting and it seems like there is no real indication of aggregates present. In addition, the samples are also not eluting at the exclusion limit of the columns (refer Figure 4.6 for experimental conditions) which were experimentally determined to be 5.80 mL. Note that the small 'peaks' appearing just before the main peak of the RI trace in image **B**, are due to the high viscosity of the DMSO, which also affects the signal of the RI detector (baseline noise).

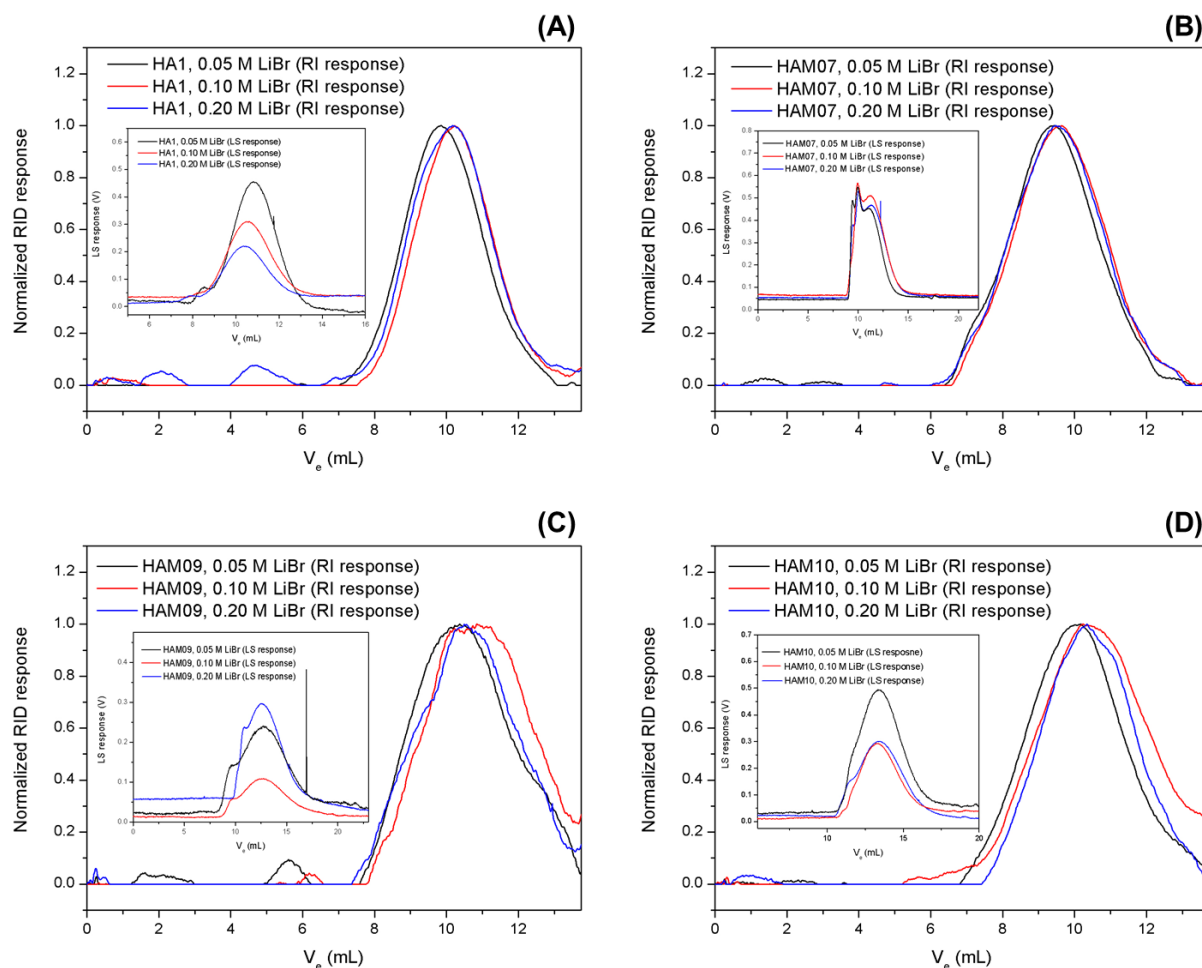


**Figure 4.7:** Overlays of the RI and LS traces (inset) for (A) HA1 (unsubstituted); (B) HAM07 (DS = 0.4); (C) HAM09 (DS = 2.5) and (D) HAM10 (DS = 1.5) at variable LiBr salt concentrations in the presence of DMSO:H<sub>2</sub>O/LiBr; Injection volume: 100  $\mu$ L (conc. = 1.5 mg/mL); Sample solvent and eluent: DMSO: H<sub>2</sub>O + X mmol/L LiBr (X = 50 (black), 100 (red) and 200 (blue)); Column: PSS-GRAM 1000 Å (300 mm x 80 mm I.D., 10  $\mu$ m) at 40 °C; RI temperature, 40 °C; Flow rate: 0.350 mL/min; Detectors: MALLS and RI.

After establishing that the addition of LiBr has a positive effect on sample dissolution and recovery, the mobile phase was then further investigated at variable salt concentrations of 0.05 M, 0.10 M and 0.20 M. This experiment was conducted in order to identify the amount of salt required to eliminate aggregation completely. The resulting RI and corresponding LS traces at variable salt concentrations are depicted for four representative samples (HA 1, unmodified; HAM 07, DS = 0.4; HAM 09, DS = 2.5 and HAM 10, DS = 1.5) in **Figure 4.7**.

For (image **A**) HA1 (unsubstituted) and (image **D**) HAM10 (DS = 1.5) the bimodality has been suppressed in both the RI and LS traces. However, taking samples (**B**) HAM07 (DS = 0.4) and (**C**) HAM09 (DS = 2.5) into consideration the LS traces look somewhat different when compared to the other two samples. The reason for the different LS traces can possibly be some sample alteration i.e. degradation with time or that these samples are still not fully solvated. However, it is still unclear as to why these samples behave slightly differently to the other samples, and further investigations are required to fully understand the nature of these samples. When looking at the RI and LS traces, it does not appear that the increased LiBr concentration makes a significant difference regarding the de-aggregation process (see **Figure 4.7**). A shift in the main LS peak with an increase in salt concentration to higher elution volumes would demonstrate a change in aggregation (less aggregation). An increase in the salt concentration above 0.05 M does not seem to influence the elution position of the main RI peaks. One notable point is that the LS traces tend to decrease in intensity as the LiBr concentration is increased.

From literature<sup>21, 22</sup> it is known that the pH of the mobile phase plays a pivotal role in the degradation and rheological properties of HA. At pH levels above and below 11 and 1.5, respectively, HA is irreversibly degraded. In a pH range of 5.0–11.0, the intrinsic viscosity  $[\eta]$  remains constant. Furthermore, the molecular radius and  $\eta$  decrease reversibly at a pH below 5 due to the protonation of the glucuronic acid groups. The pH of the current mobile phase was measured as 5.65. The assumption was made that the HA's do not undergo any form of degradation in the current mobile phase, which was therefore used without any additional solvent modifiers such as a buffer.

After establishing that the 0.05 M LiBr mobile phase is a viable option, the  $dn/dc$  values were required to obtain molar mass information from light scattering measurements. The  $dn/dc$  values for the samples were determined in DMSO:H<sub>2</sub>O/0.05 M LiBr at 40 °C. The  $dn/dc$  values enter by a power of 2 into the Rayleigh-Debye equation,<sup>23</sup> therefore, a slight change in the  $dn/dc$  value results in a large deviation in molar mass. As a result, the  $dn/dc$  values for the HA's have to be determined as accurately as possible. To our knowledge there are no  $dn/dc$  data for the HA samples in DMSO:H<sub>2</sub>O/LiBr available in literature. It is known that for some cellulose derivatives the  $dn/dc$  values change with DS.<sup>24, 25</sup> In order to establish whether the HA's would undergo the same trend as the cellulose derivatives, we investigated the  $dn/dc$  values as a function of DS. **Figure 4.8** illustrates the dependence of the  $dn/dc$  on DS for the HA's in the presence of DMSO:H<sub>2</sub>O/LiBr.

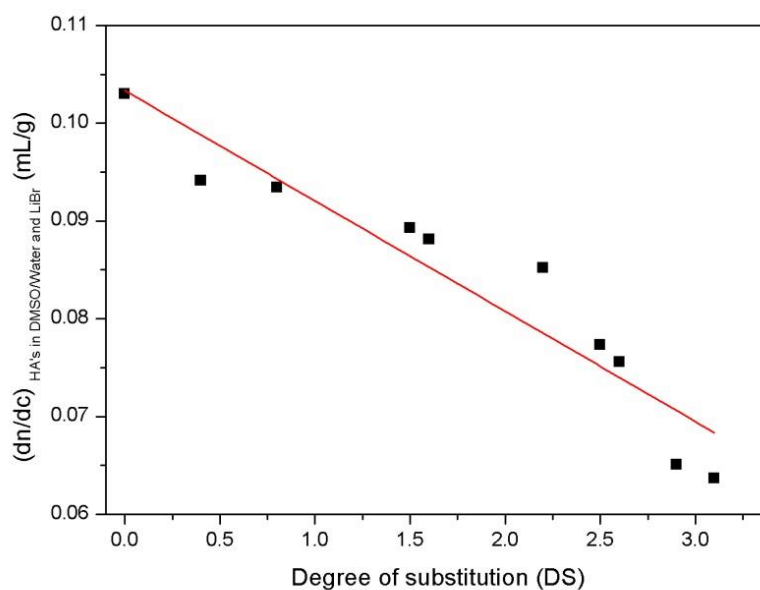


**Figure 4.8:**  $dn/dc$  values obtained in DMSO:H<sub>2</sub>O (60:40)/ 0.05M LiBr at 40 °C as a function of DS.

From **Figure 4.8** it is evident that the  $dn/dc$  values for the HA's do in fact change with DS (for the precise value obtained at each DS please refer to **Appendix B, Table B.1**). It was found that the  $dn/dc$  values for the HA's range from 0.0637 mL/g (for highest DS sample HAM 01, DS = 3.1) to 0.103 mL/g (for unmodified HA). The experimental procedure for determining the  $dn/dc$  values are given in section 4.2. The linear trend of the  $dn/dc$  as a function of DS can be described by **Equation 3.7**:

$$\left(\frac{dn}{dc}\right)_{\text{HA in DMSO/Water and LiBr}} = (0.103 - 0.011 \times DS) \text{ mL/g} \dots \dots \dots \text{Equation 3.7}$$

The  $dn/dc$  values for the samples can be calculated from Equation 3.7 once the DS value is known.

It is evident from literature that when working with DMSO as solvent the signal-to-noise (S/N) ratio is poor, especially when working at lower sample concentrations. It is also known that SEC is susceptible to column overloading for high molar mass polymers, resulting in certain problems (e.g. loss of resolution or concentration dependent molar masses).<sup>26–28</sup> Sample concentration studies are therefore crucial, since in SEC the sample concentration needs to be below the critical overlap concentration ( $c^*$ ). The critical overlap concentration is defined as the boundary between near-infinitely-dilute and semi-dilute solutions. Performing analysis above the  $c^*$  can lead to increased band broadening (due to a phenomenon known as

viscous fingering) as well as late elution, since the polymer becomes more compact at concentrations exceeding the  $c^*$ . Furthermore, it can invalidate the theoretical basis of certain detection methods. For example, light scattering detection theories assume the near-infinitely-dilute solutions model, and performing analysis above the  $c^*$  invalidates the calculations and conclusions associated with it.<sup>29</sup> Therefore, the effect of sample concentration was examined to determine what concentrations will provide good S/N ratios and do not result in column overloading. **Figure 4.9** depict two samples, HA 1 (DS = 0) and HAM 10 (DS = 1.5), tested at various sample concentrations.

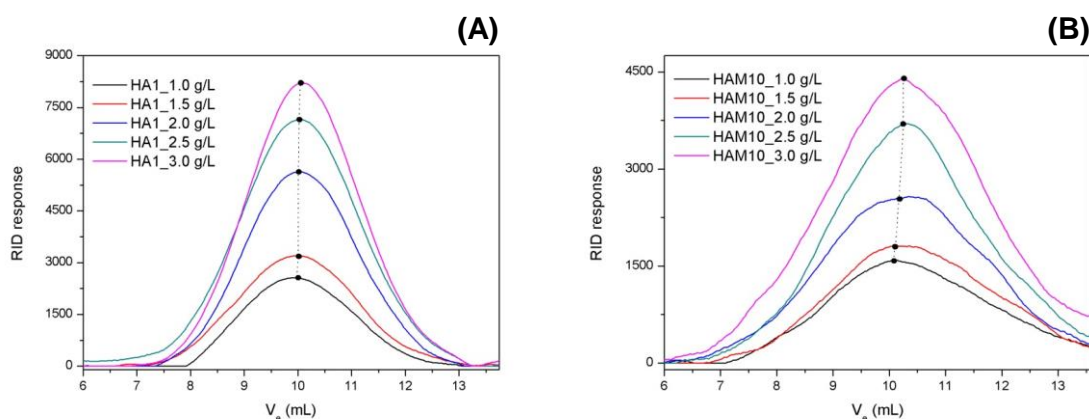


**Figure 4.9:** Overlaid RI traces at variable concentrations for samples (A) HA1 (unmodified) and (B) HAM10 (DS = 1.5) in the presence of DMSO:H<sub>2</sub>O/LiBr; Injection volume: 100  $\mu$ L; Sample solvent and eluent: DMSO: H<sub>2</sub>O + 50 mmol/L LiBr; Column: PSS-GRAM 1000 Å (300 mm x 80 mm I.D., 10  $\mu$ m) at 40 °C; RI temperature, 40 °C; Flow rate: 0.350 mL/min; Detector: RI.

It is clear from **Figure 4.9** that a sample concentration of 1.0 – 3.0 mg/mL has no major effect on the chromatographic behaviour of the samples, since the different concentrations produce good S/N ratios and there is no shift in the main RI peak. For the experiments that followed a concentration of 1.5 mg/mL was chosen, even though higher sample concentrations do not seem to affect the results. This was to ensure that the data obtained would obey the theories of light scattering since a MALLS detector was utilized to extract the absolute molar masses.

After the establishment of optimized SEC conditions for the HA's, SEC-MALLS experiments were conducted to obtain the absolute molar mass averages ( $M_n$  and  $M_w$ ) for the samples. In performing SEC-MALLS on the samples, information regarding the dependence of the molar mass on elution volume could also be evaluated. The results obtained for the absolute molar

mass averages, the molar mass dispersity values as well as the degrees of polymerization (DP) are tabulated in **Table 4.2**.

**Table 4.2:** Molar mass data obtained for samples HA01 – HAM11 using SEC-MALLS.

Sample Code (SU)	DS	Mn (g/mol)	Mw (g/mol)	Đ	DP <sub>w</sub>
HA 01	-	32 140	44 450	1.38	117
HA 02	-	30 700	47 120	1.54	124
HA 03	-	16 230	28 090	1.73	74
HA 1	-	16 240	28 060	1.73	74
HA 2	-	20 170	31 220	1.55	82
HAM 01	3.1	53 050	62 690	1.18	115
HAM 02	3.4	–	–	–	–
HAM 03	2.9	412 600	546 000	1.32	1019
HAM 04	2.6	39 400	55 810	1.42	107
HAM 05	2.2	30 010	36 360	1.21	73
HAM 06	0.8	39 320	135 700	3.45	321
HAM 07	0.4	31 410	79 040	2.52	197
HAM 08	2.6	28 240	65 290	2.31	126
HAM 09	2.5	33 020	57 750	1.75	112
HAM 10	1.5	32 970	62 240	1.89	135
HAM 11	1.6	37 800	58 650	1.55	126

From the results obtained for the DMSO:H<sub>2</sub>O/0.05M LiBr (60:40) mobile phase, it is clear that the addition of the salt was an improvement when compared to the mobile phase containing a 0.1M NaCl water solution and 300 mg/L NaN<sub>3</sub>. The occurrence of peak fronting, peak bimodality and aggregation has been minimized with the DMSO:H<sub>2</sub>O/0.05M LiBr (60:40) mobile phase. However, no molar mass information could be retrieved from sample HAM 02 (DS = 3.4), due to sample degradation. In the table, the degree of polymerization of each sample is also reported. The DP<sub>w</sub> values were determined from the obtained M<sub>w</sub> values. The calculations were performed using **Equation 3.8**, taking the change in molar mass of the monomer unit as a function of DS into account:

$$DP_w = \frac{(M_w)_{HA}}{(M_r)_{HA}} \dots \dots \dots \text{Equation 3.8}$$

where the  $(M_r)_{HA}$  is the molar mass of either the (1) unmodified or the (2) modified HA's, determined as follows:

(1) For unmodified samples  $(M_r)_{HA}$  is:

$$(M_r)_{HA} = 379.3 \text{ g/mol}$$

(2) For modified samples  $(M_r)_{HA}$  is calculated by **Equation 3.9**:

$$(M_r)_{HA} = 375.3 + (DS \times 55.06) + (4 - DS) \dots \dots \dots \text{Equation 3.9}$$

The samples used in this study are not all based on the same parent material, as is evident from by the degree of polymerization (DP) data. Assuming that the samples all consisted of the same parent material, and that the esterification reaction on the HA did not alter the backbones of the samples, the DP in theory should remain relatively constant. However, looking at **Table 4.2** there is no defined trend for the samples. However, some of the samples consisting of the same parent material do show the expected trend, for instance, samples HAM 08, HAM 09 and HAM 10 where modified from sample HA 1, and looking at their  $DP_w$  values, one can see there is no major difference. The molar masses of the samples should increase with an increase in DS, due to the addition of the acrylic anhydride fragment onto the HA backbone. Since the samples do not consist of the same parent material it is rather difficult to observe this trend.

### 4.3.3 SEC Coupled to LC Transform with FTIR

After the separation of the HA's according to molar mass, the coupling of a selective detector (e.g. FT-IR) was used to determine the degree of substitution as a function of molar mass. SEC was hyphenated to a LC-Transform interface in order to collect solvent-free separated fractions, followed by analysing them with FT-IR spectroscopy. After the establishment of the optimum conditions for the LC-Transform instrument (see experimental), the HA's were successfully collected on the collection interface (Germanium disc). However, a solvent-free deposition of the SEC fractions was unsuccessful, due to the presence of the LiBr salt. After a sample was deposited onto the Germanium disc, within 2–5 min the hygroscopic LiBr was almost completely saturated with moisture (see **Figure 4.10**). This led to very poor S/N ratios, making reproducibility an impossible task. An alternative to performing off-line analysis would be to try and modify the FT-IR interface in such a way to allow for the continues purging of the interface with an inert gas such as nitrogen or argon to obtain a moisture-free environment. The same approach can also be explored on-line FT-IR analysis.<sup>30, 31</sup> Another option is to employ a salt that can be evaporated with the solvent. As mentioned in section 3.1, ammonium acetate salt was tested as a possible H-bond disrupter. However, the recovery tests conducted after filtration in the presence of ammonium acetate proved that this salt is not ideal since the sample recoveries were moderate (ca. 60%) and would not allow for the true representation of the bulk sample. Attempts were made to



analyse the samples in the presence of ammonium acetate salt, but our attempts failed as well due to very bad S/N ratios. This was ascribed to very low sample concentrations being deposited onto the collection interface.

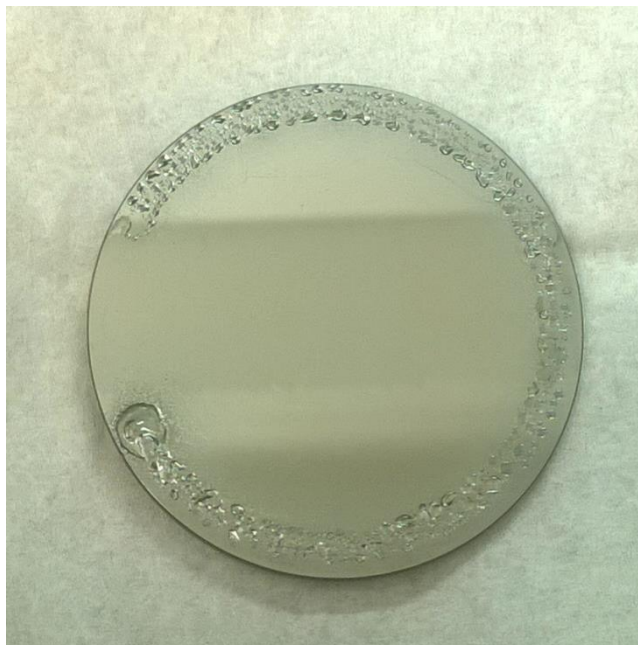


**Figure 4.10:** Sample deposition on Germanium disc after SEC. 5 min after removal from the LC-Transform instrument, the presence of moisture is apparent due to the presence of the LiBr salt.

#### 4.4 Conclusion

In conclusion, the newly developed LiBr salt-modified mobile phase is a major improvement compared to the NaCl mobile phase generally utilized for unmodified HA's. The presence of aggregates has been minimized, as evidenced by the RI and complementary LS traces, and the samples did not elute at the exclusion limit of the SEC column. Furthermore, LS is shown to be a suitable method for determining the absolute molar masses of the samples providing additional information on the nature of the samples. MALLS detection also eliminates the use of calibration standards, which tend to have a certain degree of uncertainty associated with it, regarding the different chemical compositions of the analytes and the calibrants.

## References

- [1] Yu-Jin, J.; Ubonvan, T.; Kim, D. *J. Pharm. Invest.* **2010**, 40, 33–43.
- [2] Balazs, E. A.; Leshchiner, A. U.S. Patent No. 4,582,865. 15 Apr. **1986**.
- [3] Illum, L.; Farraj, N. F.; Fisher, A. N.; Gill, I.; Miglietta, M.; Benedetti, L. M. *J. Controlled Release.* **1994**, 29 (1), 133–141.
- [4] Ciric, J.; Oostland, J.; De Vries, J. W.; Woortman, A. J. J.; Loos, K. *Anal Chem.* **2012**, 84 (23), 10463–10470.
- [5] Gidley, M. J.; Hanashiro, I.; Hani, N. M.; Hill, S. E.; Huber, A.; Jane, J.-L.; Liu, Q.; Morris, G. A.; Rolland-Sabate, A.; Striegel, A. M.; Gilbert, R. G. *Carbohydr. Polym.* **2010**, 79, 255–261.
- [6] Cave, R. A.; Seabrook, S. A.; Gidley, M. J.; Gilbert, R. G. *Biomacromolecules.* **2009**, 10, 2245–2253.
- [7] Rinaudo, M. *Polym. Int.* **2008**, 57 (3), 397–430.
- [8] Striegel, A.; Yau, W. W.; Kirkland, J. J.; Bly, D. D. *Modern size-exclusion liquid chromatography: practice of gel permeation and gel filtration chromatography.* John Wiley & Sons, Hoboken, New Jersey, USA, **2009**, 234–239.
- [9] Held, D.; Kilz, P. *The Column.* **2008**, 4 (10), 17–20.
- [10] Held, D. *The Column.* **2013**, 9 (18), 2–5.
- [11] Huglin, M.B. (Ed.). *Light Scattering from Polymer Solutions.* Academic Press, London, **1972**, 41–54, 165–203, 397–448, 459–466.
- [12] Coppola, G.; Fabbri, P.; Pallesi, B.; Bianchi, U. *J. Appl. Polym. Sci.* **1972**, 16 (11), 2829–2834.
- [13] Hann, N. D. *J. Polym. Sci., Polym. Chem. Ed.* **1977**, 15 (6), 1331–1339.
- [14] Connors, W. J.; Sarkanen, S.; McCarthy, J. L. *Holzforschung.* **1980**, 34 (3), 80–85.
- [15] Ludlam, P. R.; King, J. G. *J. Appl. Polym. Sci.* **1984**, 29, (12), 3863–3872.
- [16] Yeung, B.; Marecak, D. *J. Chromatogr. A.* **1999**, 852, 573–581.
- [17] Podzimek, S.; Hermannova, M.; Bilerova, H.; Bezakova, Z.; Velebny, V. *J. Appl. Polym. Sci.* **2010**, 116, 3013–3020.
- [18] Tanner, D. W.; Berry, G. C. *J. Polym. Sci., Polym. Phys. Ed.* **1974**, 12 (5), 941–975.
- [19] Chuang, J.-Y.; Sydor, R. J. *J. Appl. Polym. Sci.* **1987**, 34, 1739–1748.
- [20] Hernández, J. M.; Gaborieau, M.; Castignolles, P.; Gidley, M. J.; Myers, A. M.; Gilbert, R. G. *Biomacromolecules.* **2008**, 9, 954–956.
- [21] Gura, E.; Hüchel, M.; Müller, P.J. *Polymer Degradation and Stability.* **1998**, 59, 297–302.
- [22] Gatej, I.; Popa, M.; Rinaudo, M. *Biomacromolecules.* **2005**, 6, 61–67.
- [23] Bloomfield, V.A. *Biopolym.* **2000**, 54 (3), 168–172.
- [24] Badger, R. M.; Blaker, R. H. *J. Phys. Colloid Chem.* **1949**, 53 (7), 1056–1069.
- [25] Das, B.; Choudhury, P. K. *J. Polym. Sci., Part A-1: Polym. Chem.* **1967**, 5 (4), 769–777.
- [26] Eldson, W. L.; Goldwasser, J. M.; Rudin, A. *J. Polym. Sci., Polym. Lett. Ed.* **1981**, 19 (10), 483–493.
- [27] Mori, S. *J. Appl. Polym. Sci.* **1976**, 20 (8), 2157–2164.
- [28] Song, M. S.; Hu, G. X.; Li, X. Y.; Zhao, B. *J. Chromatogr. A.* **2002**, 961 (2), 155–170.
- [29] Teraoka, I. *Polymer solutions: An introduction to physical properties.* John Wiley & Sons, New York, USA, **2002**.
- [30] Beskers, T. F.; Hofe, T.; Wilhelm, M. *Polymer Chemistry.* **2015**, 6 (1), 128–142.

- [31] Beskers, T. F.; Hofe, T.; Wilhelm, M. *Macromol. Rapid Commun.* **2012**, 33 (20), 1747–1752.

## Chapter 5

### LAC Method Development for the HA's

*The development of a gradient LAC method for the separation of HA according to chemical composition is reported in this chapter. The chemical composition of the HA's was systematically investigated to obtain more insight into their structure-property relationships. Furthermore, the analysis of the HA's by gradient LAC-FTIR is described. The chapter is divided into an introductory part, experimental procedure, results and discussion as well as a conclusion part.*

#### 5.1 Introduction

When developing a gradient LAC method for the separation of HA's according to their DS, the primary step is to find a suitable stationary phase that will be proficient for the separations to be established. The second step is to establish which solvents will be most suitable to allow the effective separation of the selected samples. For gradient LAC separations at least two solvents of different strength (polarity) are required. Gradient LAC is governed by two main mechanisms, (1) an adsorption-desorption mechanism and, (2) a precipitation-dissolution mechanism. Gradient LAC can be performed in either the reversed phase (RP) or normal phase (NP) mode. NP-LAC is the older of the two modes, and works as follows: a polar stationary phase is utilized in conjunction with a gradient whose polarity index increases over the course of the chromatographic run. The sample is, generally, dissolved in a thermodynamically good solvent, which then follows the injection of the sample into the chromatographic column comprising of a mobile phase of weak(er) eluent strength. Since the mobile phase at the beginning of the injection has a lower polarity index than that of the stationary phase, it will result in the adsorption of the sample to the stationary phase. Desorption of the sample will then continuously occur as the strength of the mobile phase is increased over the course of the chromatographic run. The order of elution in NP-LAC is as follows, the more polar (less substituted) samples will elute at higher volumes, whereas the less polar (more substituted) samples will have a lower elution volume. The desorption of the polymeric materials will occur at different mobile phase compositions, which in turn should relate to the chemical composition of the individual polymeric chains. There is a variant of NP-LAC known as hydrophilic interaction liquid chromatography (HILIC), which partly overlaps with other chromatographic techniques such as ion chromatography as well as RP-LAC. In the case of HILIC, it comprises of a

hydrophilic (polar) stationary phase, such as in NP-LAC, however, is operated with reversed phase type eluents (any aprotic solvent miscible with water). The separation mechanism in HILIC is described as a liquid-liquid partition chromatography, since it is hypothesized that the mobile phase forms a water-rich layer on the polar stationary phase opposed to the water deficient mobile phase. This result in analytes partitioning between the two liquid layers, creating the liquid-liquid extraction mechanism. The order of elution in HILIC is the same as in NP-LAC, where the analytes elute in order of increasing polarity.<sup>1</sup> In RP-LAC, a less polar stationary phase is utilized with a gradient whose polarity index decreases over the chromatographic run. The order of elution is the inverted scenario of NP-LAC.<sup>2</sup>

## **5.2 Experimental**

### **Solvents and Chemicals**

Water (H<sub>2</sub>O) (Sigma-Aldrich), acetonitrile (ACN) (Merck), dimethyl sulfoxide (DMSO) (Sigma-Aldrich), tetrahydrofuran (THF) (Sigma-Aldrich), methanol (MeOH) (Romil-SPS™) and hexane (Hex) (Merck), all solvents were of HPLC-grade and were used as received.

### **Analytical Techniques**

#### **Gradient Liquid Adsorption Chromatography (LAC)**

HPLC analysis was performed on an Agilent 1200 series HPLC instrument (Agilent Technologies, Boblingen, Germany) consisting of the following components: an on-line degasser, quaternary pump, auto-sampler, thermostatted column compartment, variable wavelength (UV) detector and an Agilent 1260 infinity evaporative light scattering (ELSD) detector. Data collection and processing were performed using WinGPC Unity software (Version 7.0). Different stationary and mobile phases were explored, however, only two stationary phases will be presented in this work. The stationary phase of choice was a Discovery® cyano (CN) column (250 x 4.6 mm I.D., 100 Å pore size, 5 µm particle size (Supelco Bellefonte, USA)). Preliminary results obtained on a Zorbax RX-C8 column (150 x 2.1 mm I.D., 100 Å pore size, 5 µm particle size (Agilent, USA)) will also be presented.

The experimental procedure for the analysis of the HA's according to their chemical composition was as follows, unless stated otherwise: The HA samples (0.5 mg) were dissolved in 1 mL of DMSO:H<sub>2</sub>O (60:40) [v/v%] for a dissolution period of 16 hours at ambient temperature with agitation at 500 rpm. The samples were covered with aluminium foil, due to the possibility of degradation by light. After the dissolution period the samples

were then filtered through a 0.45  $\mu\text{m}$  RC filter. An injection volume of 20  $\mu\text{L}$  at an operating temperature of 30  $^{\circ}\text{C}$  with a flow rate of 0.50 mL/min was used for the all the HA's. For detection the evaporative light scattering detector was operated at an evaporation temperature of 100  $^{\circ}\text{C}$  and a pressure of 3.0 bars with a signal gain of 9.0 mV. The two eluents used in the gradient LAC separation were ACN and H<sub>2</sub>O. The gradient profile used for the separation of the HA's according to chemical composition is given in **Table 5.1**.

**Table 5.1:** Description of the optimized linear gradient profile.

Time Interval (min)	Mobile Phase Composition (%)
0	100 % ACN: 0 % Water
3	100 % ACN: 0 % Water
38	0 % ACN: 100 % Water
48	0 % ACN: 100 % Water
50	100 % ACN: 0 % Water
80	100%ACN: 0 % Water

} Column re-equilibration step

## LC-FTIR and FTIR Spectroscopy

### Analyte Deposition by LC-Transform Interface

Refer to section 4.2 for instrumental details. A mobile phase flow rate of 0.50 mL/min was used. The nozzle and transfer line temperatures of the LC-Transform were set to 70 and 30  $^{\circ}\text{C}$ , respectively. For the disk stage, a temperature of 120  $^{\circ}\text{C}$  with a pressure gradient of 350–150 torr was used. The pressure gradient systematically decreased with the linear gradient. This was done in order to ensure the complete removal of the water.

### FTIR Analysis of the Deposited Analytes

FTIR analyses were carried out as reported in section 4.2.

## 5.3 Results and Discussion

### 5.3.1 Separation of the HA's according to DS

The separation of the HA's according to their degree of substitution will be described in this chapter. Gradient LAC was selected for the purpose of this study, since the aim was to first separate the polar unmodified HA's from the less polar modified HA's, followed by the separation of the modified HA's according to their DS. Since the HA samples contain polar

hydroxyl groups they should interact with a polar stationary phase and result in some sort of adsorption. Therefore, normal phase LAC was used to separate the samples. With the aid of a suitable mobile phase, the polar unmodified HA's will interact with the polar stationary phase and elute at higher elution volumes compared to the modified HA's. The unmodified HA's are highly polar due to the presence of the hydroxyl groups on the polymer backbone. With the introduction of the acrylic groups onto the HA polymer backbone the polarity of the HA's is reduced, hence a reduced water solubility is obtained. The degree to which the modified HA's are less polar than the starting material depends on the degree of substitution.

In order to establish which eluent will be suitable for the use in gradient LAC of the HA samples, we made use of the solubility results obtained in Chapter 3 (section 3.1). As we have come to see from the solubility studies conducted on the HA samples, DMSO:H<sub>2</sub>O (60:40) is the only solvent that dissolves all the samples, irrespective of their DS. Furthermore, it was also clear from the solubility studies that the use of ACN and water as eluent would be suitable for gradient LAC, since certain ratios of ACN to water result in the solubility of samples with a specific DS (see **Table 3.2**). At the same time ACN-water is compatible with the sample solvent. Therefore, ACN and water would be favourable in the separation of the HA's according to their DS. Since DMSO/water/LiBr would be the preferred sample solvent to use (as evident from Chapter 4), a problem arises with this sample solvent for gradient LAC application. LiBr is a non-volatile salt and is, therefore, incompatible with ELSD detection. Thus DMSO/water without the addition of a salt was employed as sample solvent for gradient LAC. Furthermore, the use of DMSO and water as eluents in gradient LAC would be the preferred choice since it gives the best solubility results and does not deviate too much with regard to polarity from the sample solvent. However, the use of DMSO as initial eluent is not recommended due to its high viscosity producing excessively high back pressure at the given operating temperatures. At the same time, its strength as initial solvent and also the fact that DMSO shows a significant amount of detector noise does not make it a preferred choice as mobile phase.

When the HA samples are injected into 100% ACN as initial eluent onto a polar stationary phase, they should get adsorbed owing to the lower polarity of ACN compared to the stationary phase. With the introduction of a stronger eluent (more polar than ACN) such as water, the samples should desorb from the column, resulting in their elution. Preliminary chromatographic experiments had to confirm that the HA's (dissolved in a DMSO/water mixture) adsorbed onto the cyano (CN) stationary phase due to the ACN as initial solvent, and with the gradual addition of water will result in desorption. A simple linear gradient was tested going from 100% ACN to 100% water with a CN stationary phase (see **Table 5.1**).

The results obtained showed that, when ACN was used as initial eluent followed with the gradual change from ACN to water, the modified HA's eluted before the unmodified HA's, as expected. This meant that under these conditions ACN was acting as adsorption promoting solvent and water was acting as desorption promoting solvent.

As can be seen from the results obtained (**Figure 5.1**), all the samples elute within the established gradient, but at different elution volumes ( $V_e$ ) according to the previously determined DS. The column dead volume ( $V_0$ ) was experimentally determined to be 2.8 mL. From **Figure 5.1** it can be seen that all samples elute after 2.8 mL, which indicates that the separations occur in LAC mode. This finding proves that HA's with different degrees of substitution elute at different mobile phase compositions. Furthermore, it is indicative that all the samples are initially adsorbed onto the CN stationary phase (even though some part of the sample, or the solvent or matrix elutes early as is evident by the pre-peak arising at an elution volume of 4mL), regardless of the fact that DMSO/water was used as sample solvent.



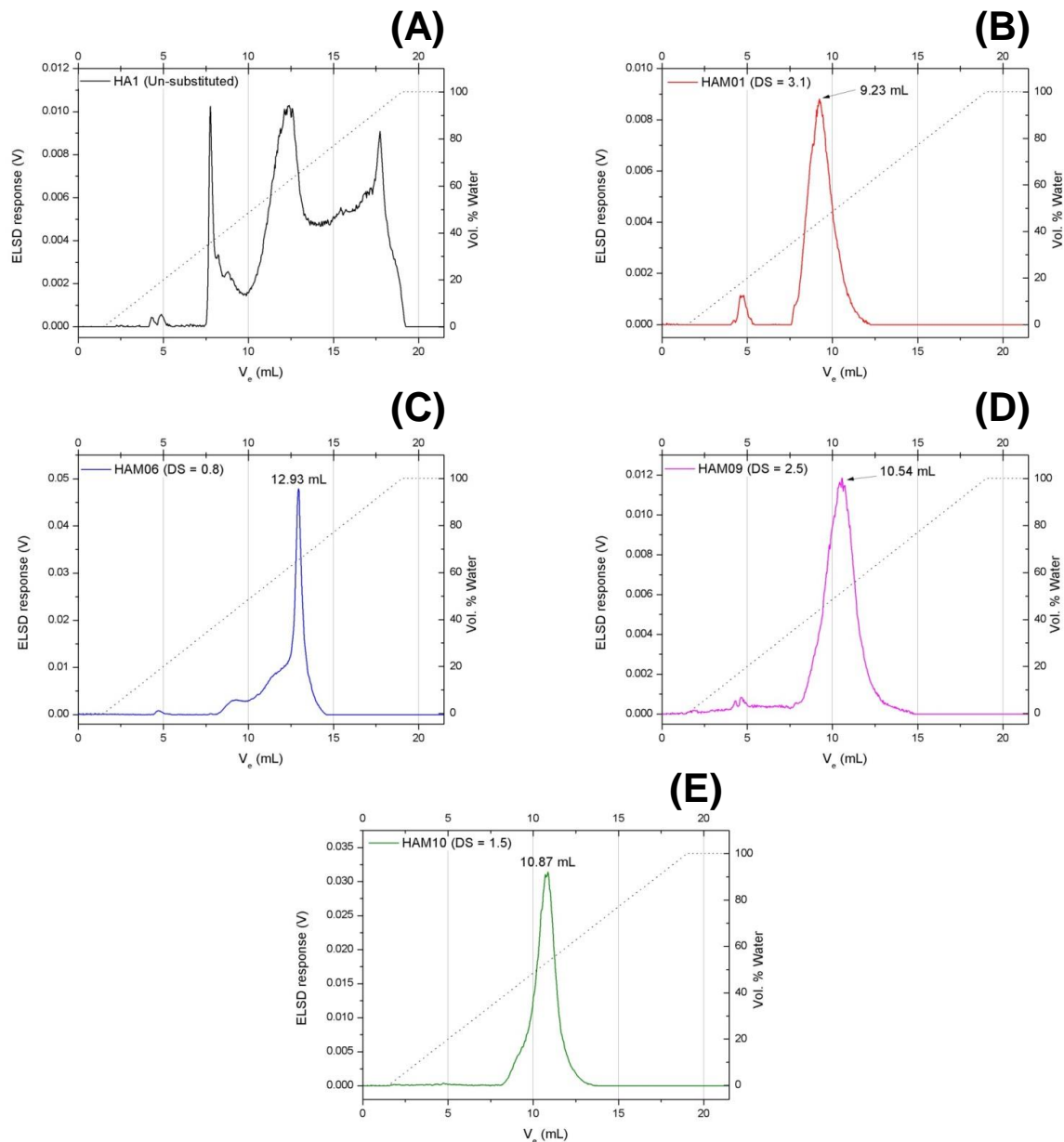


**Figure 5.1:** Chromatograms of HA's having different DS values; Sample solvent: DMSO:H<sub>2</sub>O (60:40) (v/v%); Injection volume: 30  $\mu$ L (conc. = 0.5 mg/mL); Gradient profile: linear gradient from 100% ACN to 100% H<sub>2</sub>O. (A) sample HA1 (un-substituted), (B) sample HAM 01 (DS = 3.1), (C) sample HAM 06 (DS = 0.8), (D) HAM 09 (DS = 2.5) and (E) sample HAM 10 (DS = 1.5).

The samples presented in **Figure 5.1** were selected in such a way that they would cover the largest DS range. It is clear from **Figure 5.1** that the unmodified (A) and low modified (C) samples, respectively, show a rather different elugram shape compared to the samples of higher DS. This can possibly be ascribed to the high chemical heterogeneity of these samples. As can also be seen from the figures, there is a fairly good separation of the HA's,

when comparing the peak apex elution volumes, with the selected DS range. Furthermore, in NP chromatography the change in temperature, in general, will only have minor effects on sample selectivity (band spacing of compound). However, changes in the selectivity may occur with temperature variations for mobile phases that contain localizing solvents (solvents showing a higher affinity to interact with the stationary phase) such as acetonitrile in the present case. Therefore, the use of different temperatures to change the selectivity in NP chromatography was explored. A temperature change with a localizing solvent can have an effect on the overall retention of all the compounds.<sup>2</sup> Different temperatures were investigated on the CN column, however, in the current case it has been found that the optimal separation temperature is 30 °C for the HA's with the solvents being employed.

After establishing that the CN column does provide separation of the HA's with the applied linear gradient, the next step was to test the reproducibility of HA's chromatograms on the CN column. **Figure 5.2** shows the resulting repeatable chromatograms of two selected samples, **(A)** sample HAM 10 (DS = 1.5) and **(B)** sample HAM 01 (DS = 3.1).

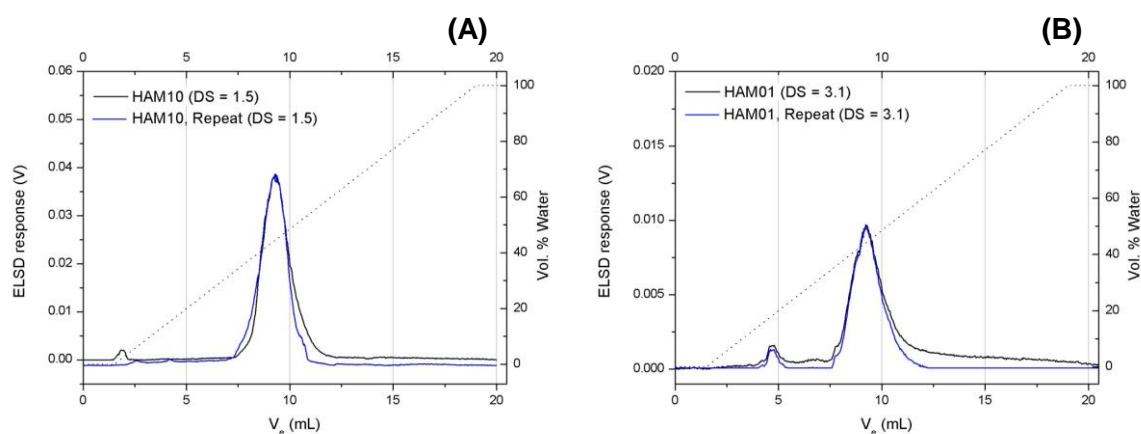


**Figure 5.2:** Illustration of the reproducibility of separation using overlaid chromatograms of two HA samples varying in DS value; Sample solvent: DMSO:H<sub>2</sub>O (60:40) (v/v%); Injection volume: 30 μL (conc. = 0.5 mg/mL); Gradient profile: linear gradient from 100% ACN to 100% H<sub>2</sub>O. **(A)** Sample HAM 10 (DS = 1.5), **(B)** sample HAM 01 (DS = 3.1).

As can be seen from **Figure 5.2**, the resulting chromatograms are nearly identical. These results show that the developed method is reproducible. Following the reproducibility tests, sample recovery tests had to be conducted to verify that there is no irreversible adsorption to the chromatographic column. It is well known from literature that the ELSD response is dependent upon various parameters, such as the type of sample, mobile phase and

instrumental parameters e.g. molar mass, chemical composition, mobile phase composition and gas flow.<sup>3, 4</sup> For the HA's under investigation, the predominant factor was the mobile phase composition, since different mobile phase compositions have a significant effect on the ELSD response (see **Appendix C, Figure C.1**).

It is evident from literature that the eluent composition at the time an analyte elutes from the column in gradient LAC is close or equal to the critical conditions at which the analyte elutes from the column in an isocratic experiment.<sup>5</sup> In order to determine the recoveries of the samples on the CN column as accurately as possible, the mobile phase composition at the elution volume apex of the samples was determined and used. Fraction collection was performed on all the samples. The sample peak areas obtained from the evaporative light scattering detector were analysed and compared before and after fractionation. The results obtained showed that the CN column provides recoveries of more than 90% of all the samples, which can be regarded as quantitative recoveries for the applied method.

In order to investigate the origin of the pre-peaks arising at lower elution volumes ( $V_e = 4$  mL) as seen in **Figure 5.1**, the influence of experimental parameters, e.g. injected volume and injected amount of sample was investigated. The first investigation was to study the influence of the injection volume of the sample solvent (DMSO:H<sub>2</sub>O (60:40)) on the pre-peak occurring at lower elution volumes. For the purpose of this investigation the same amount (ca. 0.5 mg) of sample HAM 09 (DS = 2.5) was injected by varying the injected volume, the range selected was 1  $\mu$ L – 50  $\mu$ L in order to obtain a more complete picture. The results obtained for this investigation are illustrated in **Figure 5.3**. Only one sample was used for the purpose of the test, sample HAM 09 (DS = 2.5). The investigation also aided in the determination of what the best suited injected volume would be for analysis on the CN column.

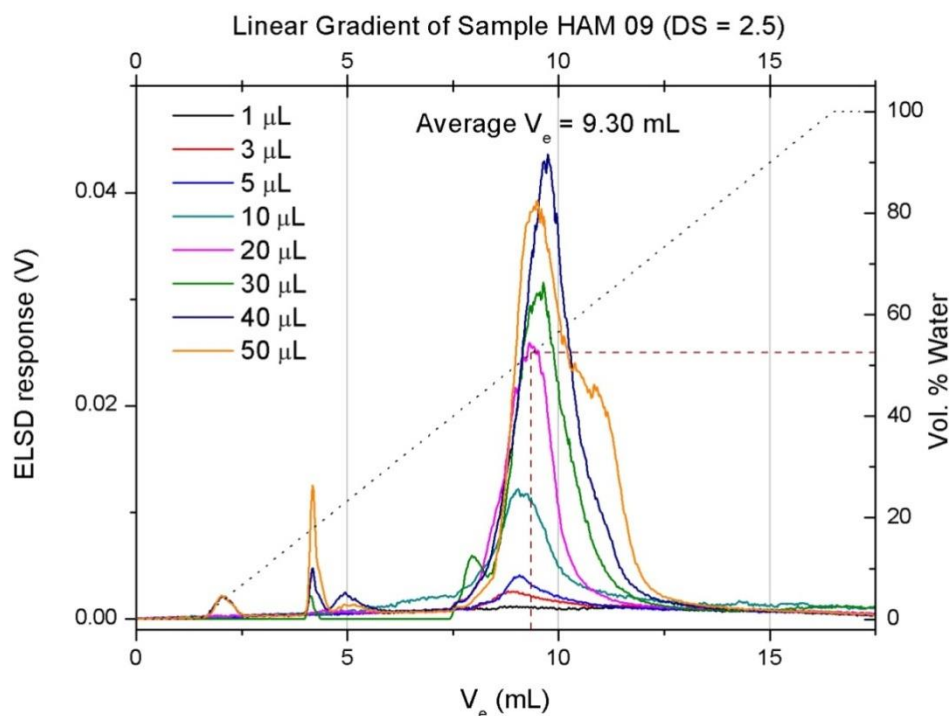


**Figure 5.3:** Influence of variable injected volumes of sample HAM 09 (DS = 2.5) on the CN column on the intensity of the pre-peak; Sample solvent: DMSO:H<sub>2</sub>O (60:40)(v/v%); Gradient profile: linear gradient from 100% ACN to 100% water in 30 min. The dashed line is a representative of the mobile phase composition at the detector.

From **Figure 5.3** it is clear that with a change in the injected sample volume, there is a change in the peak area of the broad main peak ( $V_e = 7.5 - 12.5$  mL) that increases with an increased injected volume. Taking a closer look at the peak apex ( $V_e = 9.3$  mL), it elutes at relatively the same position. The smaller pre-peak ( $V_e = 4$  mL) also does not change position, however, it does tend to increase in peak area with an increase in the injected volume. The small pre-peak which elutes after the column dead volume of 2.8 mL, can be a result of a breakthrough effect, which is caused by a sudden change in eluent strength between ACN and that of the sample solvent comprising of a mixture of DMSO/water (60:40) (v/v%). In a study conducted by Jiang et al.<sup>6</sup> they investigated the parameters causing the breakthrough phenomenon. They drew the conclusion that when a polymer is dissolved in a thermodynamically strong eluent and then injected into an eluent of weaker strength, breakthrough peaks may occur.<sup>6</sup> In the present case breakthrough peaks appear at higher injected volumes (>30  $\mu$ L). Therefore, injected volumes were restricted to <30  $\mu$ L in the following experiments, where a mixture of DMSO/water (60/40) was used as sample solvent.

An injection volume of 20  $\mu\text{L}$  was chosen in order to minimize the breakthrough peak as well as not to overload the column, and allow for effective separations.

It is known that for an adsorption-desorption separation mechanism the retention volume of a sample may have a correlation to the sample concentration. With an increase in the sample concentration there might be a decrease in the retention volume, which is a good result of the adsorption isotherm becoming non-linear (i.e. column overloading).<sup>7-9</sup> Since this generalized behaviour can have an effect on the samples under investigation, experiments were performed in order to determine what the influence of the sample concentration is on the retention volume. The resulting chromatograms are illustrated in **Figure 5.4**, where a linear gradient has been applied to sample HAM 10 (DS = 1.5), injected at various concentrations ranging between 0.5 – 1.5 mg/mL.

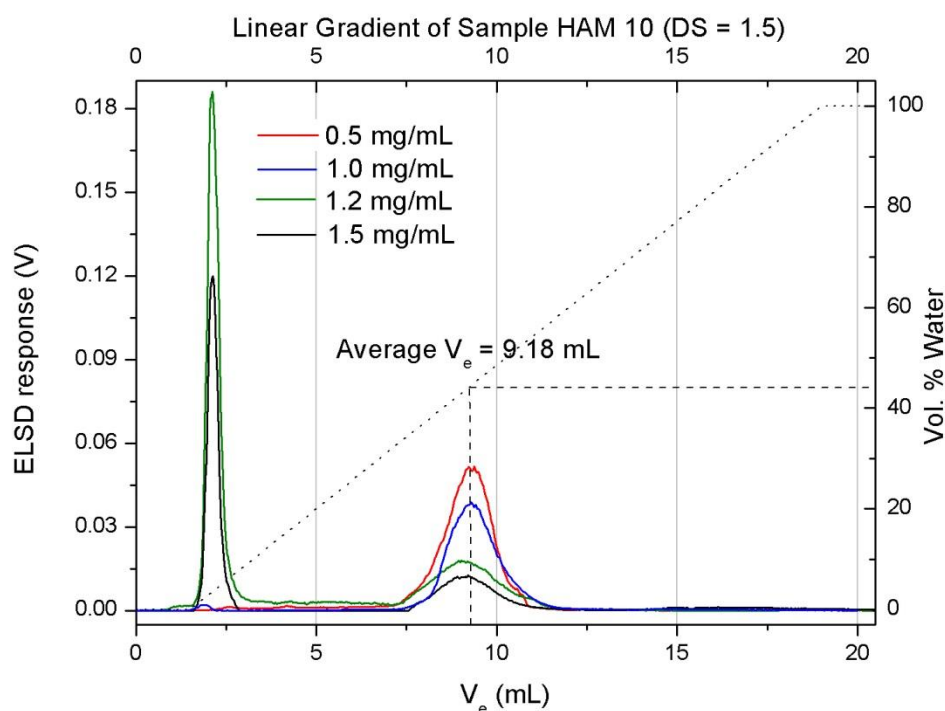


**Figure 5.4:** Illustration of the effect of variable injected concentrations on the retention behaviour of sample HAM 10 (DS = 1.5) on the CN column; Sample solvent: DMSO:H<sub>2</sub>O (60:40)(v/v%); Injection volume: 20  $\mu\text{L}$ ; Gradient profile: linear gradient from 100% ACN to 100% water in 35 min. The dashed line is a representative of the mobile phase composition at the detector.

What is apparent from **Figure 5.4** is that a sharp and intense pre-peak is observed at around ca. 2.2 mL at concentrations exceeding 1.0 mg/mL. The intensity of the pre-peak also

increases with an increase in the sample concentration. There is no notable shift in elution volume of either the pre-peak (2.2 mL) or main peak (7.5 – 11 mL) of the sample. Thus, no column overloading was observed for the sample at the concentrations evaluated. An interesting observation is that the main peak intensity decreases with an increase in sample concentration. This is due to the fact that more material is eluting in the pre-peak. The exclusion limit (1.7 mL) and column dead volume (2.8 mL) were experimentally determined for the CN column. Taking these values into account, the pre-peak arising at 2.2 mL can possibly be ascribed to either aggregation of the sample or a breakthrough peak since it eluted between the exclusion limit and the column dead volume. However, the assumption was made that it is more likely to be aggregates, since it elutes closer to the exclusion limit of the CN column. Large aggregates cannot enter the pores of the stationary phase, and as a result are excluded from the chromatographic column. This is probably due to the fact that no salt is used to screen hydrogen bond formation of the samples in the sample solvent developed for HPLC. The presence of aggregates probably has a direct correlation to the intensity of the pre-peak. Thus the assumption was made that with an increase in the sample concentration, the probability of aggregation increases and as aggregation increases, a greater part of the sample will be excluded from the chromatographic column, resulting in an increased pre-peak and decreased main peak. Since no salt has been added to the gradient HPLC method, we decided to use a concentration of 0.5 mg/mL for the samples in all the experiments, seeing that it provides the best signal response without the undesired pre-peak occurring.

After the establishment of the most effective sample concentration and injection volume, separations were conducted on all the samples. The optimized gradient profile used for this purpose is tabulated in **Table 5.1**.

The dependence of the DS on the elution volume (using the peak apexes of the samples) is illustrated in **Figure 5.5**. Irrespective of some scattering occurring around the regression line, it is clear that the samples elute in an expected order, from highest DS to lowest DS, which is in agreement with the expected course of separation in NP chromatography on a CN column. The reason for the observed trend is due to the weaker interaction strength of the higher DS HA's, as result of less hydroxyl groups available to interact with the CN column for lower DS samples. From this finding we can conclude that separation on the CN column is a function of the degree of substitution.

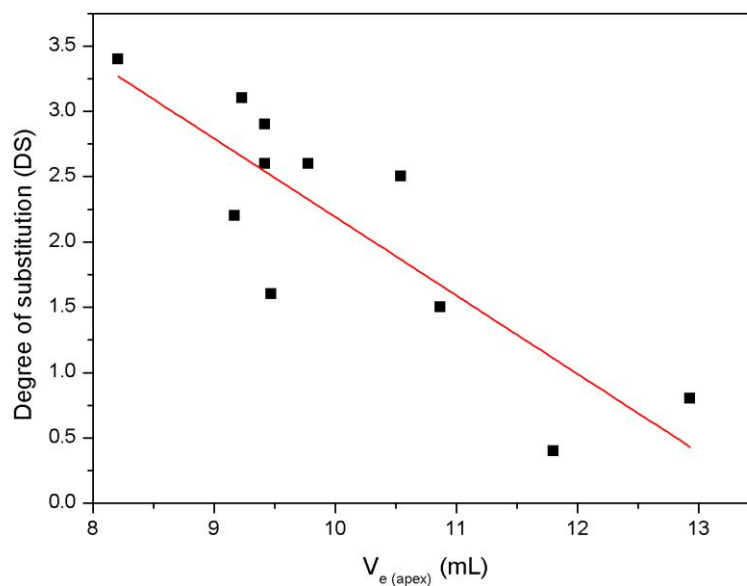


**Figure 5.5:** Illustration of the chromatographic retention as a function of the DS for all the HA samples (DS range of 0.4–3.1).

An interesting observation made from **Figure 5.5** is that some of the higher DS samples and lower DS samples have more or less the same elution volumes. In order to understand this observation some of the samples were overlaid to obtain more insight. **Figure 5.6** shows the overlaid elugrams of some selected samples that would represent the entire DS range.

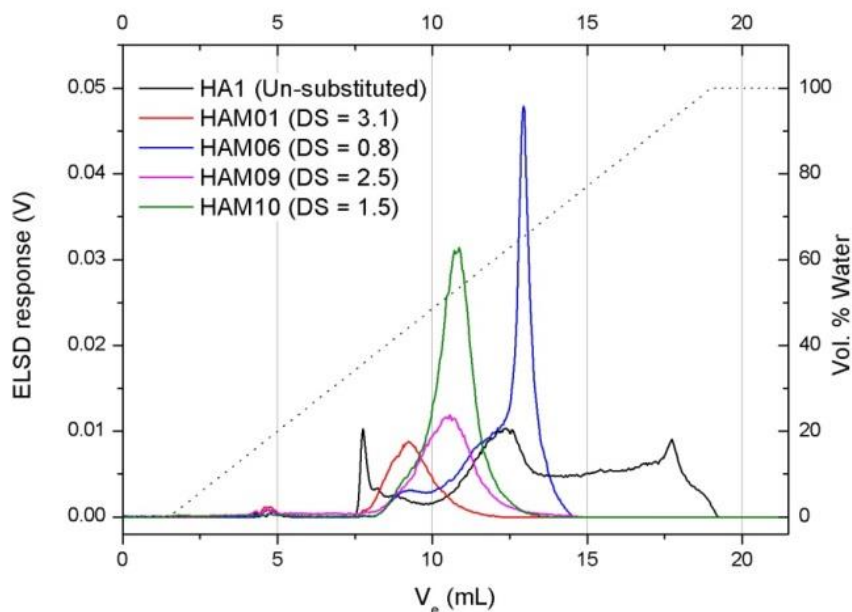


**Figure 5.6:** Overlaid chromatograms of HA samples representing the biggest part of the DS range. Experimental conditions are the same as in **Figure 5.1**.

As can be seen for the overlaid samples, the elution volume at the peak apexes for samples HA 1 (unsubstituted) and HAM 06 (DS = 0.8) are more or less the same; this is also true for samples HAM 09 (DS = 2.5) and HAM 10 (DS = 1.5). However, taking their elution profiles into account, these samples are all intrinsically different. For example, sample HAM 06 (DS = 0.8) has an elution volume peak apex at 12.93 mL, which corresponds to the main peak of the unmodified sample HA 1. However, this is not a true representation of the DS for sample HAM 06, since the chromatogram does not have a well-defined narrow peak shape but rather a broad elution profile, where there is a broad section with two observable shoulders before the peak apex. The fraction represented by the peak apex may possibly have a chemical composition more similar to that of an unmodified HA sample.

The gradient method developed can be used to calculate the DS of the HA's from the elution volume; however, the values obtained from this calculation will have a relatively large percentage error for certain samples, since only the elution volumes at peak apexes are considered and not the entire elution peak. In order to perform this calculation for the DS, the dependence of the DS on elution volume was fitted by linear regression to obtain a suitable equation (see **Figure 5.7**). A linear regression was employed, since the assumption was made that when using a simple linear gradient, the retention of the HA's will have a linear retention as a function of the DS. The DS calculation from elution volume can be described by the following equation:



$$DS_{V_e} = 8.199 - 0.6008 \times (x) \dots \dots \dots \text{Equation 5.1}$$

Where  $DS_{V_e}$  is the DS corresponding to a given elution volume and  $x$  is the elution volume at the peak apex.

### 5.3.2 Sample stability studies

In the experimental section it was mentioned that the samples were covered with aluminium foil, since there is the possibility of altering the chemical composition of the samples by light. To test whether our hypothesis holds true, light degradation experiments were conducted. For this investigation the samples were prepared as mentioned in the experimental section 5.2. After the dissolution period the samples were injected into the CN column. The same set of samples was then exposed to light for a period of seven days and re-injected into the CN column. The resulting chromatograms of two samples, HA 1 (unmodified) and HAM 01 (DS = 3.1) are depicted in **Figure 5.7**.

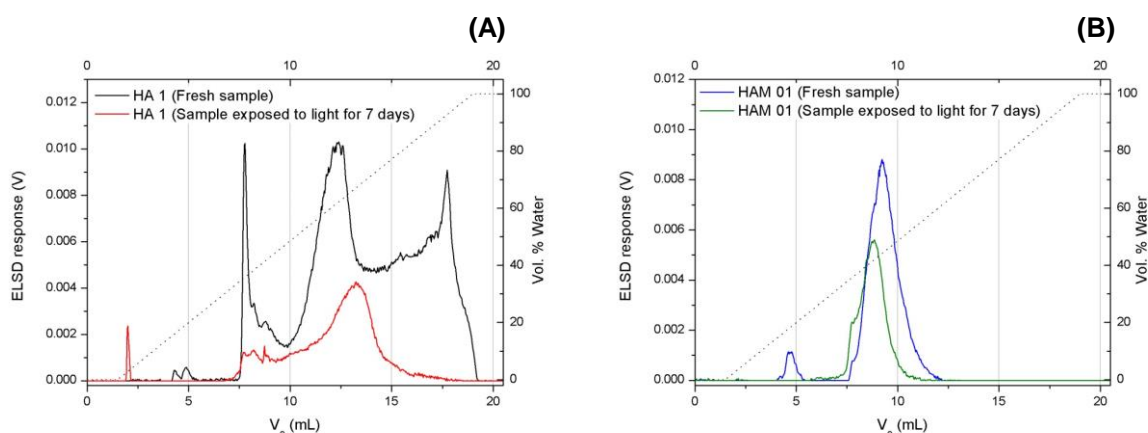


**Figure 5.7:** Elution profiles of samples (A) HA 1 (unmodified) and (B) HAM 01 (DS = 3.1) before and after exposure to light. Same experimental conditions as used in **Figure 5.4**.

What is evident is that the elugrams before and after exposure to light are not the same with regard to peak position and intensity. There is a slight shift in the peak apex for both the samples, in sample HA 1 (image **A**) it seems that the peak apex of the middle peak shifts to higher elution volumes and for sample HAM 01 (image **B**) the peak apex shifts to lower elution volumes. Furthermore, the intensities of the elugrams after light exposure also decreased. This is even more severe for sample HA 1 (image **A**), since not all the peaks are observed in the sample exposed to light. It is also apparent from the **Figure 5.7** that

unmodified HA is less stable than modified HA. This confirms our hypothesis that light does in fact alter the chemical composition of the samples to a certain extent. It is not yet clear what exactly is happening to the samples when they are exposed to light. We assume that the samples either photo-polymerize, resulting in crosslinking of the samples, or undergo some sort of cleavage resulting in the degradation of the sample.<sup>10–15</sup> However, this should be subject to further investigations.

### 5.3.3 Gradient LAC Coupled to LC transform with FTIR

For more structural information HPLC was coupled to FT-IR due to its sensitivity, simplicity as well as speed of analysis.<sup>16, 17</sup> FT-IR provides an in-depth look into the chemical substructure and additional information on a given specimen when used with separation techniques such as LAC. In this work the aim behind the hyphenation of gradient LAC with FT-IR was to analyse the HA's according to their degree of substitution as a function of chemical composition and possibly different functional groups. The hyphenation with FT-IR should also confirm the validity of the developed LAC method as well as shed some insight onto the pre-peak arising at low elution volumes ( $V_e = 4$  mL). As a test for the applicability of the LC-FTIR approach, sample HAM 09 (DS = 2.5) was analysed by gradient LAC-FTIR (refer to **Figure 5.4** depicting the chromatogram of HAM 09 after gradient LAC separation). **Figure 5.8** presents the information obtained on the chemical composition of sample HAM 09 (DS = 2.5) after chromatographic separation.

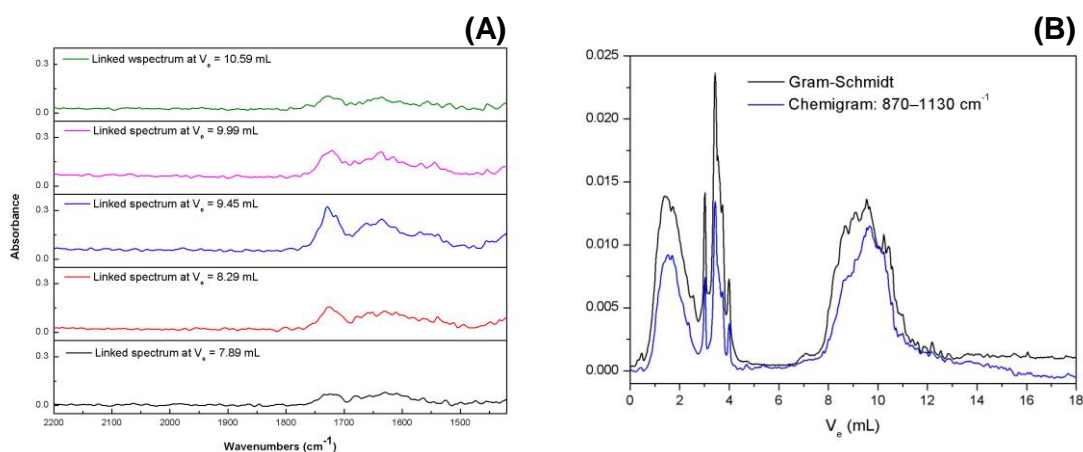


**Figure 5.8:** (A) Linked FT-IR spectra and (B) selected chemigram of the gradient LAC-FTIR analysis of sample HAM 09 (DS = 2.5). Stationary phase: CN column; Sample solvent: DMSO:H<sub>2</sub>O (60:40)(v/v%); Sample concentration: 1 mg/mL; Injection volume: 100  $\mu$ L; Gradient profile: linear gradient from 100% ACN to 100% water in 35 min. Additional experimental conditions as explained in section 5.2.

From image (A) the evolution of the characteristic absorption region ( $1680\text{--}1790\text{ cm}^{-1}$ ) for the acrylic moiety (which is directly related to the DS) can be observed. Only certain spectra were selected to illustrate the change. As can be seen in **Figure 5.8 (A)**, there is an increased intensity in the characteristic absorption region of  $1680\text{--}1790\text{ cm}^{-1}$  after which a maximum is reached, followed by a decrease in intensity again. This holds a direct correlation to certain fractions with different degrees of substitution that elute from the chromatographic column. As a result of the measurements, chemigrams are obtained, which present the intensity profile of a certain absorption band across the elution profile. The typical absorption fingerprint region for HA are the skeletal C-O group at  $870\text{--}1130\text{ cm}^{-1}$ . As seen from image (B), the concentration profile shows one significant peak at an elution volume of  $7\text{--}12\text{ mL}$ . This elution peak corresponds to that of **Figure 5.4** as well as revealing the absorption of the fingerprint region for HA. The observation made in the chemigram is confirmed by the overlay of the Gram-Schmidt plot, which is representative of the sum of all absorptions and relates to the sample concentration. Furthermore, the dependence of the degree of substitution on the elution volume is shown in **Figure 5.9**.

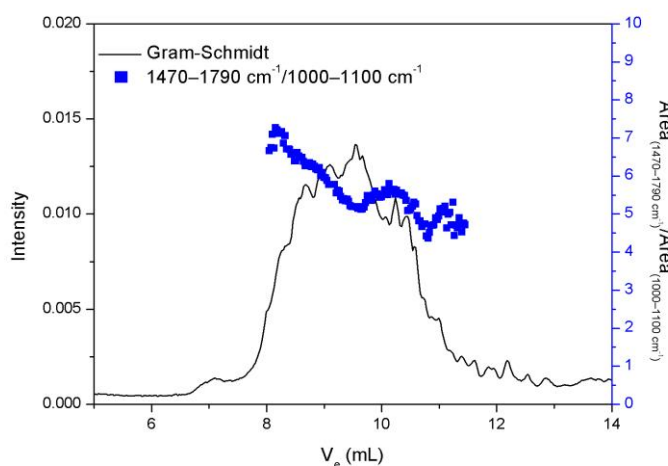


**Figure 5.9:** Elution profile of the main peak and concentration of carbonyl groups across the elution profile. Refer to **Figure 5.8** for experimental conditions.

A clear trend can be observed from the figure, with an increase in the elution volume there is a decrease in the peak area of the ratio between the characteristic and fingerprint regions. These regions hold a direct correlation to the degree of substitution as previously determined in section 3.2. This finding also indicates that separation according to the degree of substitution was accomplished within a single sample as well. To address the pre-peak arising at an elution volume of  $4\text{ mL}$  for the majority of the samples, a three dimensional plot was constructed, revealing the absorption bands that correspond to the pre-peak, see

**Figure 5.10.** As seen from **Figure 5.8 (B)** the intensity of the pre-peak is also more severe than previously shown, the reason being that higher concentrations (1 mg/mL) with higher injection (100  $\mu$ L) volumes were utilized to obtain adequate absorption spectra from FT-IR.

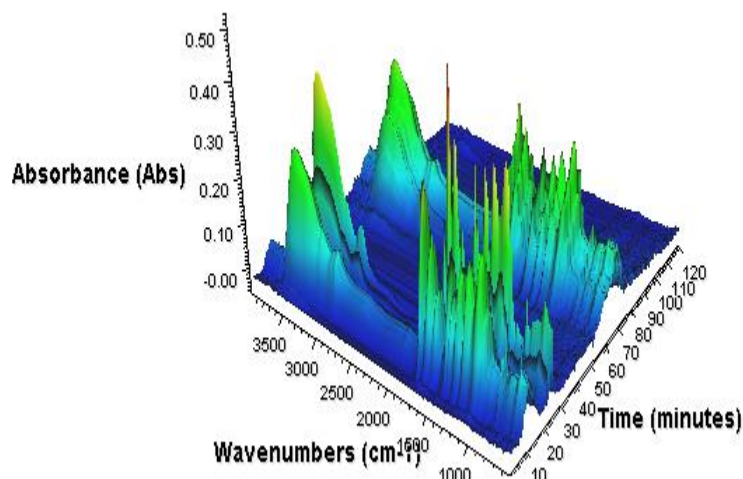


**Figure 5.10:** The absorbance and wavenumbers as a function of elution time determined by gradient LAC-FTIR. Refer to **Figure 5.8** for experimental conditions.

As seen from **Figure 5.10** the pre-peak arising at an elution volume of 1.5 – 4 mL (10 – 45 min.) has an almost identical absorption spectrum compared to the main peak observed at an elution volume of 7 – 12 mL (60 – 80 min.). FT-IR spectroscopy cannot prove whether the pre-peak is due to aggregation or a breakthrough peak. Nevertheless, it supports the assumptions drawn from the results obtained by gradient LAC that the pre-peak may possibly be a result of a breakthrough peak, or aggregates (when higher concentration of the HA samples are dissolved in the sample solvent without the addition of a salt), since the pre-peak has a chemical composition similar to that of the main peak. Thus, the conclusion can be drawn from the results that the CN column does in fact separate the HA's according to their degree of substitution and confirms the validity of the developed chromatographic method. It is also clear from gradient LAC-FTIR that the addition of a salt (preferably ESLD compatible) is required to ensure that no information is lost due to the presence of aggregates. Further investigations have to be conducted on an entire array of HA samples with varying DS to ensure that the conclusions drawn are in fact valid for all separations conducted on the CN column.

### 5.3.4 Preliminary C8 column results

After performing gradient LAC on the CN column and establishing that it works relatively well for the HA samples under investigation, another column, namely a C8 column, was investigated in reversed phase mode. This test was done to determine whether separation of the HA's is possible in the reversed phase mode and as a possible alternative to the CN column. The details of the C8 column used are given in the experimental section. For the purpose of this investigation the same experimental conditions as employed for the CN column were used, with the only difference being that water was used as the initial eluent. **Figure 5.11** illustrates the preliminary results obtained on the C8 column, using a linear gradient from 100% water to 100% ACN.

In **Figure 5.11**, two distinct peaks can be seen for all modified HA samples. The first peak eluting at around 2 – 5.5 mL can possibly be attributed to either a breakthrough peak or unmodified HA fragments since it elutes after the column dead volume of 0.5 mL. The peak eluting between 6 – 11 mL is ascribed to the modified HA samples and varies according to the DS in the given elution range. The results obtained on the C8 column are very promising, since separation is obtained for all samples in the DS range investigated, and the elution profiles of the samples are well defined, with no undesired interactions resulting in odd elution profiles. Furthermore, sample recoveries on the C8 column were very promising, with more than 95% of the injected sample masses being recovered from the column. Looking at image (F) in **Figure 5.11**, it is clear that samples with varying DS elute at different elution volumes. However, the elution ranges for the modified HA's are very close to each other, and further investigations to optimize the conditions for the C8 column could possibly provide baseline separation between samples of varying DS. The order of elution for the modified HA samples is in accordance with the reversed phase mechanism, with more polar (less substituted) samples eluting before the less polar (more substituted) samples. The first peak eluting at around 4 mL for all the modified samples was assumed to be either a breakthrough peak or unmodified HA fragments, although, this should be confirmed. From the preliminary results conducted on the C8 column, it is clear that the use of a C8 column in reversed phase mode can possibly be employed as alternative to the CN column used in normal phase mode.

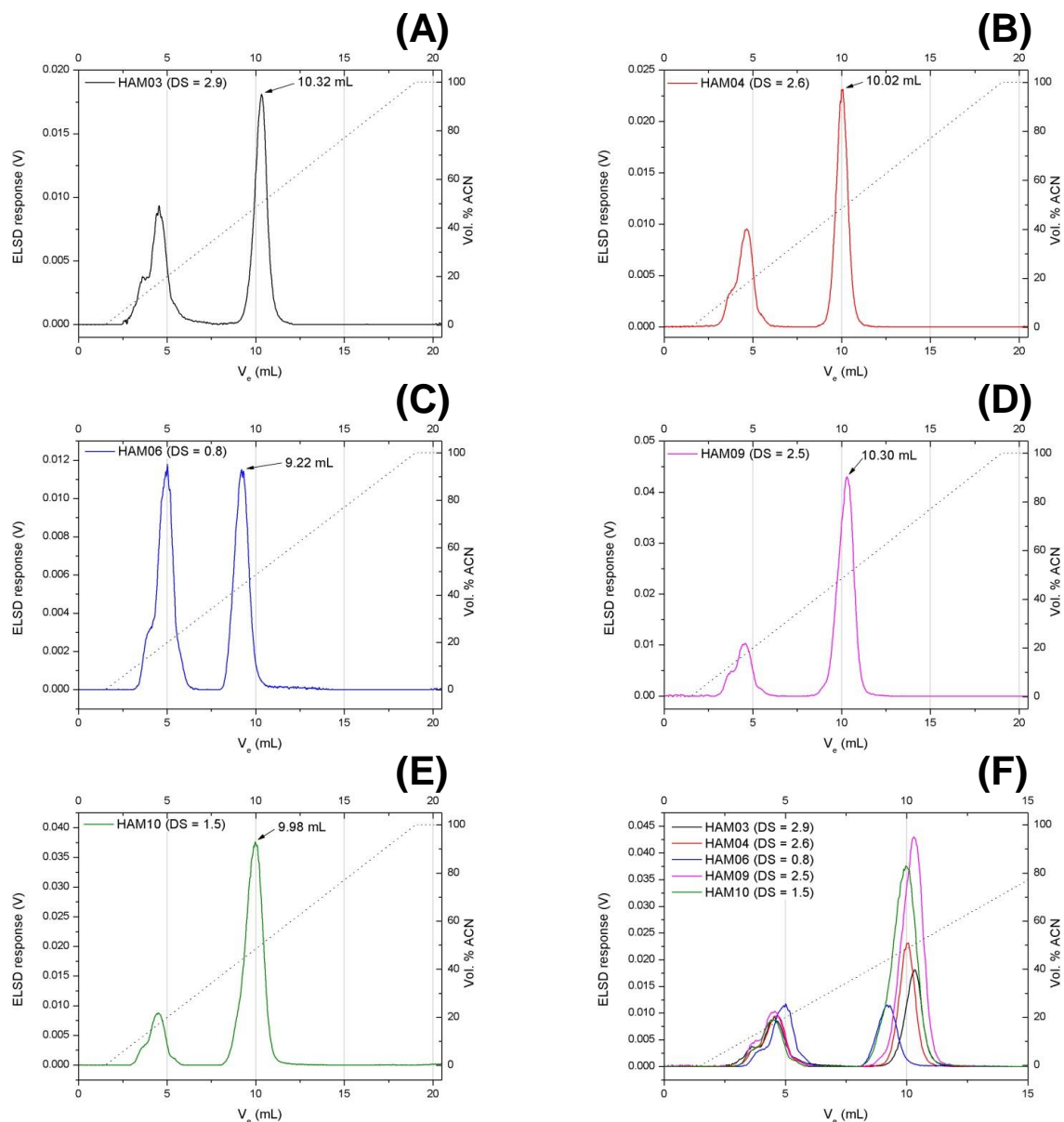


**Figure 5.11:** Chromatograms of HA's with different DS values separated on a C8 column; Sample solvent: DMSO:H<sub>2</sub>O (60:40) (v/v%); Injection volume: 20  $\mu$ L (conc. = 0.5 mg/mL); Gradient profile: linear gradient from 100% H<sub>2</sub>O to 100% ACN. (A) sample HAM 03 (DS =2.9), (B) sample HAM 04 (DS = 2.6), (C) sample HAM 06 (DS = 0.8), (D) HAM 09 (DS = 2.5), (E) sample HAM 10 (DS = 1.5) and image F an overlay of samples A–E.

## 5.4 Conclusion

From the results obtained on the CN column it is clear that the HA's are separated according to their degree of substitution. The CN column provides good recoveries of >90% for all samples, as well as good reproducibility. Furthermore, the separation according to chemical composition was supported by hyphenation with FT-IR. Thus, the validity of the developed chromatographic method for the HA's is confirmed. Even though relatively good results were obtained with the CN column as stationary phase, it should still further be improved by modifying the sample solvent. In the present case, no salt was added to the sample solvent and as a result undesired aggregation occurred, particularly at higher sample concentration, which can have an effect on the separation of the samples. The use of a C8 column in reversed phase mode has the potential to be an alternative and more effective method for the separation of the HA samples according to chemical composition, however, further investigations on the C8 column are required to verify this hypothesis.

## References

- [1] Alpert, A. J. *J. Chromatogr. A*, **1990**, *499*, 177–196.
- [2] Snyder, L. R.; Kirkland, J. J.; Glajch, J. L. *Practical HPLC method development*. John Wiley & Sons, New York, USA, **2012**, 278–283.
- [3] Guiochon, G.; Moysan, A.; Holley, C. *J. Liq. Chromatog.* **1988**, *11* (12), 2547–2570.
- [4] Mathews, B. T.; Higginson, P. D.; Lyons, R.; Mitchell, J. C.; Sach, N. W.; Snowden, M. J.; Taylor, M. R.; Wright, A. G. *Chromatographia*. **2004**, *60* (11–12), 625–633.
- [5] Bashir, M. A.; Brüll, A.; Radke, W. *Polymer*. **2005**, *46*, (10), 3223–3229.
- [6] Jiang, X.; van der Horst, A.; Schoenmakers, P. J. *J. Chromatogr. A*, **2002**, *982* (1), 55–68.
- [7] Glöckner, G. *In Gradient HPLC of copolymers and chromatographic cross-fractionation*, Springer-Verlag: Berlin, Germany, **1991**.
- [8] Engelhardt, H.; Czok, M.; Schultz, R.; Schweinheim, E. *J. Chromatogr.* **1988**, *458*, 79–92.
- [9] Glöckner, G.; Engelhardt, H.; Wolf, D.; Schultz, R. *Chromatographia*. **1996**, *42* (3–4), 185–190.
- [10] Matsumura, G.; Herp, A.; Pigman, W. *Radiat. Res.* **1966**, *28* (4), 735–752.
- [11] Prestwich, G. D.; Marecak, D. M.; Marecek, J. F.; Vercruyse, K. P.; Ziebell, M. R. *J. Control. Release*. **1998**, *53* (1), 93–103.
- [12] Luo, Y.; Kirker, K. R.; Prestwich, G. D. *J. Control. Release*. **2000**, *69* (1), 169–184.
- [13] Kogan, G.; Šoltés, L.; Stern, R.; Gemeiner, P. *Biotechnol. Lett.* **2007**, *29* (1), 17–25.
- [14] Burdick, J. A.; Chung, C.; Jia, X.; Randolph, M. A.; Langer, R. *Biomacromolecules*. **2005**, *6* (1), 386–391.
- [15] Zhong, S. P.; Campoccia, D.; Doherty, P. J.; Williams, R. L.; Benedetti, L.; Williams, D. F. *Biomater.* **1994**, *15* (5), 359–365.
- [16] Pasch, H. *Phys. Chem. Chem. Phys.* **1999**, *1* (17), 3879–3890.
- [17] Pasch, H. *Polym. Chem.* **2013**, *4* (9), 2628–2650.



## Chapter 6

### Summary, Conclusions and Future Work

#### 6.1 Summary

The aim of the study was to analyse the molar mass and chemical heterogeneity of hyaluronic acid before and after chemical modification with acrylate moieties. This was achieved by using various advanced analytical techniques. The correlation of the information obtained from these techniques will be useful in determining the end-use properties of HA in both its modified and unmodified states.

#### 6.2 Conclusions

The present investigations were conducted on sets of virgin HA and HA that was modified with acrylate groups. All samples analysed in this study were obtained from L'Oréal (Paris, France). No additional modifications were performed on these samples, and they were used as received.

In extensive solubility studies, it was found that the combination of an organic modifier, i.e. dimethyl sulfoxide (DMSO), in conjunction with water was the most suitable solvent to dissolve HA samples in a broad DS range. The solubility studies showed a clear trend that indicated that the solubility of the samples is a direct function of DS, which has a direct correlation to the overall polarity of the HA's. It was also apparent from the solubility studies that solvent systems comprising of certain ratios of acetonitrile (ACN) and water can be useful in gradient LAC. It was found that when a ratio of 50:50 ACN to water is used only the unmodified HA's are soluble, while when a ratio of 80:20 ACN to water was used only the modified HA's are soluble. Therefore, ACN-water solvent gradients appeared to be promising candidates for chromatographic experiments.

The average DS of the modified HA samples was successfully determined via  $^1\text{H-NMR}$  spectroscopy and was found to be between 0 and 3.4. However, due to the use of relatively large amounts of sample, costly deuterated solvents and instrumentation, as well as the solubility issue of the HA's at high concentration levels required to produce  $^1\text{H-NMR}$  spectra with good signal-to-noise ratios, an alternative method was explored for  $^1\text{H-NMR}$

spectroscopy. FT-IR/ATR was investigated due to its simplicity and sensitivity. FT-IR/ATR proved to be a fast and effective alternative for a quick estimation of the average DS. Since FT-IR proved successful in the DS determination with only small amounts of HA sample required, this method opened up the possibility to be hyphenated to liquid chromatography and to allow for the analysis of chromatographic fractions with respect to DS as a function of either molar mass or chemical composition.

SEC analysis with a RI detector was carried out on the HA's with a well-known mobile phase used in literature (0.1 M NaCl aqueous solution with 300 mg/L  $\text{NaN}_3$ ) for unmodified HA as a starting point in the SEC method development of the HA's. It became clear from the results that this mobile phase was not effective for the modified HA's, since it did not break up unfavoured aggregation, resulting in the samples eluting at the exclusion limit of the SEC columns. Furthermore, the use of calibration standards (pullulan) for molar mass analysis was replaced by using a MALLS detector, since a MALLS detector enabled the determination of absolute molar masses of the HA's. The results obtained from the solubility studies were used to find a more suitable solvent system that would dissolve all the HA's irrespective of their DS. From the solubility studies, DMSO:H<sub>2</sub>O (60:40) (v/v%) was the solvent that proved to be the most promising. It was used as a new mobile phase in SEC-MALLS-RI analysis of the HA's. However, it was apparent from the results that this mobile phase without an additional modifier would not be suitable since aggregation was still a major issue. SEC-MALLS investigations in DMSO:H<sub>2</sub>O (60:40) (v/v%) revealed that aggregates could be completely suppressed with the addition of an inorganic salt, LiBr. After the establishment of the new salt-modified mobile phase, the  $dn/dc$  values of the samples were measured and used to obtain molar mass information from a MALLS-RI detector setup. From initial spectroscopic investigations it became clear that FT-IR could possibly be hyphenated with LC. SEC was coupled to FT-IR via the LC Transform interface to determine the degree of substitution as a function of molar mass for the HA's. However, these experiments failed mainly due to the highly hygroscopic nature of LiBr, which resulted in very poor signal-to-noise ratios. The LiBr salt was replaced by a salt that would evaporate with the mobile phase – ammonium acetate was used. These experiments failed due to very low sample recoveries when using ammonium acetate as the mobile phase modifier.

For the separation of the HA's with regard to chemical composition, a normal phase gradient LAC method was found to be capable of separating the HA's with respect to their DS. The separations of the HA's was performed using a linear gradient of ACN and water on a cyano stationary phase. The developed method enabled the separation of the HA's according to chemical composition in the investigated DS range. LC-FTIR was employed in order to

investigate the degree of substitution of the HA's as a function of chemical composition. The developed gradient LAC method allowed for the effective separation of the HA's according to their degree of substitution. Furthermore, preliminary tests were conducted on a C8 column in reversed phase mode to investigate alternative methods to separate the HA's according to their DS. However, this should still be subject to future investigations.

It is clear from the present research that the newly developed techniques provide new detailed insights into the complex molecular structure of HA's that are functionalized with acrylate moieties.

### **6.3 Recommendations for Future Work**

Future work may include the following aspects: an in-depth study on the influence of different ELSD-compatible salts with the current mobile phase should be explored, to obtain better and more reproducible results from SEC-FTIR and to enable the hyphenation of SEC with LAC. The separation methods devised in this work, with reference to SEC, should be compared to thermal field flow fractionation (ThFFF). The idea behind this suggestion is the fact that SEC requires the samples to be filtered, resulting in a certain degree of information lost due to sample loss. In ThFFF there is no need to filter the samples since an open channel is used as opposed to a stationary phase of packed porous particles. It would provide additional insight into the molecular complexity of the HA samples when unfiltered samples were fractionated.

In the case of gradient LAC, the developed method can be fine-tuned with the addition of an appropriate ELSD-compatible salt that would also completely suppress any form of aggregation. Further comparison of the normal phase method to the reversed phase method can be conducted, since it is known that reversed phase liquid chromatography is generally more robust in the separation of very polar analytes. Preliminary work already carried out in this direction has proven to be positive; for this purpose a C8 column was utilized with ACN and water as eluents. From the results obtained on the C8 column, promising separations of all HA samples in the DS range investigated was achieved.

Finally, it is recommended to perform two-dimensional (2D) liquid chromatography, where gradient LAC is hyphenated to SEC to obtain comprehensive information on all chemically different species of the fractionated samples regarding their molar mass and chemical composition.

## **Appendix A**

Complete summary of the results obtained for the solubility studies under different experimental conditions.

**Table A.1:** Solubility study at 25 °C and a concentration of 1 mg/mL (+ soluble, +/- partial soluble, - insoluble).

Solvent	HA 01	HA 02	HA 03	HAM 01	HAM 02	HAM 03	HAM 04	HAM 05	HAM 06	HAM 07
	25 °C	25 °C	25 °C	25 °C	25 °C	25 °C	25 °C	25 °C	25 °C	25 °C
DMSO	+	+/-	+/-	-	-	-	-	-	-	-
CHCl <sub>3</sub>	+/-	+/-	+/-	-	-	-	-	-	-	-
H <sub>2</sub> O	+	+	+	+/-	+	+	+	+/-	+	+
Acetone	+/-	-	+/-	-	-	-	-	-	-	-
DCM	+/-	+/-	+/-	-	-	- (swell)	- (swell)	- (swell)	- (swell)	-
DMAc	-	-	-	-	-	-	-	-	-	-
DMF	-	-	+/-	-	-	-	- (swell)	- (swell)	-	-
THF	-	-	-	-	-	-	-	- (swell)	-	-
MeOH	+/-	+/-	+/-	+	- (swell)	+	+	- (swell)	- (swell)	-
Hexane	-	-	+/-	-	- (swell)	-	- (swell)	-	-	-
Ethyl Acetate	+/-	+/-	+/-	-	-	-	-	-	-	-
Butanone	+/-	+/-	+/-	-	-	-	-	-	-	-
Toluene	+/-	+/-	+/-	+	+	- (swell)	- (swell)	+	- (swell)	- (swell)
H <sub>2</sub> O:MeOH (70:30)	+	+	+	+	+	+	+	+	+	+
2-Propanol	+/-	+/-	+/-	-	-	-	-	-	-	-
Ethanol	+/-	+/-	+/-	-	- (swell)	- (swell)	- (swell)	- (swell)	- (swell)	-
0.1M NaCl + H <sub>2</sub> O:MeOH (50:50)	+	+	+	+	+	NA	NA	+	NA	NA
0.2M NaCl + H <sub>2</sub> O:MeOH (50:50)	+	+	+	+	+	NA	NA	+	NA	NA
0.3M NaCl + H <sub>2</sub> O:MeOH (50:50)	+	+	+	+	+	NA	NA	+	NA	NA
0.1M NaCl + 300 mg/L NaN <sub>3</sub>	+	+	+	+	+/-	+	+/-	+	+	+

Table A.2: Solubility study at 40 °C and a concentration of 1 mg/mL (+ soluble, +/- partial soluble, - insoluble).

Solvent	HA 01	HA 02	HA 03	HAM 01	HAM 02	HAM 03	HAM 04	HAM 05	HAM 06	HAM 07
	40 °C	40 °C	40 °C	40 °C	40 °C	40 °C	40 °C	40 °C	40 °C	40 °C
DMSO	+/-	+/-	+/-	-	+(swell)	+	+(swell)	+(swell)	-	-
CHCl <sub>3</sub>	+/-	+/-	+/-	-	-	-	-	-	-	-
H <sub>2</sub> O	+	+	+	+	+(swell)	+	+	+/-	+	+
Acetone	+/-	-	+/-	-	-	-	-	-	-	-
DCM	+/-	+/-	+/-	-	-	-(swell)	-(swell)	-(swell)	-(swell)	-
DMAc	+/-	+/-	+/-	-	-(swell)	+(swell)	-(swell)	-	-	-
DMF	+/-	+/-	+/-	-	-(swell)	-(swell)	+(swell)	+(swell)	-	-
THF	+/-	+/-	+/-	-	-(swell)	-	-	-(swell)	-	-
MeOH	+/-	+/-	+/-	+(swell)	-(swell)	+(swell)	+(swell)	-(swell)	-(swell)	-
Hexane	+/-	+/-	+/-	-	-	-	-	-	-	-
Ethyl Acetate	+/-	+/-	+/-	-	-	-	-	-	-	-
Butanone	+/-	+/-	+/-	-	-	-	-(swell)	-	-	-
Toluene	+/-	+/-	+/-	+(swell)	+(swell)	-(swell)	-(swell)	+(swell)	+(swell)	-(swell)
H <sub>2</sub> O:MeOH (70:30)	+	+	+	+	+(swell)	+	+	+(GL)	+	+
0.5M NaOH	+	+	+	+	+/-	+	+	+/-	+	+
DMSO:H <sub>2</sub> O (50:50)	+	NA	NA	+/-	+/-	NA	NA	NA	NA	NA
DMSO:H <sub>2</sub> O (60:40)	+	+	+	+	+	+	+	+	+	+
DMSO:H <sub>2</sub> O (70:30)	+	+	+	+	+/-	+	+	+	+	+
DMSO:H <sub>2</sub> O (80:20)	+	+	+	+	+/-	+	+	+/-	+/-	+/-
0.02% NaN <sub>3</sub>	+	NA	NA	NA	+(swell)	+	NA	+/-	NA	+
0.1M NaNO <sub>3</sub>	+	NA	NA	NA	+(swell)	+	NA	+/-	NA	+

## Appendix A: Solubility Studies

2015

0.1M AmAc	+	NA	NA	NA	+	+	NA	+/-	NA	+
PBS	+/-	+/-	+/-	+	+/-	NA	NA	+	NA	+
Toluene:MeOH (50:50)	+/-	+/-	+/-	NA	NA	+/-	NA	+/-	NA	+/-
0.02M PB:MeOH (90:10)	+/-	NA	NA	+	+/-	NA	NA	+	NA	+
H <sub>2</sub> O:1.4-Dioxane (50:50)	+/-	+/-	+/-	+	+/-	+	+	+	+	+
ACN:H <sub>2</sub> O (50:50)	-	-	-	+	+	+	+	+	+	+
ACN:H <sub>2</sub> O (20:80)	+	+	+	-	-	-	-	-	-	-
0.1M NaCl + 300 mg/L NaN <sub>3</sub>	+	+	+	+	+/-	+	+/-	+	+	+

**Table A.3:** Solubility study at 40 °C and a concentration of 0.5 mg/mL (+ soluble, +/- partial soluble, - insoluble).

Solvent	HA 01	HA 02	HA 03	HAM 01	HAM 02	HAM 03	HAM 04	HAM 05	HAM 06	HAM 07
	40 °C	40 °C	40 °C	40 °C	40 °C	40 °C	40 °C	40 °C	40 °C	40 °C
DMSO	+	+/-	+/-	-	-	-	-	-	-	-
DMAc	+/-	+/-	+/-	-	- (swell)	+/-	+/-	- (swell)	-	-
DMF	+/-	+/-	+/-	-	- (swell)	- (swell)	+	+	-	-
MeOH	+/-	+/-	+/-	+	+	+	+	+	- (swell)	-
H <sub>2</sub> O:MeOH (70:30)	+	+	+	+	+	+	+	+	+	+

**Table A.4:** Solubility study at 40 °C and a concentration of 0.5 mg/mL in the presence of a salt\* (+ soluble, +/- partial soluble, - insoluble).

Solvent	HA 01	HA 02	HA 03	HAM 01	HAM 02	HAM 03	HAM 04	HAM 05	HAM 06	HAM 07
	40 °C	40 °C	40 °C	40 °C	40 °C	40 °C	40 °C	40 °C	40 °C	40 °C
DMSO	+/-	+/-	+/-	+	+	+	+	+	- (swell)	- (swell)
DMAc	+/-	+/-	+/-	+	- (swell)	+/-	+/-	- (swell)	-	-
DMF	+/-	+/-	+/-	-	- (swell)	- (swell)	+	+	-	-

**\*0.1M NaCl for all the samples**

**Swell (+)** – Positive swelling (possibility of dissolving)

**Swell (-)** – Negative swelling (dissolving more problematic)

**GL** – gel like

**[NOTE:** In the Tables, HA refers to unmodified hyaluronic acid and HAM refers to modified hyaluronic acid.]



## Appendix B

The  $dn/dc$  values obtained for each DS can be seen in **Table B.1**. Since the  $dn/dc$  values have a direct correlation to the DS in our case, all the  $dn/dc$  values had to be determined to get the most accurate MM information from SEC-MALLS.

**Table B.1:** Description of the  $dn/dc$  values used for molar mass determination.

<b>DS value</b>	<b><math>dn/dc</math> value (mL/g)</b>
1. Unmodified	0.103
2. 0.4	0.0941
3. 0.8	0.0934
4. 1.5	0.0893
5. 1.6	0.0881
6. 2.2	0.0852
7. 2.5	0.0773
8. 2.6	0.0756
9. 2.9	0.0651
10. 3.1	0.0587

## Appendix C

The effect the mobile phase has on the ELSD response for the HA samples with varying DS is represented in **Figure C.1**

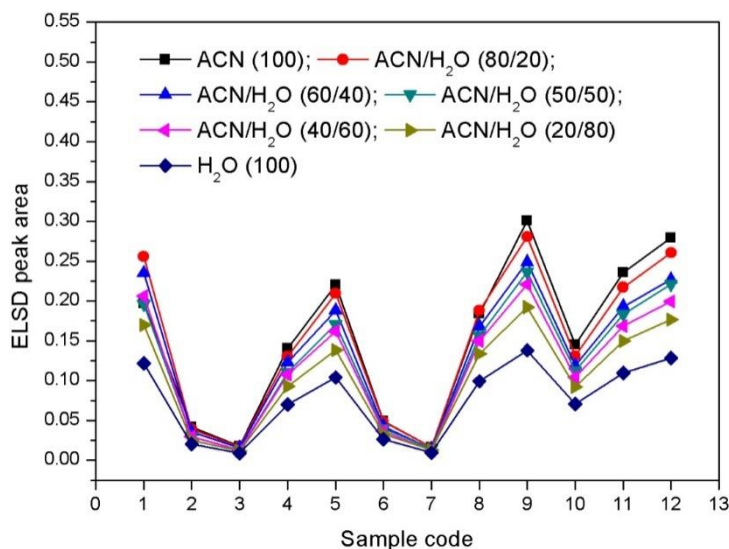


**Figure C.1:** Influence of mobile phase composition on the ELSD response; No column; flow rate: 0.50 mL/min.; Temperature 30 °C; Injected volume 30 µL; sample codes: (1) HA 1 (unmodified), (2) HAM 01 (DS = 3.1), (3) HAM 02 (DS = 3.4), (4) HAM 03 (DS = 2.9), (5) HAM 04 (DS = 2.6), (6) HAM 05 (DS = 2.2), (7) HAM 06 (DS = 0.8), (8) HAM 07 (DS = 0.4), (9) HAM 08 (DS = 2.6), (10) HAM 09 (DS = 2.5), (11) HAM 10 (DS = 1.5), (12) HAM 11 (DS = 1.6). Eluent profile: 3 min isocratic run with the desired solvent or solvent mixture; Detector: ELSD (Nebulization temp. = 100 °C, evaporation temp. = 100 °C and gas flow = 3.0 bar).